U.PORTO
FEUP FACULDADE DE ENGENHARIA
UNIVERSIDADE DO PORTO

Marine Biofilm Formed by Coccoid Cyanobacteria: Development and Control

A Dissertation presented to the
UNIVERSITY OF PORTO
for the degree of Doctor in
Chemical and Biological Engineering
by

Sara Isabel da Silva Faria

Supervisor: Prof. Filipe J. Mergulhão
Co-supervisor: Rita Teixeira dos Santos

lepabe
Laboratory for Process Engineering, Environment, Biotechnology and Energy

LEPABE – Laboratory for Process Engineering, Environment, Biotechnology and Energy
Department of Chemical Engineering
Faculty of Engineering, University of Porto
November, 2021

This PhD project was funded by “CVMAR+i – Industrial Innovation and Marine Biotechnology Valorization” international project, financed by INTERREG V-A Spain – Portugal (POCTEP) (0302_CVMAR_I_1_P) and by Base Funding - UIDB/00511/2020 of the Laboratory for Process Engineering, Environment, Biotechnology and Energy – LEPABE - funded by national funds through the FCT/MCTES (PIDDAC).

“A tarefa não é tanto ver aquilo que ninguém viu, mas pensar o que ninguém ainda pensou sobre aquilo que todo mundo vê.”

Arthur Schopenhauer

Acknowledgments

In completing another journey, which led me to a PhD in Chemical and Biological Engineering, I am grateful to those who contributed to my academic and scientific enrichment. Therefore, the elaboration of this thesis would not be possible without the collaboration, encouragement and support of several people.

First of all, I would like to express my sincere gratitude to my supervisor Professor Filipe Mergulhão for the scientific supervision and support throughout my studies. I also would like to thank his pertinent suggestions and criticisms, as well as the invaluable trust, availability, encouragement and persistence, that contributed to improving my skills. The knowledge I acquired from him has been precious and will definitely be crucial to my future professional career and personal life.

I am also grateful to Dr. Rita Santos, my co-supervisor, for all suggestions, support, and contribution throughout my studies. Definitely, she was one of the major contributors to the realization of this thesis project and for my progress as a researcher. Your help gave me more confidence to overcome my insecurities, improving my scientific and academic skills. I hope our friendship is for life.

I also would like to say thank you to Dr. Luciana Gomes! Thank you for helping me to overcome the obstacles during these three years and for your friendship. I learned from you the importance of persevering and not giving up even when everything doesn't seem to work.

To all those in the Department of Chemical Engineering and LEPABE, I would like to express my sincere thanks for providing good working facilities.

I would like to thank Dr. Vítor Vasconcelos and Dr. João Morais from the Interdisciplinary Centre of Marine and Environmental Research (CIIMAR) group for supplying the cellular suspensions from cyanobacterial strains used on my PhD project.

To Prof. Luís de Melo, Prof. Nuno Azevedo and Dr. Andreia Azevedo for sharing their knowledge and supporting this journey.

To all my LabE007/E008 and BEL 2 colleagues, with special thanks to Maria João Romeu, Ana Claúdia Barros, Diana Oliveira, Isabel Oliveira, Beatriz Magalhães and Anabela Borges, who were with me during all these years, for advice and the good atmosphere in the lab. I also would like to thank Carla Ferreira, Sílvia Faia and Paula Pinheiro from E-101 for being always ready to help me with "stuff" problems.

I would like to thank my family, especially my parents for their patience and unconditional support. To André Castro, I thank you for all the optimism, patience and love. Without all of you on my side, none of my victories would make sense and nothing of that would be possible. You are, undoubtedly, the real drivers of this adventure that is life.

Last but not least, I would like to thank all my friends, especially Ana Azevedo, Vanessa Dinis and Isabel Vilar, for the good times we have always had together. I hope that our friendship will last a lifetime and that there will never cease to be stories to tell. Thank you for helping me to increase my confidence and build a bright future!

Thank you all for the support!

Scientific outputs

The results presented in this thesis are partially published in:

Papers in peer-reviewed journals

Faria, S. I., R. Teixeira-Santos, M. J. Romeu, J. Morais, V. Vasconcelos and F. J. Mergulhão (2020). "The Relative Importance of Shear Forces and Surface Hydrophobicity on Biofilm Formation by Coccoid Cyanobacteria." Polymers **12**(3): 653. (doi: 10.3390/polym12030653) **(Chapter 3)**

Faria, S. I., R. Teixeira-Santos, L. C. Gomes, E. R. Silva, J. Morais, V. Vasconcelos and F. J. Mergulhão (2020). "Experimental assessment of the performance of two marine coatings to curb biofilm formation of microfoulers." Coatings **10**(9):893. (doi: 10.3390/coatings10090893) **(Chapter 4).**

Faria, S. I., R. Teixeira-Santos, M. J. Romeu, J. Morais, E. de Jong, J. Sjollema,V. Vasconcelos and F. J. Mergulhão (2020). "Unveiling the antifouling performance of different marine surfaces and their effect on the development and structure of cyanobacterial biofilms." Microorganisms **9**(5): 1102. (doi: 10.3390/microorganisms9051102) **(Chapter 5).**

Faria, S. I., L. C. Gomes, R. Teixeira-Santos, J. Morais, V. Vasconcelos and F. J. Mergulhão (2021) "Developing New Marine Antifouling Surfaces: Learning from Single-Strain Laboratory Tests." Coatings **11**(1): 90. (doi: 10.3390/coatings11010090) **(Chapter 6).**

Faria, S. I., R. Teixeira-Santos, J. Morais, V. Vasconcelos and F. J. Mergulhão (2021). "The association between the initial adhesion and cyanobacterial biofilm development." FEMS Microbiology Ecology **97**(5): fiab052. (doi: 10.1093/femsec/fiab052) **(Chapter 7).**

Other outputs

Faria, S. I., F. J. Mergulhão (2019). "Influence of hydrodynamic conditions and surface properties on cyanobacterial adhesion." 3rd Doctoral Congress in Engineering in the Symposium on Chemical and Biological Engineering, Portugal (poster presentation).

Faria, S. I. (2020)**. "**Marine biofilm formed by coccoid cyanobacteria: development and control." Training School Meeting organized by European Network of multidisciplinary research to Improve the Urinary Stents (ENIUS) (COST Action CA16217), Lublin (Poland) (oral presentation) https://link.springer.com/article/10.1007/s00240-020-01218-2 .

Faria, S. I., F. J. Mergulhão (2020). "The influence of shear forces and surface hydrophobicity on coccoid cyanobacterial biofilm development." Biofilms 9, online international conference (poster presentation).

Silva E. R., A. V. Tulcidas, O. Ferreira, R. Bayón, A. Igartua. G. Mendoza, F. J. Mergulhão, **S. I. Faria**, L. C. Gomes, S. Carvalho, J. C. M. Bordado (2021). "Assessment of the environmental compatibility and antifouling performance of an innovative biocidal and foul-release multifunctional marine coating". Environmental Research **198** (doi: 10.1016/j.envres.2021.111219).

Neves, A. R., R. Ruivo, J. Sousa, L. Gomes, **S. I. Faria**, E. Sousa, M. Pinto, M. Santos, F. J. Mergulhão, E. Silva, M. C. Silva (2021). "Synthesis, antibiofilm properties and application into marine coatings of a new eco-friendly polyphenolic compound." 4th International Conference on Biological and Biomimetics Adhesives (ICBBA 2021), Aveiro, Portugal, online international conference (oral presentation by Ana Neves).

Nomenclature

Abbreviations

2D	Two-dimensional
3D	Three-dimensional
AF	Antifouling
AFM	Atomic force microscopy
CFD	Computational fluid dynamics
CIIMAR	Interdisciplinary centre of marine and environmental research
CLSM	Confocal laser scanning microscopy
EPS	Extracellular polymeric substances
FRC	Fouling release coatings
GHG	Greenhouse gases
HEMA	Hydrophilic hydroxyethyl methacrylate
HPG	Hyperbranched polyglycerol
IAS	Invasive alien species
IMO	International maritime organization
LEGE-CC	Blue biotechnology and ecotoxicology culture collection
MTPs	Microtiter plates
OCT	Optical coherence tomography
OD	Optical density
PDMS	Polydimethylsiloxane
PEG	Polyethylene glycol
PFA	Hydrophobic perfluorodecyl acrylate
QS	Quorum sensing
TBT	Tributyltin
UV	Ultraviolet

Symbols

γ^{LW}	Lifshitz van der Waals components (mJ/m^2)
$\gamma-$	Electron donor components (mJ/m^2)
$\gamma+$	Electron acceptor character (mJ/m^2)
γ_l^{Tot}	Total surface energy (mJ/m^2)
γ^{AB}	Lewis acid-base components (mJ/m^2)
ΔG	Surface hydrophobicity (mJ/m^2)
ΔG^{Adh}	Free energy of adhesion (mJ/m^2)
R*a*	Average roughness (nm)
θ	Surface angle (°)
θ_w	Contact angles with water (°)
θ_F	Contact angles with formamide (°)
θ_B	Contact angles with α- *bromonaphthalene* (°)

Table of contents

List of figures

Chapter 4

Chapter 6

Chapter 7

List of tables

Chapter 7

Abstract

Marine biofouling is an undeniable problem for the marine sector since it is responsible for several economic losses and ecological problems all around the world. The main goal of this thesis was to understand the initial process of biofouling development, from adhesion to the formation of marine biofilms by microfouler organisms, and evaluate the antifouling (AF) performance of marine surfaces on the reduction and/or control of marine microfouling.

The hydrodynamic conditions and surface properties have been described as relevant modulating factors of the biofilm formation process. Thus, the relative importance of these parameters was first assessed in this study, during the cyanobacterial biofilm formation process. On this first task, the hydrodynamic conditions demonstrated to have a higher impact on coccoid cyanobacteria biofilm development than surface hydrophobicity, although a combined effect of these two parameters was also verified.

The surface properties, and their interaction with microfoulers in the biofilm formation process, were evaluated in more detail in order to clarify and encourage the research community to improve the effectiveness of existing AF surfaces and/or develop new environmentally friendly AF materials for marine applications. The AF performance of several surfaces was tested. A commercial silicone-based paint and an epoxy resin showed to reduce the amount of biofilm formed and affect the biofilm structure (thickness, density, porosity, and homogeneity).

The most realistic studies available to assess the performance of AF surfaces in marine contexts are the immersion of marine surfaces in seawater. Nevertheless, this strategy can be dangerous for non-target marine organisms since the tested components can be toxic, and results are highly dependent on sea conditions. Therefore, there has been a concern to create *in vitro* safe tests that mimic the real marine environment as much as possible. Throughout this Ph.D. project, they demonstrated to be a useful tool for initial screening and comparing the effectiveness of AF surfaces, with the advantage of mimicking a spectrum of marine conditions.

In this work, the impact of microorganisms diversity was evaluated to understand whether using a mixed population for the *in vitro* tests yields substantially different results than using single strains. It was shown that the use of a single-strain strategy represents a

good compromise between the high complexity of i*n vivo* marine ecosystems and the convenience of *in vitro* testing.

Additionally, the potential of short-time adhesion assays to estimate how biofilm development occurs was evaluated, and the results revealed a significant correlation between the number of adhered and biofilm cells. These findings demonstrated the high potential of initial adhesion assays to estimate marine biofilm development and as a screening tool for novel AF marine surfaces.

In conclusion, this study contributed to understanding the biofilm formation process of microfouler organisms and defining the experimental conditions to be used in marine *in vitro* tests to assess the AF potential of surfaces. The results are likely to contribute to the development of more efficient approaches to control bio-encrustation in the marine context.

Keywords: Biofouling, marine biofilm, microfouler organisms, cyanobacterial, hydrodynamic conditions, surface properties, antifouling strategies, antifouling surfaces, *in vitro* assay.

Resumo

A bioincrustação marinha é um problema inegável para o setor marinho uma vez que é responsável por diversas perdas económicas e problemas ecológicos em todo o mundo. O principal objetivo desta tese foi compreender o processo inicial de formação da bioincrustação, da adesão até à formação de biofilmes marinhos, e avaliar o potencial de superfícies marinhas em controlar e/ou reduzir a bioincrustação por microorganismos.

As condições hidrodinâmicas e as propriedades de superfícies têm sido descritas como fatores determinantes no processo de formação de biofilme. Assim, na primeira fase deste estudo, a importância relativa desses parâmetros foi investigada durante o processo de formação de biofilme de cianobactérias. As condições hidrodinâmicas testadas tiveram um maior impacto no desenvolvimento de biofilmes de cianobactérias cocóides do que a hidrofobicidade da superfície, embora um efeito combinado desses dois parâmetros também tenha sido verificado.

As propriedades da superfície e a sua interação com microrganismos, durante o processo de formação de biofilme, foram testadas com detalhe neste estudo, de forma a esclarecer e a encorajar a comunidade científica a melhorar a eficácia das superfícies anti-incrustrantes existentes e/ou desenvolver novos materiais anti-incrustantes, amigos do ambiente, para aplicações marinhas. O desempenho anti-incrustante de várias superfícies foi testado, e uma tinta à base de silicone comercial e uma resina epóxi mostraram ser capazes de reduzir a quantidade de biofilme formado, tendo causado impacto na estrutura do biofilme (espessura, densidade, porosidade e homogeneidade).

Os estudos atualmente disponíveis para avaliar o desempenho de superfícies anti-incrustantes em contexto marinho incluem a imersão de superfícies marinhas na água do mar. No entanto, esta estratégia pode ser perigosa para os organismos marinhos uma vez que os componentes testados podem ser tóxicos, para além de que os resultados podem ser fortemente influenciados pelas condições marítimas. Logo, tem havido uma preocupação crescente em implementar testes *in vitro* seguros e que mimetizem o ambiente marinho real. Ao longo deste projeto de Doutoramento, os testes *in vitro* demonstraram ser uma ferramenta útil para estudos iniciais de avaliação da eficácia das superfícies anti-incrustantes, com a vantagem de permitir avaliar facilmente um amplo espectro de condições marinhas.

Neste trabalho, o impacto da diversidade biológica foi avaliado a fim de entender se o uso de uma população mista para os testes *in vitro* produz resultados substancialmente diferentes comparativamente ao uso de uma única espécie. Este estudo demonstrou que o uso de monocultura representa um bom compromisso entre a elevada complexidade dos ecossistemas marinhos e a conveniência dos testes *in vitro*.

Além disso, o potencial dos ensaios de adesão de curto prazo, relativamente ao desenvolvimento do biofilmes, foi avaliado e os resultados revelaram existir correlação entre o número de células aderidas e o número de células do biofilme. Esses resultados demonstraram o alto potencial dos ensaios de adesão inicial para estimar o desenvolvimento do biofilme marinho, podendo ser utilizados para testes preliminares de novas superfícies marinhas com propriedades anti-incrustantes.

Em conclusão, este estudo permitiu compreender o processo de formação dos biofilmes marinhos e ajudou na definição das condições experimentais ideais para testes *in vitro* de avaliação do potencial anti-incrustamento de superfícies. Os resultados obtidos poderão ter impacto no desenvolvimento de abordagens mais eficientes para controlar o problema da bio-incrustação em contexto marinho.

Palavras-chave: Bio-incrustação, biofilme marinho, microorganismos marinhos, cianobactérias, condições hidrodinâmicas, propriedades de superfície, estratégias anti-incrustamento, superfícies anti-incrustantes, ensaios *in vitro*.

1.

Introduction

1.1. Relevance and motivation

In marine environments, submerged surfaces and marine structures are quickly colonized by marine micro and macroorganisms, in a process known as biofouling. Biofouling is a natural process responsible for several economic and environmental problems that affect different maritime sectors around the world, being considered one of the most important issues facing marine technology (Silva et al. 2019, Tian et al. 2020). The attachment of fouling organisms to marine vessels promotes surface corrosion and increases drag resistance. Consequently, it leads to greater maintenance costs and increases fuel consumption (Almeida et al. 2007, Tian et al. 2020). Higher fuel consumption increases the emission of greenhouse gases (GHG) and other harmful carcinogenic effluents that contribute to environmental pollution, global warming and climate change, as well as health problems (Mathew et al. 2021).

In addition to the problems associated with frictional drag, marine biofouling can have other environmental implications such as the bioinvasion of exotic species from different geographic areas when fouling organism travel in marine vessels, having a negative impact on global biodiversity (King et al. 2006, Lacoursière-Roussel et al. 2012, Tian et al. 2020). This phenomenon is also aggravated at both community (species richness) and

population (genetic diversity) levels by the intense shipping activity in ports (Lacoursière-Roussel et al. 2012, Neves et al. 2020).

Marine biofouling also affects the underwater structures used for on-site weekly, monthly or continuous monitoring of parameters such as dissolved oxygen, turbidity, conductivity, pH, or fluorescence (Delauney et al. 2010). Bio-incrustation causes incorrect measurements on optical and electrochemical marine devices such as sensors and housings in less than a week (Delauney et al. 2010, Romeu et al. 2019). Additionally, biofouling can damage a wide diversity of underwater marine facilities, including net cages for aquaculture, bridges, pontoons and oil production platforms (Tian et al. 2020).

Overall, the consequences of marine biofouling involve an increase of direct costs either for maintenance and cleaning procedures as well as indirect costs resulting from productivity loss of maritime industries (Bannister et al. 2019, Mathew et al. 2021).

Biofouling is a dynamic process that involves several marine organisms (micro and macroorganisms) and their interactions in sequential steps (Vladkova et al. 2014). Firstly, a conditional film is formed on the marine surface, which promote bacteria and algae (microfoulers) surface adhesion and biofilm formation. This microfouling layer is the basis for later settlement of macrofouling organisms (e.g., bryozoans, mollusks, polychaeta, tunicates, coelenterates or fungi) (Jamal et al. 2018). The biofilm is characterized as a complex and organized consortium of microorganisms, attached to the surface, and embedded on a slimy matrix of extracellular polymeric substances (EPS) that confer protection against adverse conditions (Bannister et al. 2019). The biofilm formation is influenced by innumerous factors, including surface properties, hydrodynamic conditions, temperature, pH and nutrient availability (Allen et al. 2018, Rao 2010). Amongst all the parameters, the physicochemical factors related to the surface and flow velocity play a crucial role in marine biofilms development (Faria et al. 2020, Romeu et al. 2019). Therefore, it is important to understand the impact of these factors on adhesion and biofilm formation processes in marine environments in order to design new strategies to control biofouling and, consequently, mitigate its implications.

Another promising approach to prevent and control biofouling is the use of efficient AF compounds that inhibit or delay the adhesion and biofilm formation on submerged

surfaces since these steps correspond to the early stage of biofouling development and can prevent the attachment of macroorganisms (Eduok et al. 2017, Silva et al. 2019). Up to date, a wide range of control and prevention strategies have been exploited, such as the use of chemical agents and other compounds, which are effective in fouling mitigation. However, the use of some of these compounds has limitations since often they do not comply with the evolving regulatory framework. Most of them affect marine ecosystems and cause significant health issues to humans through air, land and water pollution (Amara et al. 2018, Breinlinger et al. 2021, Mathew et al. 2021).

Therefore, the necessity to develop AF strategies continues to require efforts from the scientific community to overcome these problems and create an acceptable, sustainable, universal and environmentally friendly AF strategies (Miller et al. 2020, Silva et al. 2019). Recently, different coatings have been developed to overcome some of the disadvantages of common chemical agents typically used in the past (Basu et al. 2020, Silva et al. 2019). However, their efficiency and effectiveness are often not verified using laboratory testing conditions that simulate the real marine environment. Thus, results indicating poor surface performance are only attained after prolonged and expensive field tests.

In the real marine environment, marine structures are exposed to different species of micro and macroorganisms, and marine biofilms are mainly composed of diverse species of bacteria and diatoms (de Carvalho 2018). Therefore, for AF studies, it is important to verify if the behavior of single species marine biofilms is similar to mixed culture biofilms organisms in order to evaluate if singles species can be used as a first screening approach in controlled conditions.

A recommended first step for testing new AF surface consists of exposing them to microfouling organisms under laboratory conditions that mimic the marine environments and analyse for several weeks since the direct evaluation of coatings in the ocean can be very expensive and the agents tested can be toxic to marine organisms (Faria et al. 2020, Romeu et al. 2019, Romeu et al. 2020, Zecher et al. 2018). Recent work has shown that the results obtained with these tests can be comparable to those obtained with field tests performed in the Atlantic Ocean (Silva et al. 2021). Although laboratory assays provide the first indications

about AF performance and allow a better understanding of the dynamics of biofilm formation they are laborious and time-consuming, requiring on average 6 weeks to provide representative results of a real marine scenario (Silva et al. 2021). In this sense, it may be wiser to develop alternative short-term assays that can serve as a primary screening procedure of the AF potential of developed coatings.

1.2. Objectives and outline

The main objective of this thesis was to understand the dynamic of adhesion and biofilm formation of coccoid cyanobacterial under distinct hydrodynamic conditions and substratum surfaces, simulating what happens in the real marine environment, in order to develop strategies to prevent and control marine microfouling, and consequently biofouling development and associated problems. It was also an important objective to study strategies that contribute to improving the conditions of *in vitro* tests in order to obtain more reliable results in a more efficient manner.

In order to answer these main goals, the following specific objectives were defined:

1. Assessment of the relative importance of shear forces and surface hydrophobicity on biofilm formation by coccoid cyanobacterial;
2. Evaluate the AF potential of different marine surfaces to prevent or reduce biofilm formation by marine microorganisms, under controlled hydrodynamic conditions.
3. Improving the assay conditions used to evaluate AF potential of marine surfaces.
    a. Understanding if biofilm forming by single species of marine microorganisms can be indicative of the AF performance of a surface;
    b. Evaluate the potential of short-time adhesion assays to assess the AF behavior of surfaces.

This thesis is outlined as follows:

Chapter 2 consists of a brief literature review describing the state of the art, which was the basis for the development of this thesis.

In **Chapter 3,** a detailed study was made to evaluate the relative importance of shear forces and surface hydrophobicity on cyanobacterial biofilm development in marine settings. In that study, we followed biofilm development in defined hydrodynamic conditions (including those that can be found in harbors), using two cyanobacterial coccoid strains with different biofilm-forming capacities and two model surfaces with different hydrophobicity (glass and an epoxy polymeric coating).

After this initial evaluation, which concluded that hydrodynamics had a stronger impact on biofilm development than surface hydrophobicity, the following studies analysed the performance of marine AF surfaces under the hydrodynamic conditions prevailing around a ship hull in a harbor. Understanding how AF surfaces interact with microfoulers can clarify and help to improve their efficacy, leading to the development of new AF coatings to control and/or reduce biofouling.

In **Chapter 4,** the performance of AF marine surfaces (silicone-based paint and an epoxy resin) against biofilm formation by two common microfouling organisms, *Pseudoalteromonas tunicata* and *Cyanobium* sp. LEGE 10375 was evaluated, under defined hydrodynamic conditions.

In **Chapter 5,** the AF performance of five surface materials (glass, perspex, polystyrene, epoxy-coated glass, and a silicone hydrogel coating) against biofilm formation by cyanobacteria, under defined hydrodynamic conditions, were evaluated. The surface effects on biofilm architecture were analysed.

The microorganisms selected in the previous studies, coccoid cyanobacteria and marine bacteria, were used as model microorganisms since they are one of the first colonizers of

marine surfaces. However, the marine environment presents a much higher biological complexity. The time spent in screening the AF potential of surfaces and coatings is also an important aspect to bear in mind during development. The optimization of *in vitro* in terms of biological complexity and assay duration may enable faster surface development.

In **Chapter 6,** we assessed if there are benefits in varying the degree of complexity of marine cultures when the goal is to get the first indications about the AF materials' performance. A polymeric coating commonly used to coat the hulls of small recreational vessels and with known antibiofilm activity was tested against mono-species and dual-species cultures, in order to identify which culture conditions generate the worst-case scenario, being the most appropriate for *in vitro* experiments, particularly during the initial screening of the performance of novel AF marine surfaces.

In **Chapter 7,** the association between the initial adhesion and biofilm formation was investigated to evaluate the potential of short-time adhesion assays to estimate the biofilm development and, consequently, the AF efficacy of a given surface. For this purpose, the initial adhesion and biofilm formation of three coccoid cyanobacteria isolated from different geographic areas were evaluated using different surfaces and hydrodynamic conditions.

Finally, **Chapter 8** contains the main conclusions of this thesis and some suggestions for future work.

1.3. References

Allen, A., O. Habimana and E. Casey (2018). "The effects of extrinsic factors on the structural and mechanical properties of Pseudomonas fluorescens biofilms: A combined study of nutrient concentrations and shear conditions." Colloids and Surfaces B: Biointerfaces **165**: 127-134.

Almeida, E., T. C. Diamantino and O. de Sousa (2007). "Marine paints: the particular case of antifouling paints." Progress in Organic Coatings **59**(1): 2-20.

Amara, I., W. Miled, R. B. Slama and N. Ladhari (2018). "Antifouling processes and toxicity effects of antifouling paints on marine environment. A review." Environmental toxicology and pharmacology **57**: 115-130.

Bannister, J., M. Sievers, F. Bush and N. Bloecher (2019). "Biofouling in marine aquaculture: a review of recent research and developments." Biofouling **35**(6): 631-648.

Basu, S., B. M. Hanh, J. I. Chua, D. Daniel, M. H. Ismail, M. Marchioro, S. Amini, S. A. Rice and A. Miserez (2020). "Green biolubricant infused slippery surfaces to combat marine biofouling." Journal of colloid and interface science **568**: 185-197.

Breinlinger, S., T. J. Phillips, B. N. Haram, J. Mareš, J. A. M. Yerena, P. Hrouzek, R. Sobotka, W. M. Henderson, P. Schmieder and S. M. Williams (2021). "Hunting the eagle killer: A cyanobacterial neurotoxin causes vacuolar myelinopathy." Science 371(6536).

de Carvalho, C. C. (2018). "Marine biofilms: a successful microbial strategy with economic implications." Frontiers in Marine Science **5**: 126.

Delauney, L., C. Compere and M. Lehaitre (2010). "Biofouling protection for marine environmental sensors." Ocean Science **6**(2): 503-511.

Eduok, U., O. Faye and J. Szpunar (2017). "Recent developments and applications of protective silicone coatings: A review of PDMS functional materials." Progress in Organic Coatings **111**: 124-163.

Faria, S. I., R. Teixeira-Santos, M. J. Romeu, J. Morais, V. Vasconcelos and F. J. Mergulhão (2020). "The Relative Importance of Shear Forces and Surface Hydrophobicity on Biofilm Formation by Coccoid Cyanobacteria." Polymers **12**(3): 653.

Jamal, M., W. Ahmad, S. Andleeb, F. Jalil, M. Imran, M. A. Nawaz, T. Hussain, M. Ali, M. Rafiq and M. A. Kamil (2018). "Bacterial biofilm and associated infections." Journal of the Chinese Medical Association **81**(1): 7-11.

King, R. K., G. J. Flick, S. A. Smith, M. D. Pierson, G. D. Boardman and C. W. Coale (2006). "Comparison of bacterial presence in biofilms on different materials commonly found in recirculating aquaculture systems." Journal of Applied Aquaculture **18**(1): 79-88.

Lacoursière-Roussel, A., B. M. Forrest, F. Guichard, R. F. Piola and C. W. McKindsey (2012). "Modeling biofouling from boat and source characteristics: a comparative study between Canada and New Zealand." Biological invasions **14**(11): 2301-2314.

Mathew, N. T., J. Kronholm, K. Bertilsson, M. Despeisse and B. Johansson (2021). Environmental and Economic Impacts of Biofouling on Marine and Coastal Heat Exchangers. EcoDesign and Sustainability II. Springer: 385-398.

Miller, R. J., A. S. Adeleye, H. M. Page, L. Kui, H. S. Lenihan and A. A. Keller (2020). "Nano and traditional copper and zinc antifouling coatings: metal release and impact on marine sessile invertebrate communities." Journal of Nanoparticle Research **22**: 1-15.

Neves, A. R., J. R. Almeida, F. Carvalhal, A. Câmara, S. Pereira, J. Antunes, V. Vasconcelos, M. Pinto, E. R. Silva and E. Sousa (2020). "Overcoming environmental problems of biocides: Synthetic bile acid derivatives as a sustainable alternative." Ecotoxicology and environmental safety **187**: 109812.

Rao, T. (2010). "Comparative effect of temperature on biofilm formation in natural and modified marine environment." Aquatic Ecology **44**(2): 463-478.

Romeu, M. J., P. Alves, J. Morais, J. M. Miranda, E. D. de Jong, J. Sjollema, V. Ramos, V. Vasconcelos and F. J. Mergulhão (2019). "Biofilm formation behaviour of marine filamentous cyanobacterial strains in controlled hydrodynamic conditions." Environmental microbiology **21**(11): 4411-4424.

Romeu, M. J., D. Domınguez-Pérez, D. Almeida, J. Morais, A. Campos, V. Vasconcelos and F. J. Mergulhão (2020). "Characterization of planktonic and biofilm cells from two filamentous cyanobacteria using a shotgun proteomic approach." Biofouling **36**(6): 631-645.

Silva, E., O. Ferreira, P. Ramalho, N. Azevedo, R. Bayón, A. Igartua, J. Bordado and M. Calhorda (2019). "Eco-friendly non-biocide-release coatings for marine biofouling prevention." Science of the Total Environment **650**: 2499-2511.

Silva, E. R., A. V. Tulcidas, O. Ferreira, R. Bayón, A. Igartua, G. Mendoza, F. J. Mergulhão, S. I. Faria, L. C. Gomes and S. Carvalho (2021). "Assessment of the environmental compatibility and antifouling performance of an innovative biocidal and foul-release multifunctional marine coating." Environmental Research **198**: 111219.

Tian, L., Y. Yin, H. Jin, W. Bing, E. Jin, J. Zhao and L. Ren (2020). "Novel marine antifouling coatings inspired by corals." Materials Today Chemistry **17**: 100294.

Vladkova, T., D. Akuzov, A. Klöppel and F. Brümmer (2014). "Current Approaches to Reduction of Marine Biofilm Formation." Journal of Chemical Technology & Metallurgy **49**(4).

Zecher, K., V. P. Aitha, K. Heuer, H. Ahlers, K. Roland, M. Fiedel and B. Philipp (2018). "A multi-step approach for testing non-toxic amphiphilic antifouling coatings against marine microfouling at different levels of biological complexity." Journal of microbiological methods **146**: 104-114.

2.

Literature review

2.1. Biofouling development

Marine biofouling is an undesirable natural process in which submerged marine structures, including ship hulls, oil production platforms, oceanographic instrumentation, heat exchangers, and aquaculture systems, are attached by different molecules and colonized by marine organisms (Carteau et al. 2014, Caruso 2020, Selim et al. 2017). This process occurs spontaneously in marine environments and involves two major groups of organisms – micro- and macrofouling organisms – divided according to their size (Abioye et al. 2019), which participate in different stages of biofouling development (Selim et al. 2017, Telegdi et al. 2016). While microfouling organisms such as bacteria, cyanobacteria, and diatoms, are the first colonizers of underwater surfaces and lead to biofilm formation (Arrhenius et al. 2014), macrofouling organisms, including bryozoans, molluscs, polychaeta, coelenterates, and fungi, settle later and form mature fouling communities (Menesses et al. 2017, Telegdi et al. 2016). The diversity and prevalence of fouling organisms are dependent on geographic location and seasonal variations (Salta et al. 2013).

Marine biofouling involves several consecutive steps and is modulated by different factors related to both environmental conditions and the physical-chemical nature of the substrates (Caruso 2020). In particular, in ship hulls, there is a wide diversity of materials and structures that are prone to biofouling development (Salta et al. 2013) (Figure 2.1. A).

The surface colonization process is described as a succession of three main stages, as shown in Figure 1B: conditioning film formation, surface colonization and biofilm formation

by microfouling organisms (microfouling), and settlement of macrofouling organisms (macrofouling) (Caruso 2020, Salta et al. 2013).

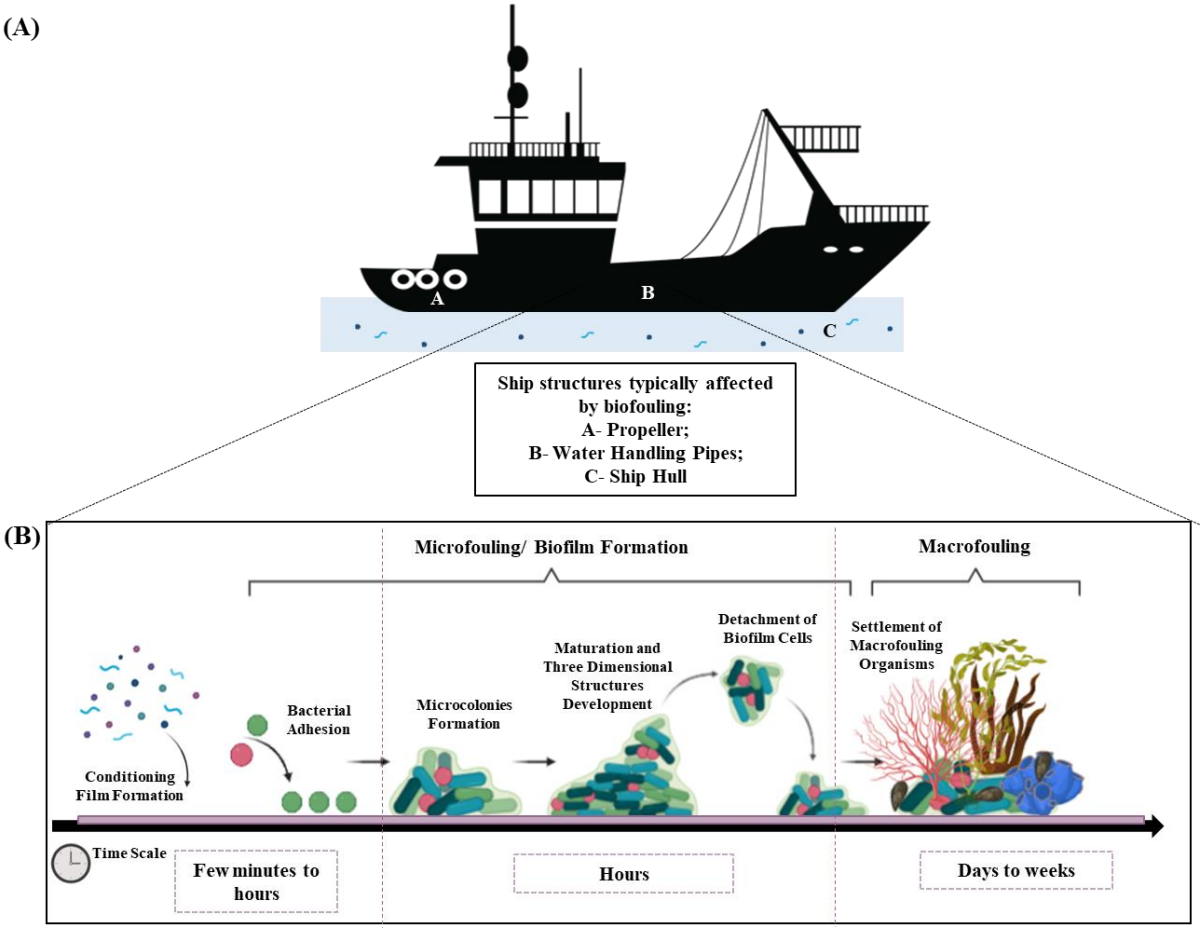

Figure 2.1. Schematic representation of (A) ship structures typically prone to biofouling and (B) main stages of biofouling development (adapted from Antunes et al. 2019, Vinagre et al. 2020).

Submerged surfaces rapidly adsorb organic molecules that are dissolved in the surrounding aquatic environment forming conditioning films (Vinagre et al. 2020). These are mostly composed of glycoproteins, proteoglycans, and polysaccharides, which facilitate the initial attachment of microfouling organisms (Caruso 2020, Flemming and Wingender 2010, Selim et al. 2017) (Figure 2.1. B). At the initial stage of surface colonization, the pioneer species produce biomolecules that favour microbial adhesion to the substrate (Caruso 2020). Cell attachment to marine surfaces is a reversible process that occurs through microbial appendages and weak physical forces, such as Van der Waals forces and hydrogen

bonds (Telegdi et al. 2016). Subsequently, when cell attachment becomes irreversible, the formation of microcolonies by pioneer species builds a suitable substrate for colonization by other microfouling organisms leading to biofilm formation (Figure 2.1. B). When the biofilm reaches its maturation stage presenting three-dimensional structures, the nutritional competition among microfouling organisms leads to cell death and/or detachment of biofilm cells which are transported by flow and colonize other surface locations (Caruso 2020), allowing biofilm proliferation (Arunasri and Mohan 2019, Jamal et al. 2018, Kumar et al. 2017) (Figure 2.1. B).

Biofilm formation is the first step in biofouling development, constituting the substrate for the colonization and settlement of macrofouling organisms (Caruso 2020). The microbial communities that initially attach to marine surfaces are important drivers of the biofouling process, influencing its later stages (Salta et al. 2013). Within days to weeks, macrofouling organisms settle and form macrofouling communities (Figure 2.1. B), creating microhabitats that favor further settlements. Biofouling communities reach their maturity within a few years, increasing their species diversity and richness (Vinagre et al. 2020).

The influence of biofilms on the settlement of macrofouling organisms is modulated by the spatial and temporal heterogeneity of marine environments, which suffer changes in terms of hydrodynamics, topography, nutrients and organic matter availability, and biological dispersal and aggregation at the level of microhabitats (Caruso 2020).

2.1.1. Marine biofilms

Since biofilm formation is the initial colonization stage of marine biofouling, building the basis and driving later settlement by macrofouling organisms, it deserves particular attention.

Marine biofilms consist of organized communities of mixed microfouling organisms, surrounded by a self-produced matrix of EPS, whose composition depends on the microbial interactions with environmental factors (Antunes et al. 2019, Salta et al. 2013). EPS has a significant role in microbial adhesion, acting as a glue, as well as in cohesion and protection of biofilms against environmental alterations (Bruno and Valle 2017, Telegdi et al. 2016). In

addition to EPS and microorganisms, biofilms are also composed of water (75-90%) and organic and inorganic compounds (Jamal et al. 2018, Telegdi et al. 2016).

Biofilm formation results from both cell-surface and cell-cell interactions. In turn, cell-to-cell communication is mediated by quorum sensing (QS) mechanisms involving signaling molecules called autoinducers, which command diverse cellular processes, including cell division and growth (Jamal et al. 2018, Selim et al. 2017).

Biofilm structure is extensively characterized by its heterogeneity and by the presence of pores, or empty spaces, which allow nutrient flow and confer to cells a higher resistance to physical and chemical stresses, including pH changes, ultraviolet (UV) radiation, osmotic shock, desiccation, and antimicrobial effect of biocides (Selim et al. 2017). In general, biofilms are dynamic systems that include different structural and functional complexity levels, which are constantly changing in response to marine environmental variations (Antunes et al. 2019, Arunasri and Mohan 2019, Caruso 2020, Jamal et al. 2018).

Although marine biofilms are composed of a vast diversity of marine species, bacteria, diatoms, and cyanobacteria are typically initial colonizers and boosters of biofilm development (Antunes et al. 2019, Arrhenius et al. 2014). In particular, cyanobacteria are found to be the most important colonizers of marine surfaces being able to determine the structure and function of mature biofilms (de Carvalho 2018). Cyanobacteria are prokaryotic photoautotrophic bacteria with a large variety of species and diverse morphology. These microorganisms exist in filamentous and coccoid forms and can be found in practically all habitats in the world (e.g., rocks, soils, forests, lakes, reservoirs, ice, desert, etc.) due to their high adaptability to a wide range of environmental conditions (Brito et al. 2012, Popović et al. 2016). The successful adaptation of cyanobacteria is largely due to their morphology, functional versatility, and capability to produce large amounts of EPS, which allow them to maintain the biofilm structure and contribute to a higher attachment of microbial cells on marine surfaces (Brito et al. 2012). The initial attachment of these organisms modifies surface properties and influences the attachment of subsequent colonizers (Antunes et al. 2019).

Several factors related to environmental conditions and substrate surface nature have been indicated as modulators of microbial adhesion and biofilm development (Caruso 2020, Doiron et al. 2018). The biotic factors are related to the biology of the different microfouling organisms and their specific interactions, which will dictate how biofilm development occurs

on submerged marine surfaces (Vinagre et al. 2020). In turn, the abiotic factors include the physical-chemical features of aquatic environments, such as temperature, salinity, pH, nutrient concentration, and light availability (Caruso 2020). Besides, hydrodynamic conditions and surface properties have been described as one of the most relevant factors affecting adhesion and marine biofilm formation on the initial stage and its structure in maturation phases (Flemming and Wingender 2010, Romeu et al. 2019, Telegdi et al. 2016).

2.1.1.1. Influence of hydrodynamic conditions

In marine environments, biofilms are exposed to a wide range of hydrodynamic conditions, which depend on their geographical location associated with the movement of the waves and/or tidal currents (Shields et al. 2011). The hydrodynamic forces influence not only the diffusional flow of nutrients and oxygen supply, but also modulate microbial cell adhesion and biofilm development on a given surface (Busscher and van der Mei 2006, Catão et al. 2019, Chang et al. 2020, Risse-Buhl et al. 2017, Simoes et al. 2007). Moreover, hydrodynamic also affect the composition and architecture of marine biofilms (Catão et al. 2019, Chang et al. 2020, Risse-Buhl et al. 2017). In fact, shear forces have been associated with biofilm mass transfer, growth rate, EPS production, energy metabolism, cell concentration, detachment, and the occurrence of genetic and/or molecular modifications during biofilm development (Catão et al. 2019, Krsmanovic et al. 2020, Moreira et al. 2015, Paul et al. 2012, Romeu et al. 2020, Romeu et al. 2021).

Several studies have shown that biofilms developed under higher shear forces are thinner and display a lower concentration of microfouling organisms. However, biofilm cells are strongly adhered and there are few pores or empty spaces in the biofilm structure (Chang et al. 2020, Horn et al. 2003, Howell 2009, Rickard et al. 2004, Tsai 2005). Higher flow rates, are usually associated with high shear forces and higher diffusional flux of nutrients, that increase erosion and detachment of biofilm portions, thus decreasing the amount of biomass attached to surfaces (Catão et al. 2019, Chang et al. 2020, Risse-Buhl et al. 2017). On the other hand, a higher transport of nutrients within the biofilm channels facilitates the growth of microorganisms that do not have direct access to the nutrients, contributing to a higher microbial development and EPS production (Eberl et al. 2000).

In opposition, biofilms developed at lower shear forces present higher species diversity, diffusivity, and cell density (Chang et al. 2020, Horn et al. 2003, Howell 2009, Rickard et al. 2004, Tsai 2005).

In general, hydrodynamic studies show that fluid flow velocity modulates biofilm formation at different levels during its development (Howell 2009, Krsmanovic et al. 2020, Rickard et al. 2004, Tsai 2005).

2.1.1.2. Influence of surface properties

The biofilm formation process begins with the attachment of planktonic microbial cells to submerged substrate surfaces (Caruso 2020, Flemming and Wingender 2010, Jamal et al. 2018, Selim et al. 2017). Microorganisms easily adhere to marine surfaces since they confer protection against adverse environmental conditions and facilitate access to nutrients and light (Doiron et al. 2018). However, surface properties, including roughness, wettability, hydrophobicity, surface polarization, and tension may affect the extension of microbial adhesion and, consequently, biofilm formation (Caruso 2020, Kuliasha et al. 2019, Palmer et al. 2007, Telegdi et al. 2016, Wilhelm et al. 2014).

Surface properties exert a greater impact, particularly during the early stages of biofilm development, where cell-surface interactions are very important (Zang et al. 2015, Wang et al. 2021). The physical-chemical properties of marine surfaces can, affect the chemistry of the water-substratum interface, influencing the formation and composition of conditioning films. The formation of these films can change surface properties, affecting the diversity and density of microorganisms present on the substratum and thus facilitating biofilm formation (Hwang et al. 2012, Lorite et al. 2011, Talluri et al. 2020, Vinagre et al. 2020, Wang et al. 2021). However, the microorganisms' response to surface materials depends on other factors such as species, temperature, and depth (Vinagre et al. 2020). Subsequently, during biofilm development, the impact of surface properties is attenuated since the surface is progressively covered by microorganisms and other biofilm components (Wang et al. 2021).

Several studies have demonstrated that surface topography and roughness influences the physical and environmental conditions presented to microorganisms (Dantas et al. 2016,

De-la-Pinta et al. 2019, Vinagre et al. 2020). It is known that more heterogeneous substrata display a larger surface area, allowing to accommodate a greater density and diversity of microorganisms with low competition between species, and protect them from adverse environmental conditions (Caruso 2020, Vinagre et al. 2020). In turn, surfaces displaying lower roughness are directly related to low microbial adhesion (Dantas et al. 2016). Also, surface hydrophobicity influences the initial microbial attachment (Cerca et al. 2005). Several authors have demonstrated that the adhesion to hydrophobic and non-polar substrata (e.g., teflon, silicone and plastics) occurs to a greater extent than that to hydrophilic surface materials like metals and glass (Caruso 2020, Cerca et al. 2005, Donlan 2002, Jamal et al. 2018, Vinagre et al. 2020). However, since microbial adhesion depends on several biotic and abiotic factors, it is not possible to establish a direct association between surface properties and the adhesion strength of microorganisms.

2.2. Economic and environmental impacts of marine biofouling

Biofouling is one of the major challenges faced by the marine industry, having severe economic and environmental implications worldwide (Kuliasha et al. 2019, Silva et al. 2019, Tian et al. 2020). This natural phenomenon is responsible for a considerable number of undesirable effects, including increased marine shipping and maintenance costs, increased fuel consumption and carbon dioxide (CO_2) emission, and the introduction of exotic species into local ecosystems (Kuliasha et al. 2019).

A wide diversity of marine structures, such as ship hulls, oil production platforms, aquaculture systems, and industrial water inlet systems (Caruso 2020, Silva et al. 2019, Tian et al. 2020), can be easily colonized and damaged by fouling organisms, leading to substantial economic losses for marine industries (Table 2.1.) (Tian et al. 2020). Similarly, biofouling can cause incorrect measurements in underwater equipment such as devices or sensors (Delgado et al. 2021, Romeu et al. 2019, Tian et al. 2020). Moreover, fouling organisms attached to marine vessel hulls accelerate surface corrosion, resulting in higher dry-docking periods and maintenance costs (Kuliasha et al. 2019, Tian et al. 2020, Zhu et al. 2020). In addition, biofouling development increases drag resistance and, consequently, decreases

vessel speed (Basu et al. 2020, Neves et al. 2020, Silva et al. 2019). As such, higher fuel consumption is required to attain reasonable cruise speeds, increasing GHG emissions and atmospheric pollution (Neves et al. 2020, Silva et al. 2019). According to the International Maritime Organization (IMO), without preventive and/or corrective actions, gas emissions from world shipping fleets could increase from 150% to 250% by 2050, compared to the emissions in 2007 (IMO 2009) and, in an extreme scenario, the CO_2 emissions can even double by 2030, posing serious environmental problems (IMO, 2009, Silva et al. 2019). Marine biofouling is also associated with the introduction of non-indigenous species traveling in marine vessels (ships, yachts, or sailing boats) between different geographic areas into local ecosystems, which play a negative impact on global diversity (Lacoursière-Roussel et al. 2016, Mineur et al. 2007, Neves et al. 2020). This process is aggravated at both community (species richness) and population (genetic diversity) levels by the intense shipping activity in ports (Lacoursière-Roussel et al. 2016, Neves et al. 2020). The negative impact of bio-invasion promoted by biofouling has motivated marine conservation entities to investigate strategies to reduce the introduction and spread of fouling species in local ecosystems. In 2015, the European regulation on invasive alien species (IAS), regulation 1143/2014), entered into force, setting out rules to prevent, minimize and mitigate the adverse impacts caused by invasive species through the study of their introduction routes and spread (Vinagre et al. 2020). Likewise, in other countries, strict regulations and control measures have already been implemented to maintain the vessel hulls clean (Georgiades and Kluza 2017, Hellio and Yebra 2009, McClay et al. 2015, Zecher et al. 2018). However, regular cleaning procedures are also associated with significant costs for the marine sector (Zecher et al. 2018).

Overall, the economic and environmental consequences of marine biofouling have prompted research on AF strategies that inhibit microbial colonization and consequent biofilm formation.

Table 2.1. Estimated economic losses caused by biofouling for marine industries (Adapted from de Carvalho, 2018).

INDUSTRY	PROBLEM	ESTIMATED COST	REFERENCES
Aquaculture	Biofouling on marine facilities (aquaculture nets, offshore oil platforms and ship hulls)	1.5 - 3 billion U.S dollars per year	(Fitridge et al. 2012, Schultz et al. 2011)
	Biofouling on fish cages and shellfish harvesting sites	5-10% of the industry value in Europe (approximately 260 million euros per year)	(Lane and Willemsen 2004)
	Replacement of cages and application of AF compounds	Approximately 120.000 euros per year	(Willemsen 2005)
Oil and gas industry	Microbial corrosion.	20-30% of corrosion-related costs	(Skovhus et al. 2017)
Maritime transport	Effects in hydrodynamic performance (increased drag resistance)	35-50% increased fuel consumption	(Flemming and Wingender 2010, Schultz et al. 2011)
	Biofouling of ballast water tanks with non-indigenous species	1.6-4% of annual operating costs for a ship	(Fernandes et al. 2016)
	Coating and Cleaning procedures	56 million euros per year	(Schultz et al. 2011)
	Activities related to invasive species (cleaning procedures and regulation implementation)	513.9 million dollars in 1999 and 631.5 million dollars in 2000	(Warziniack et al. 2021)
Water desalination	Biofouling of reverse osmosis membranes	5-20% of operational costs for cleaning	(Flemming 1997, Maddah and Chogle 2017)
Miscellaneous-Heat exchanger	Decreased heat transfer and induced corrosion	Approximately 7.5% of maintenance costs of a process plant	(Ibrahim 2012)

2.3. Antifouling strategies

In the last decades, numerous efforts have been made to develop efficient marine AF strategies to inhibit biofilm formation by microfouling organisms since it precedes settlement by macrofouling organisms, thus decreasing biofouling development and its undesirable consequences (Delgado et al. 2021, Jayaprakashvel et al. 2020, Silva et al. 2019).

One of the most successful coatings throughout history was the self-polishing copolymer coatings containing tributyltin (TBT), which have not only highly effective AF properties but also are self-polishing and smoothing (Howell and Behrends 2010). Although TBT was developed about 150 years ago, it only was applied as an AF agent in the early 1970s, in combination with several copper compounds (Batista-Andrade et al. 2018, Han et al. 2021, Howell and Behrends 2010, Ulaeto et al. 2017). However, rapidly TBT was found to be toxic for non-target organisms and able to persist for long periods in the aquatic environment (Batista-Andrade et al. 2018, Han et al. 2021, Hellio and Yebra 2009, Howell and Behrends 2010, Ulaeto et al. 2017), and in 2008, IMO banned its use (Howell and Behrends 2010). Beyond its negative environmental impact, several authors have found that TBT causes adverse effects to the human body due to its bioaccumulation on the marine environment and its potential biomagnification in the food webs (Antizar-Ladislao 2008). In addition to TBT, other toxic agents for marine organisms and human health have also been banned (Delgado et al. 2021).

In this context, the desirable characteristics of a marine AF coating are to be effective against a wide range of fouling organisms at the site of release (e.g., ship hulls), but non-toxic to non-target organisms, as well as present high degradation in the marine environment and a low bioaccumulation rate (Howell and Behrends 2010). Therefore, the development of non-toxic, environmentally-friendly, inexpensive, and efficient antifouling coatings is urgent (Selim et al. 2017, Tian et al. 2020).

Given the growing concern on the harmful side effects of non-natural biocidal coating on the environment, three main strategies have been applied in designing environmental-friendly AF coatings (Table 2.2.): (1) matrix-degrading and killing of fouling organisms; (2) fouling resistance (preventing the attachment of fouling organisms); (3) fouling release (reducing the strength of adhesion of fouling organisms).

2.3.1. Natural biocide-based coatings

Natural products and metabolites from a large variety of microorganisms and biological resources have been investigated as promising AF agents able to control marine biofouling development (Cui et al. 2014, Jayaprakashvel et al. 2020, Vilas-Boas et al. 2020). Coatings based on the biocidal activity of natural compounds may be grouped into three categories according to their release mechanisms: i) contact leaching coatings; ii) controlled depletion polymer coatings; and iii) self-polishing copolymer coatings. Among them, enzymatic AF coatings have been extensively explored over the past 20 years, and their mode of action consists of the application of biocidal or adhesive enzymes and enzymatic generation of biocides from substrates or coating compounds (Pradhan et al. 2019). Compared to organometallic AF agents, enzymes have more advantages, including high efficiency and biodegradability (Wang et al. 2019). Several authors have already demonstrated that enzymes produced by marine organisms have evident inhibitory effects on biofilm formation by diatoms (Table 2.2.) (Essock-Burns et al. 2016, Wang et al. 2019). However, it is difficult to obtain sufficient amounts of these AF agents from the ocean and their chemical synthesis is expensive, which may impair their massive application on marine structures (Gu et al. 2020).

2.3.2. Fouling-resistant coatings

Fouling-resistant coatings are essentially composed of amphiphilic polymers, which present low polymer-water interfacial energies conferring higher resistance to protein adsorption and settlement of fouling organisms (Hu et al. 2020, Selim et al. 2017). Several hydrophilic polymer coatings, including polyethylene glycol (PEG), hydrogel, zwitterionic, and hyperbranched polymers (Table 2.2.), have been developed in the last years as marine AF coatings (Hu et al. 2020, Selim et al. 2017).

Polyethylene materials have been explored due to their ability to increase surface hydrophilicity and decrease the attraction forces with fouling organisms by the formation of hydrogen bonds with water (Misdan et al. 2016, Pradhan et al. 2019, Selim et al. 2017). PEG

is a non-toxic, highly hydrophilic, and neutrally charged compound (Selim et al. 2017). Currently, a typical strategy to prevent protein adhesion and fouling organisms attachment is the employment of PEG nanocomposites (Table 2.2.). Sham et al. developed a PEG-polydimethylsiloxane (PDMS) composite that reduced the viability of adhered bacteria by 4 Log (Sham et al. 2017).

Likewise, hydrogels composed of hydrophilic polymer networks and with high water content (80%) are effective in inhibiting protein adhesion (Selim et al. 2017). In addition, hydrogels are non-toxic, highly elastic, and inert against bio-macromolecule adhesion. In 2008, Ekblad et al. demonstrated that PEG-hydrogel composites were able to reduce the cell density of green algae and diatoms by 95% compared to glass surfaces (Ekblad et al. 2008).

In the last decade, zwitterionic polymers have been widely explored as a new generation of fouling-resistant materials because of their excellent hydration capacity combined with strong hydrophilicity (Pradhan et al. 2019, Selim et al. 2017). However, although there are few studies about the performance of zwitterionic polymers in inhibiting biofilm formation, Hibbs et al. demonstrated that this type of coating provides minimal resistance against bacterial biofilm formation but facilitates the removal of attached microbial biomass by exposure to a water-jet apparatus that generated hydrodynamic shearing forces (Hibbs et al. 2015).

Lastly, highly branched coatings with hydrophilic terminals have also been explored to confer biofouling resistance to surfaces. In fact, hyperbranched composites provide surfaces with compositional and topographical complexities that hamper interactions with adhesive biomolecules secreted by marine organisms (Selim et al. 2017). In 2016, Pranantyo et al. demonstrated that the hyperbranched polyglycerol (HPG) coatings significantly reduced the adhesion and biofilm formation of marine bacteria and that bacterial adhesion was dependent on coating density and surface hydrophilicity (Pranantyo et al. 2016).

2.3.3. Fouling-release coatings

Fouling release coatings (FRC) have been presented as successful alternatives that inhibit the attachment of marine organisms by conferring to surfaces low drag resistance and high smooth topology, which hinders the interaction between organisms and surface (Selim

et al. 2017). Thus, the attached organisms can be rapidly removed by the water shear force coming from mechanical cleaning or for the shear forces of the ship's navigation (Hu et al. 2020). Several authors have demonstrated that these coatings are able to inhibit the biofilm development by different microorganisms typically found in the marine environment (Dobretsov and Thomason 2011, Martinelli et al. 2011, Selim et al. 2016, Selim et al. 2019)

The currently used FRC are fluoropolymers and silicone-based coatings, such as superhydrophobic coatings, photo-induced coatings and amphiphilic coatings (Hu et al. 2020, Selim et al. 2017).

Fluoropolymers form non-porous and smooth surfaces with low surface tension and good antiadhesive properties against fouling organisms. Dobretsov and Thomason developed a commercial fluoropolymer coating, Intersleek 900, which was able to significantly reduce the number of adhered cells of marine bacteria (Dobretsov and Thomason 2011).

In turn, silicone-based coatings are characterized by their superior anti-fouling properties, surface inertness, hydrophobicity, and high heat resistance. The mode of action of these coatings consists of decreasing the interfacial tension of the surface and enhancing its hydrophobicity and self-cleaning performance (Selim et al. 2017).

Super hydrophobic FRC gained worldwide attention due to their easy cleaning, non-stick, and eco-friendly characteristics, and high potential to repel water (superhydrophobic or lotus effect, e.g., biomimetic surfaces). Selim et al. developed a superhydrophobic FR β-MnO_2 nanocomposite which was capable to significantly reduce the number of viable adhered cells compared to control (PDMS). The high performance of the β-MnO_2 nanocomposite was achieved due to suitable roughness, superhydrophobicity and low free energy of surface (Selim et al. 2019).

Photo-induced coatings change their wettability by UV light exposure, decreasing fouling settlement and maintenance costs by reducing the surface free energy for self-cleaning operations (Selim et al. 2017). Selim et al. demonstrated that TiO_2 nanocomposites induced by UV light radiation displayed biofilms with low surface coverage compared to control (PDMS blank) (Selim et al. 2016).

Lastly, amphiphilic coatings combine hydrophilic and hydrophobic materials providing surfaces with high antifouling properties (Selim et al. 2017). In 2017, Bucs et al. synthetized a hydrophilic hydroxyethyl methacrylate (HEMA) and hydrophobic

perfluorodecyl acrylate (PFA) coating that decreased 6-fold the biomass of marine biofilms and affected their composition (lower polysaccharide and higher protein content than the control (Bucs et al. 2017).

Although there are a wide diversity of available AF strategies, the efficacy of most of them is not well characterized concerning biofilm prevention and control, and further research is needed in this field.

Table 2.2. Main future directions of marine antifouling coatings that aim to inhibit biofilm formation.

Strategy	Antifouling compounds/Coatings	Mechanism of action	Composites	Major Conclusions	Ref.
Matrix-degrading and killing of fouling organisms	**Enzyme-based coatings**	Release of active molecules embedded in a polymer matrix.	Proteases	Proteases have a significant effect on the decomposition of barnacle cement and diatom secretion.	(Wang et al. 2019)
			Amylase, trypsin and lysozyme	Enzymes effectively remove the biofilm of diatoms (60 – 90%).	(Essock-Burns et al. 2016)
Fouling resistant	**Amphiphilic polymer**				
	PEG	Increase surface hydrophilicity and minimize attraction forces with fouling organisms.	PEG-PDMS composites	Marine bacteria adhered to PEG-PDMS films reduced their viability by 4 Log.	(Sham et al. 2017)
	Hydrogel	Decrease protein adhesion avoiding fouling attachment.	PEG-based hydrogel	The density of green algae and diatoms cells on the hydrogel surface was reduced by 95% compared to glass.	(Ekblad et al. 2008)
	Zwitterionic	These polymers comprise positive and negative charges, establishing potent and stable ionic bonds with water molecules and increasing surface hydrophilicity.	Polysulfone and polyacrylate-based zwitterionic coatings	The zwitterionic polymer coatings provided minimal resistance against bacterial biofilm retention and microalgal cell attachment but facilitated the removal of attached microbial biomass.	(Hibbs et al. 2015)

Strategy	Antifouling Compounds/Coatings	Mechanism of action	Composites	Major Conclusions	Ref.
Fouling resistant	Hyperbranched polymers	Form extremely hydrophilic surfaces with high compositional and topographical complexities that hamper any interactions with adhesive biomolecules secreted by marine organisms.	HPG	HPG modified surfaces significantly reduced the adhesion of Gram-negative and -positive marine bacteria and inhibited biofilm formation (10-fold).	(Pranantyo et al. 2016)
Fouling release coatings	**Fluoropolymers**	Produce non-porous and smooth surfaces with low surface tension and good anti-adhesion performance toward fouling organisms; these coatings also create a weak interface with adhesive molecules and thus fouling attachment can be disrupted by shear stress.	Fluoropolymer coating (Intersleek 900)	Biofilms developed on Intersleek 900-coated surfaces were significantly thinner and showed lower bacterial density compared to control (tie coat).	(Dobretsov and Thomason 2011)
	Silicone-based coatings				
	Superhydrophobic FR paints	Decrease surface friction resistance.	β-MnO_2 nanocomposites	The number of adhered viable cells was lower for β-MnO_2 nanocomposite than for PDMS (control).	(Selim et al. 2019)
	Photo-induced superhydrophilic coatings	Increase surface hydrophilicity by UV light irradiation decreasing fouling settlement.	Nanocomposites of TiO_2 photo-induced by UV light radiation	Photo-induced nanocomposites reduced biofilm surface coverage.	(Selim et al. 2016)

Strategy	Antifouling compounds/Coatings	Mechanism of action	Composites	Major Conclusions	Ref.
	Silicone-based coatings				
Fouling release coatings	Amphiphilic coatings	Combines hydrophilic and hydrophilic materials improving surface fouling-prevention characteristics.	Amphiphilic copolymers (HEMA and PFA)	Inhibition of marine biofilm development composition (6 times lower active biomass than control) and affected biofilm composition (23% lower polysaccharide and 132% higher protein content than control).	(Bucs et al. 2017)

2.3.4. Laboratory tests

The most reliable method for testing the AF performance of marine surfaces is the immersion of samples in the ocean. However, sea trials require long periods to collect data, are dependent on sample location and the time of year, and may be expensive and ecologically toxic for non-target marine organisms (Briand 2009, Salta et al. 2010, Zecher et al. 2018). In this context, alternative methods have been developed to evaluate the performance of antifouling surfaces under laboratory conditions that mimic marine environments. Given the vast diversity of microfouling organisms and biological factors underlying their attachment in marine scenarios (Stafslien et al. 2011), several parameters should be considered when designing laboratory assays, including microorganisms species, temperature, and hydrodynamic conditions (Briand 2009).

The selection of fouling organisms plays a significant role in laboratory assays since the microfouling process begins with the attachment of early colonizers, which rapidly form microfouling communities composed of a wide diversity of organisms. Between the early colonizer organisms, cyanobacteria species are one of the most dominant bacterial phyla colonizing different surfaces at diverse locations, particularly in the early stages of colonization (de Carvalho 2018; Angelova et al. 2019). Several authors have shown that mixed biofilms exhibit enhanced resistance compared to single-species biofilms (Gomes et al. 2018, Lara and Lopez-Ribot 2020, Lobo et al. 2019). However, marine surfaces are typically tested against single-species biofilms (Briand 2009).

Hydrodynamics are one of the most important factors affecting the microorganism's attachment and biofilm development (Paul et al. 2012, Moreira et al. 2015, Catão et al. 2019). In marine environments, substrata surfaces are in contact with a wide range of hydrodynamic conditions according to their location, which is associated with wave's forces and movement (breaking waves) and/or tidal currents that affect the normal flow conditions (Shields et al. 2011). Thus, the hydrodynamic condition selection should take into account the real application of the AF surface under study in order to obtain representative results.

Although laboratory assays allow a better understanding of the dynamics of biofilm formation under conditions representative of real scenarios and some of them show a significant correlation with field assays, they are laborious and time-consuming, requiring on average 6 weeks to provide results (Romeu et al. 2019, Silva et al. 2021).

In order to overcome these limitations, short-term assays (2-48 h) have been developed as screening tools for AF marine surfaces (Stafslien et al. 2007, Salta et al. 2010, Stafslien et al. 2011). Most of these assays are based on the enumeration of attached cells by direct counting under a microscope after their staining (Briand 2009, Salta et al. 2010) or on the spectrophotometric or fluorometric quantification of chlorophyll (Briand 2009). Cell staining usually requires several methodological steps (e.g. cell fixation, staining and washing) to improve analysis specificity and sensitivity (Briand 2009, Salta et al. 2010). In turn, chlorophyll quantification may only be applied to chlorophyll-producing organisms (Stafslien et al. 2007, Briand 2009). Although these assays are very useful as screening tools, developing more accurate and simpler to perform alternative short-term assays is necessary.

Overall, the economic and environmental impact of marine biofouling and the limited effectiveness of available antifouling strategies continue to motivate research in this field in the development of preventive and control strategies at the level of marine biofilm formation.

2.4. References

Abioye, O. P., C. Loto and O. Fayomi (2019). "Evaluation of anti-biofouling progresses in marine application." Journal of Bio-and Tribo-Corrosion **5**(1): 22.

Angelova, A. G., G. A. Ellis, H. W. Wijesekera and G. J. Vora (2019). "Microbial Composition and Variability of Natural Marine Planktonic and Biofouling Communities From the Bay of Bengal." Frontiers in Microbiology **10**(2738).

Antizar-Ladislao, B. (2008). "Environmental levels, toxicity and human exposure to tributyltin (TBT)-contaminated marine environment. A review." Environment international **34**(2): 292-308.

Antunes, J., P. Leão and V. Vasconcelos (2019). "Marine biofilms: diversity of communities and of chemical cues." Environmental microbiology reports **11**(3): 287-305.

Arrhenius, Å., T. Backhaus, A. Hilvarsson, I. Wendt, A. Zgrundo and H. Blanck (2014). "A novel bioassay for evaluating the efficacy of biocides to inhibit settling and early establishment of marine biofilms." Marine pollution bulletin **87**(1-2): 292-299.

Arunasri, K. and S. V. Mohan (2019). Biofilms: Microbial life on the electrode surface. Microbial Electrochemical Technology. S. V. Mohan, S. Varjani and A. Pandey. Hyderabad, India, Elsevier**:** 295-313.

Basu, S., B. M. Hanh, J. I. Chua, D. Daniel, M. H. Ismail, M. Marchioro, S. Amini, S. A. Rice and A. Miserez (2020). "Green biolubricant infused slippery surfaces to combat marine biofouling." Journal of colloid and interface science **568**: 185-197.

Batista-Andrade, J. A., S. S. Caldas, R. M. Batista, I. B. Castro, G. Fillmann and E. G. Primel (2018). "From TBT to booster biocides: levels and impacts of antifouling along coastal areas of Panama." Environmental pollution **234**: 243-252.

Briand, J.-F. (2009). "Marine antifouling laboratory bioassays: an overview of their diversity." Biofouling **25**(4): 297-311.

Brito, A., V. Ramos, R. Seabra, A. Santos, C. L. Santos, M. Lopo, S. Ferreira, A. Martins, R. Mota and B. Frazao (2012). "Culture-dependent characterization of cyanobacterial diversity in the intertidal zones of the Portuguese coast: a polyphasic study." Systematic and Applied Microbiology **35**(2): 110-119.

Bruno, L. and V. Valle (2017). "Effect of white and monochromatic lights on cyanobacteria and biofilms from Roman Catacombs." International Biodeterioration & Biodegradation **123**: 286-295.

Bucs, S. S., R. V. Linares, N. Farhat, A. Matin, Z. Khan, M. C. van Loosdrecht, R. Yang, M. Wang, K. K. Gleason and J. C. Kruithof (2017). "Coating of reverse osmosis membranes with amphiphilic copolymers for biofouling control." Desalination and water treatment **68**: 1-11.

Busscher, H. J. and H. C. van der Mei (2006). "Microbial adhesion in flow displacement systems." Clinical microbiology reviews **19**(1): 127-141.

Carteau, D., K. Vallée-Réhel, I. Linossier, F. Quiniou, R. Davy, C. Compère, M. Delbury and F. Faÿ (2014). "Development of environmentally friendly antifouling paints

using biodegradable polymer and lower toxic substances." Progress in Organic Coatings **77**(2): 485-493.

Caruso, G. (2020). "Microbial colonization in marine environments: overview of current knowledge and emerging research topics." Journal of Marine Science and Engineering **8**(2): 78.

Catão, E. C., T. Pollet, B. Misson, C. Garnier, J.-F. Ghiglione, R. Barry-Martinet, M. Maintenay, C. Bressy and J.-F. Briand (2019). "Shear stress as a major driver of marine biofilm communities in the NW Mediterranean Sea." Frontiers in microbiology **10**: 1768.

Cerca, N., G. B. Pier, M. Vilanova, R. Oliveira and J. Azeredo (2005). "Quantitative analysis of adhesion and biofilm formation on hydrophilic and hydrophobic surfaces of clinical isolates of Staphylococcus epidermidis." Research in microbiology **156**(4): 506-514.

Chang, J., X. He, X. Bai and C. Yuan (2020). "The impact of hydrodynamic shear force on adhesion morphology and biofilm conformation of Bacillus sp." Ocean Engineering **197**: 106860.

Cui, Y. T., S. L. Teo, W. Leong and C. L. Chai (2014). "Searching for “environmentally-benign” antifouling biocides." International journal of molecular sciences **15**(6): 9255-9284.

Dantas, L. C. d. M., J. P. d. Silva-Neto, T. S. Dantas, L. Z. Naves, F. D. das Neves and A. S. da Mota (2016). "Bacterial adhesion and surface roughness for different clinical techniques for acrylic polymethyl methacrylate." International journal of dentistry **2016**.

de Carvalho, C. C. (2018). "Marine biofilms: a successful microbial strategy with economic implications." Frontiers in Marine Science **5**: 126.

De-la-Pinta, I., M. Cobos, J. Ibarretxe, E. Montoya, E. Eraso, T. Guraya and G. Quindós (2019). "Effect of biomaterials hydrophobicity and roughness on biofilm development." Journal of Materials Science: Materials in Medicine **30**(7): 1-11.

Delgado, A., C. Briciu-Burghina and F. Regan (2021). "Antifouling Strategies for Sensors Used in Water Monitoring: Review and Future Perspectives." Sensors **21**(2): 389.

Dobretsov, S. and J. C. Thomason (2011). "The development of marine biofilms on two commercial non-biocidal coatings: a comparison between silicone and fluoropolymer technologies." Biofouling **27**(8): 869-880.

Doiron, K., L. Beaulieu, R. St-Louis and K. Lemarchand (2018). "Reduction of bacterial biofilm formation using marine natural antimicrobial peptides." Colloids and surfaces B: Biointerfaces **167**: 524-530.

Donlan, R. M. (2002). "Biofilms: microbial life on surfaces." Emerging infectious diseases **8**(9): 881.

Eberl, H., C. Picioreanu, J. Heijnen and M. Van Loosdrecht (2000). "A three-dimensional numerical study on the correlation of spatial structure, hydrodynamic conditions, and mass transfer and conversion in biofilms." Chemical Engineering Science **55**(24): 6209-6222.

Ekblad, T., G. Bergström, T. Ederth, S. L. Conlan, R. Mutton, A. S. Clare, S. Wang, Y. Liu, Q. Zhao and F. D'Souza (2008). "Poly (ethylene glycol)-containing hydrogel surfaces for antifouling applications in marine and freshwater environments." Biomacromolecules **9**(10): 2775-2783.

Essock-Burns, T., A. Wepprich, A. Thompson and D. Rittschof (2016). "Enzymes manage biofilms on crab surfaces aiding in feeding and antifouling." Journal of Experimental Marine Biology and Ecology **479**: 106-113.

Fernandes, J. A., L. Santos, T. Vance, T. Fileman, D. Smith, J. D. Bishop, F. Viard, A. M. Queirós, G. Merino and E. Buisman (2016). "Costs and benefits to European shipping of ballast-water and hull-fouling treatment: Impacts of native and non-indigenous species." Marine Policy **64**: 148-155.

Fitridge, I., T. Dempster, J. Guenther and R. de Nys (2012). "The impact and control of biofouling in marine aquaculture: A review." Biofouling **28**(7): 649-669.

Flemming, H.-C. (1997). "Reverse osmosis membrane biofouling." Experimental thermal and fluid science **14**(4): 382-391.

Flemming, H.-C. and J. Wingender (2010). "The biofilm matrix." Nature reviews microbiology **8**(9): 623-633.

Georgiades, E. and D. Kluza (2017). "Evidence-based decision making to underpin the thresholds in New Zealand's craft risk management standard: biofouling on vessels arriving to New Zealand." Marine Technology Society Journal **51**(2): 76-88.

Gomes, L., J. Deschamps, R. Briandet and F. J. Mergulhão (2018). "Impact of modified diamond-like carbon coatings on the spatial organization and disinfection of mixed-

biofilms composed of Escherichia coli and Pantoea agglomerans industrial isolates." International journal of food microbiology **277**: 74-82.

Gu, Y., L. Yu, J. Mou, D. Wu, M. Xu, P. Zhou and Y. Ren (2020). "Research strategies to develop environmentally friendly marine antifouling coatings." Marine Drugs **18**(7): 371.

Han, X., J. Wu, X. Zhang, J. Shi, J. Wei, Y. Yang, B. Wu and Y. Feng (2021). "Special issue on advanced corrosion-resistance materials and emerging applications. The progress on antifouling organic coating: from biocide to biomimetic surface." Journal of Materials Science & Technology **61**: 46-62.

Hellio, C. and D. Yebra (2009). Advances in marine antifouling coatings and technologies. Cambridge, U.K., Woodshead Publishing. PART I: 17-31

Hibbs, M. R., B. A. Hernandez-Sanchez, J. Daniels and S. J. Stafslien (2015). "Polysulfone and polyacrylate-based zwitterionic coatings for the prevention and easy removal of marine biofouling." Biofouling **31**(7): 613-624.

Horn, H., H. Reiff and E. Morgenroth (2003). "Simulation of growth and detachment in biofilm systems under defined hydrodynamic conditions." Biotechnology and Bioengineering **81**(5): 607-617.

Howell, D. (2009). 17- Testing the impact of biofilms on the performance of marine antifouling coatings. Advances in marine antifouling coatings and technologies. C. Hellio and D. Yebra. Cambridge, UK, Woodhead Publishing Series in Metals and Surface Engineering**:** 422-442.

Howell, D. and B. Behrends (2010). Consequences of antifouling coatings–the chemist's perspective. Biofouling. S. Dürr and J. C. Thomason. Chichester, U.K. , Wiley-Blackwell**:** 226-242.

Hu, P., Q. Xie, C. Ma and G. Zhang (2020). "Silicone-based fouling-release coatings for marine antifouling." Langmuir **36**(9): 2170-2183.

Hwang, G., S. Kang, M. G. El-Din and Y. Liu (2012). "Impact of conditioning films on the initial adhesion of Burkholderia cepacia." Colloids and Surfaces B: Biointerfaces **91**: 181-188.

IMO-International Maritime Organization (2009). Prevention of Air Pollution From Ships, Second IMO Study on Greenhouse Gas (GHG) Emissions From Ships. MEPC 59/INF.10.

Ibrahim, H. A.-H. (2012). Fouling in heat exchangers. MATLAB-A Fundamental Tool for Scientific Computing and Engineering Applications-Volume 3. V. N. Katsikis. Rijeka, Croatia, InTech**:** 57-96.

Jamal, M., W. Ahmad, S. Andleeb, F. Jalil, M. Imran, M. A. Nawaz, T. Hussain, M. Ali, M. Rafiq and M. A. Kamil (2018). "Bacterial biofilm and associated infections." Journal of the Chinese Medical Association **81**(1): 7-11.

Jayaprakashvel, M., M. Sami and R. Subramani (2020). Antibiofilm, Antifouling, and Anticorrosive Biomaterials and Nanomaterials for Marine Applications. Nanostructures for Antimicrobial and Antibiofilm Applications. R. Prasad, B. Siddhardha and M. Dyavaiah. Gewerbestrasse, Switzerland, Springer**:** 233-272.

Krsmanovic, M., D. Biswas, H. Ali, A. Kumar, R. Ghosh and A. K. Dickerson (2020). "Hydrodynamics and surface properties influence biofilm proliferation." Advances in Colloid and Interface Science: 102336.

Kuliasha, C. A., R. L. Fedderwitz, J. A. Finlay, S. C. Franco, A. S. Clare and A. B. Brennan (2019). "Engineered Chemical Nanotopographies: Reversible Addition–Fragmentation Chain-Transfer Mediated Grafting of Anisotropic Poly (acrylamide) Patterns on Poly (dimethylsiloxane) To Modulate Marine Biofouling." Langmuir **36**(1): 379-387.

Kumar, A., A. Alam, M. Rani, N. Z. Ehtesham and S. E. Hasnain (2017). "Biofilms: Survival and defense strategy for pathogens." International Journal of Medical Microbiology **307**(8): 481-489.

Lacoursière-Roussel, A., D. G. Bock, M. E. Cristescu, F. Guichard and C. W. McKindsey (2016). "Effect of shipping traffic on biofouling invasion success at population and community levels." Biological Invasions **18**(12): 3681-3695.

Lane, A. and P. Willemsen (2004). "Collaborative effort looks into biofouling." Fish Farming Int **44**: 34-35.

Lara, H. H. and J. L. Lopez-Ribot (2020). "Inhibition of mixed biofilms of Candida albicans and methicillin-resistant Staphylococcus aureus by positively charged silver nanoparticles and functionalized silicone elastomers." Pathogens **9**(10): 784.

Lobo, C. I. V., T. B. Rinaldi, C. M. S. Christiano, L. De Sales Leite, P. A. Barbugli and M. I. Klein (2019). "Dual-species biofilms of Streptococcus mutans and Candida albicans exhibit more biomass and are mutually beneficial compared with single-species biofilms." Journal of oral microbiology **11**(1): 1581520.

Lorite, G. S., C. M. Rodrigues, A. A. De Souza, C. Kranz, B. Mizaikoff and M. A. Cotta (2011). "The role of conditioning film formation and surface chemical changes on Xylella fastidiosa adhesion and biofilm evolution." Journal of colloid and interface science **359**(1): 289-295.

Maddah, H. and A. Chogle (2017). "Biofouling in reverse osmosis: phenomena, monitoring, controlling and remediation." Applied Water Science **7**(6): 2637-2651.

Martinelli, E., M. Suffredini, G. Galli, A. Glisenti, M. E. Pettitt, M. E. Callow, J. A. Callow, D. Williams and G. Lyall (2011). "Amphiphilic block copolymer/poly (dimethylsiloxane)(PDMS) blends and nanocomposites for improved fouling-release." Biofouling **27**(5): 529-541.

McClay, T., C. Zabin, I. Davidson, R. Young and D. Elam (2015). Vessel biofouling prevention and management options report, Coast Guard New London CT Researh and Development Center.

Menesses, M., J. Belden, N. Dickenson and J. Bird (2017). "Measuring a critical stress for continuous prevention of marine biofouling accumulation with aeration." Biofouling **33**(9): 703-711.

Mineur, F., M. P. Johnson, C. A. Maggs and H. Stegenga (2007). "Hull fouling on commercial ships as a vector of macroalgal introduction." Marine biology **151**(4): 1299-1307.

Misdan, N., A. F. Ismail and N. Hilal (2016). "Recent advances in the development of (bio) fouling resistant thin film composite membranes for desalination." Desalination **380**: 105-111.

Moreira, J., L. Gomes, M. Simões, L. Melo and F. Mergulhão (2015). "The impact of material properties, nutrient load and shear stress on biofouling in food industries." Food and Bioproducts Processing **95**: 228-236.

Neves, A. R., J. R. Almeida, F. Carvalhal, A. Câmara, S. Pereira, J. Antunes, V. Vasconcelos, M. Pinto, E. R. Silva and E. Sousa (2020). "Overcoming environmental

problems of biocides: Synthetic bile acid derivatives as a sustainable alternative." Ecotoxicology and environmental safety **187**: 109812.

Palmer, J., S. Flint and J. Brooks (2007). "Bacterial cell attachment, the beginning of a biofilm." Journal of industrial microbiology & biotechnology **34**(9): 577-588.

Paul, E., J. C. Ochoa, Y. Pechaud, Y. Liu and A. Liné (2012). "Effect of shear stress and growth conditions on detachment and physical properties of biofilms." Water research **46**(17): 5499-5508.

Popović, S., G. S. SIMIĆ, A. Korać, I. Golić and J. Komárek (2016). "Nephrococcus serbicus, a new coccoid cyanobacterial species from Božana Cave, Serbia." Phytotaxa **289**(2): 135-146.

Pradhan, S., S. Kumar, S. Mohanty and S. K. Nayak (2019). "Environmentally benign fouling-resistant marine coatings: a review." Polymer-Plastics Technology and Materials **58**(5): 498-518.

Pranantyo, D., L. Q. Xu, K. G. Neoh, E.-T. Kang and S. L.-M. Teo (2016). "Antifouling coatings via tethering of hyperbranched polyglycerols on biomimetic anchors." Industrial & Engineering Chemistry Research **55**(7): 1890-1901.

Rickard, A. H., A. J. McBain, A. T. Stead and P. Gilbert (2004). "Shear rate moderates community diversity in freshwater biofilms." Applied and Environmental Microbiology **70**(12): 7426-7435.

Risse-Buhl, U., C. Anlanger, K. Kalla, T. R. Neu, C. Noss, A. Lorke and M. Weitere (2017). "The role of hydrodynamics in shaping the composition and architecture of epilithic biofilms in fluvial ecosystems." Water research **127**: 211-222.

Romeu, M. J., P. Alves, J. Morais, J. M. Miranda, E. D. de Jong, J. Sjollema, V. Ramos, V. Vasconcelos and F. J. Mergulhão (2019). "Biofilm formation behaviour of marine filamentous cyanobacterial strains in controlled hydrodynamic conditions." Environmental Microbiology **21**(11): 4411-4424.

Romeu, M. J., D. Domınguez-Pérez, D. Almeida, J. Morais, A. Campos, V. Vasconcelos and F. J. Mergulhão (2020). "Characterization of planktonic and biofilm cells from two filamentous cyanobacteria using a shotgun proteomic approach." Biofouling **36**: 631–645.

Romeu, M. J., D. Domınguez-Pérez, D. Almeida, J. Morais, M. Araújo, H. Osório, A. Campos, V. Vasconcelos and F. J. Mergulhão (2021). " Quantitative proteomic analysis of marine biofilms formed by filamentous cyanobacterium." Environmental Reseach (in press).

Salta, M., J. A. Wharton, Y. Blache, K. R. Stokes and J. F. Briand (2013). "Marine biofilms on artificial surfaces: structure and dynamics." Environmental microbiology **15**(11): 2879-2893.

Salta, M., J. A. Wharton, P. Stoodley, S. P. Dennington, L. R. Goodes, S. Werwinski, U. Mart, R. J. Wood and K. R. Stokes (2010). "Designing biomimetic antifouling surfaces." Philosophical Transactions of the Royal Society A: Mathematical, Physical and Engineering Sciences 368(1929): 4729-4754.

Schultz, M., J. Bendick, E. Holm and W. Hertel (2011). "Economic impact of biofouling on a naval surface ship." Biofouling **27**(1): 87-98.

Selim, M. S., S. A. El-Safty, M. A. El-Sockary, A. I. Hashem, O. M. A. Elenien, A. M. EL-Saeed and N. A. Fatthallah (2016). "Smart photo-induced silicone/TiO2 nanocomposites with dominant exposed surfaces for self-cleaning foul-release coatings of ship hulls." Materials & Design **101**: 218-225.

Selim, M. S., M. Shenashen, S. A. El-Safty, S. Higazy, M. M. Selim, H. Isago and A. Elmarakbi (2017). "Recent progress in marine foul-release polymeric nanocomposite coatings." Progress in Materials Science **87**: 1-32.

Selim, M. S., H. Yang, S. A. El-Safty, N. A. Fatthallah, M. A. Shenashen, F. Q. Wang and Y. Huang (2019). "Superhydrophobic coating of silicone/β–MnO2 nanorod composite for marine antifouling." Colloids and Surfaces A: Physicochemical and Engineering Aspects **570**: 518-530.

Sham, R. A. M., A. A. Zainuddin, S. N. S. Samion, A. Ahmad, F. H. Anuar and W. S. Aqma (2017). "Characterisation of Antibacterial and Antibiofilm Activities of Poly(Ethylene Glycol)-PolyDimethylsiloxane (PEG-PDMS) Polyurethane Copolymers Towards the Formation of Marine biofilm in Staphylococcus sp." Undergraduate Research Journal for Biomolecular Sciences and Biotechnology advances **1**: 92-99.

Shields, M. A., D. K. Woolf, E. P. Grist, S. A. Kerr, A. C. Jackson, R. E. Harris, M. C. Bell, R. Beharie, A. Want and E. Osalusi (2011). "Marine renewable energy: The

ecological implications of altering the hydrodynamics of the marine environment." Ocean & coastal management **54**(1): 2-9.

Silva, E., O. Ferreira, P. Ramalho, N. Azevedo, R. Bayón, A. Igartua, J. Bordado and M. Calhorda (2019). "Eco-friendly non-biocide-release coatings for marine biofouling prevention." Science of the Total Environment **650**: 2499-2511.

Silva, E. R., A. V. Tulcidas, O. Ferreira, R. Bayón, A. Igartua, G. Mendoza, F. J. Mergulhão, S. I. Faria, L. C. Gomes and S. Carvalho (2021). "Assessment of the environmental compatibility and antifouling performance of an innovative biocidal and foul-release multifunctional marine coating." Environmental Research **198**: 111219.

Simoes, M., M. O. Pereira, S. Sillankorva, J. Azeredo and M. J. Vieira (2007). "The effect of hydrodynamic conditions on the phenotype of Pseudomonas fluorescens biofilms." Biofouling **23**(4): 249-258.

Skovhus, T. L., D. Enning and J. S. Lee (2017). Corrosion in Oil and Gas Production. Microbiologically Influenced Corrosion in the Upstream Oil and Gas Industry. London, New York, CRC Press**:** 3-33.

Stafslien, S. J., J. Bahr, J. Daniels, D. A. Christianson and B. J. Chisholm (2011). "High-throughput screening of fouling-release properties: an overview." Journal of adhesion science and technology **25**(17): 2239-2253.

Stafslien, S. J., J. A. Bahr, J. W. Daniels, L. V. Wal, J. Nevins, J. Smith, K. Schiele and B. Chisholm (2007). "Combinatorial materials research applied to the development of new surface coatings VI: An automated spinning water jet apparatus for the high-throughput characterization of fouling-release marine coatings." Review of Scientific Instruments **78**(7): 072204.

Talluri, S. N., R. M. Winter and D. R. Salem (2020). "Conditioning film formation and its influence on the initial adhesion and biofilm formation by a cyanobacterium on photobioreactor materials." Biofouling **36**(2): 183-199.

Telegdi, J., L. Trif and L. Románszki (2016). Smart anti-biofouling composite coatings for naval applications. Smart Composite Coatings and Membranes. M. F. Montemos, Woodhead Publishing 123-155.

Tian, L., Y. Yin, H. Jin, W. Bing, E. Jin, J. Zhao and L. Ren (2020). "Novel marine antifouling coatings inspired by corals." Materials Today Chemistry **17**: 100294.

Tsai, Y.-P. (2005). "Impact of flow velocity on the dynamic behaviour of biofilm bacteria." Biofouling **21**(5-6): 267-277.

Ulaeto, S. B., R. Rajan, J. K. Pancrecious, T. Rajan and B. Pai (2017). "Developments in smart anticorrosive coatings with multifunctional characteristics." Progress in Organic Coatings **111**: 294-314.

Vilas-Boas, C., F. Carvalhal, B. Pereira, S. Carvalho, E. Sousa, M. M. Pinto, M. J. Calhorda, V. Vasconcelos, J. R. Almeida and E. R. Silva (2020). "One Step Forward towards the Development of Eco-Friendly Antifouling Coatings: Immobilization of a Sulfated Marine-Inspired Compound." Marine drugs **18**(10): 489.

Vinagre, P. A., T. Simas, E. Cruz, E. Pinori and J. Svenson (2020). "Marine biofouling: A European database for the marine renewable energy sector." Journal of marine science and engineering **8**(7): 495.

Wang, L., L. Yu and C. Lin (2019). "Extraction of protease produced by sea mud bacteria and evaluation of antifouling performance." Journal of Ocean University of China **18**(5): 1139-1146.

Wang, Y., L. P. Samaranayake and G. A. Dykes (2021). "Plant components affect bacterial biofilms development by altering their cell surface physicochemical properties: a predictability study using Actinomyces naeslundii." FEMS Microbiology Ecology **97**(1): fiaa217.

Warziniack, T., R. G. Haight, D. Yemshanov, J. L. Apriesnig, T. P. Holmes, A. M. Countryman, J. D. Rothlisberger and C. Haberland (2021). Economics of invasive species. Invasive Species in Forests and Rangelands of the United States, Springer**:** 305-320.

Wilhelm, L., K. Besemer, C. Fasching, T. Urich, G. A. Singer, C. Quince and T. J. Battin (2014). "Rare but active taxa contribute to community dynamics of benthic biofilms in glacier-fed streams." Environmental microbiology **16**(8): 2514-2524.

Willemsen, P. (2005). "Biofouling in European aquaculture: is there an easy solution." European Aquaculture Society Special Publ **35**: 82-87.

Zecher, K., V. P. Aitha, K. Heuer, H. Ahlers, K. Roland, M. Fiedel and B. Philipp (2018). "A multi-step approach for testing non-toxic amphiphilic antifouling coatings against marine microfouling at different levels of biological complexity." Journal of microbiological methods **146**: 104-114.

Zhu, H.-W., J.-N. Zhang, P. Su, T. Liu, C. He, D. Feng and H. Wang (2020). "Strong adhesion of poly (vinyl alcohol)–glycerol hydrogels onto metal substrates for marine antifouling applications." Soft matter **16**(3): 709-717.

3.

The relative importance of shear forces and surface hydrophobicity on biofilm formation by coccoid cyanobacteria[a]

Abstract

Understanding the conditions affecting cyanobacterial biofilm development is crucial to develop new antibiofouling strategies and decrease the economic and environmental impact of biofilms in marine settings. In this study, we investigated the relative importance of shear forces and surface hydrophobicity on biofilm development by two coccoid cyanobacteria with different biofilm formation capacities. The strong biofilm-forming *Synechocystis salina* was used along with the weaker biofilm-forming *Cyanobium* sp. Biofilms were developed in defined hydrodynamic conditions using glass (a model hydrophilic surface) and a polymeric epoxy coating (a hydrophobic surface) as substrates. Biofilms developed in both surfaces at lower shear conditions contained a higher number of

[a] The content of this chapter was adapted from the following publication(s):

Faria, S. I., R. Teixeira-Santos, M. J. Romeu, J. Morais, V. Vasconcelos and F. J. Mergulhão (2020). "The relative importance of shear forces and surface hydrophobicity on biofilm formation by coccoid cyanobacteria." Polymers **12**(3): 653.

cells and presented higher values for wet weight, thickness, and chlorophyll *a* content. The impact of hydrodynamics on biofilm development was generally stronger than the impact of surface hydrophobicity, but a combined effect of these two parameters strongly affected biofilm formation for the weaker biofilm producing organism. The antibiofilm performance of the polymeric coating was confirmed at the hydrodynamic conditions prevailing in ports. Shear forces were shown to have a profound impact on biofilm development in marine settings regardless of the fouling capacity of the existing flora and the hydrophobicity of the surface.

3.1. Introduction

Marine biofouling is an area of intense research particularly due to the considerable economic impacts on marine transport. Biofouling on ship hulls increases frictional drag and may result in a fuel consumption increase ranging from 6% to 45%, depending on the size of the vessel (Banerjee et al. 2011, Nurioglu and Esteves 2015, Schultz et al. 2011, Silva et al. 2019). This is associated with increased emissions of GHG and environmental pollution (Silva et al. 2019). In addition to the problems associated with frictional drag, marine biofouling poses other environmental problems such as the introduction of nonindigenous species in different habitats including the transport of pathogenic species (King et al. 2006, Lacoursière-Roussel et al. 2012).

Biofouling by macrofouling organisms such as bryozoans, mollusks, polychaeta, tunicates, coelenterates, or fungi occurs after biofilm formation by microfouling organisms such as cyanobacteria and diatoms which are early colonizers (Camps et al. 2011, de Carvalho 2018, Essock-Burns et al. 2016, Telegdi et al. 2016). Thus, it has been suggested that reducing biofilm formation may be a good strategy to delay macrofouling (Cao et al. 2011, Chambers et al. 2006, Palmer et al. 2007).

Port authorities in different countries are moving towards a "clean hull" policy where vessels must provide evidence of biofouling management before they arrive (Georgiades and Kluza 2017, McClay et al. 2015, Takata et al. 2006). The enforcement of these policies is likely to be more intense in large-sized vessels whereas small recreational

vessels may be subjected to less stringent control and may have a significant impact on the introduction of nonindigenous species. It has been recognized that around 87% of nonindigenous marine species in New Zealand are associated with biofouling on international vessels (Industries 2018, Matua 2018) and small recreational vessels may play an important role in this process as compliance with regulations is harder to guarantee.

Several parameters have been indicated as modulators of biofilm development, including surface hydrophobicity and hydrodynamic conditions (Donlan 2002, Telegdi et al. 2016). Recently, Romeu *et al.* demonstrated that lower shear forces promoted biofilm formation using different filamentous cyanobacterial strains, while the surface properties had a less pronounced effect (Romeu et al. 2019).

In this chapter, we have tested a polymeric epoxy resin commonly used to coat the hulls of small recreational vessels (such as powerboats, yachts, and sailing boats) (King et al. 2006, Taylor 1996). Particularly used in fiberglass hulls, epoxy resins are selected due to their mechanical strength and chemical resistance (Patel et al. 2018). Epoxy composites offer improved resistance to fatigue, hull durability, and enable the production of cosmetically attractive surfaces even after exposure to saltwater and UV light (Hoge and Leach 2016). In addition to the problems in ship hulls, marine biofouling also affects other surfaces. Glass surfaces can be found in underwater windows of boats, flotation spheres, moored buoys, underwater cameras, measuring devices, or sensors (Blain et al. 2004, Taylor 1996). Particularly in these latter cases, when the optical properties of glass windows are compromised, these devices produce incorrect readings and require frequent cleaning and maintenance during their operational lifetime (Delauney et al. 2010).

The main goal of this study was to evaluate the relative importance of shear forces and surface hydrophobicity on cyanobacterial biofilm development in marine settings. For that purpose, we have followed biofilm development in defined hydrodynamic conditions (including those that can be found in harbors), using two cyanobacterial coccoid strains with different biofilm-forming capacities and two model surfaces with different hydrophobicity (glass and an epoxy polymeric coating). These surfaces can be found in ship hulls and also in the windows of underwater sensors and measuring devices.

3.2. Materials and methods

3.2.1. Surface preparation

In order to assess the cyanobacterial biofilm development, two different surfaces, glass and a polymeric epoxy resin, were used. Glass coupons (1 x 1 cm; Vidraria Lousada, Lda, Lousada, Portugal) were immersed in a 2% (v/v) TEGO 2000® (JohnsonDiversey, Northampton, United Kingdom) solution, an amphoteric disinfectant used for cleaning and disinfecting surfaces (Gomes et al. 2018), for 20 min (Meireles et al. 2017) under agitation (150 rpm). Then, the coupons were washed in sterile distilled water to remove any remaining disinfectant residues, air-dried, and sterilized by autoclaving (121 ^{O}C, 15 min) (Azevedo et al. 2006). For the preparation of epoxy-coated glass surfaces, after the washing procedures, glass coupons were gently coated with 150 µL of epoxy resin and dried in two steps: i) 12 h at room temperature (approximately 25 ^{O}C), and ii) 3 h at 60 ^{O}C, according to the instructions from the manufacturer. The polymeric epoxy resin (produced by HB Química company, Matosinhos, Porto, Portugal) is a commercial resin constituted by HB Eposurf 2 resin and HB Eposurf hardener, in a ratio of 10:3. The HB Eposurf 2 resin is composed by bisphenol-A- (epichlorohydrin) and epoxy resins (average molecular weight below 700 KDa), Poly (Bisphenol A-co-epichlorohydrin), 4-4`- Isopropylidenediphenol, oligomeric reaction products with 1-cloro-2,3-epoxypropene, phenol, polymer with formaldehyde, oxiranylmethyl ether Poly[(phenyl glycidyl ether)-co-formaldehyde] and 1,6-Hexamethylenediol diglycidyl ether. The HB Eposurf hardener is composed by 3-aminomethyl-3,5,5-trimethylcyclohexylamine, 5-Amino-1,3,3-trimethylcyclohexanemethylamine, mixture of *cis* and *trans*, 5-Amino-1,3,3-trimethylcyclohexanemethylamine, mixture of *cis* and *trans*, 3-aminomethyl-3,5,5-trimethylcyclohexylamine.

Coated coupons were immersed in 70% (v/v) ethanol (VWR International S.A.A., Fontenay-sous-Bois, France) for 20 min to sterilize them, according to the indications from the manufacturer. After drying, the initial weight of each coupon was registered.

The water contact angle of both surfaces was determined in three independent measurements performed at 25 ± 2 ^{O}C, by the sessile drop method using a contact angle meter

(Dataphysics OCA 15 Plus, Filderstadt, Germany), as described in Gomes et al. 2015 (Gomes et al. 2015). In each experiment, at least 25 determinations for each material were performed.

3.2.2. Cyanobacterial strains and growth conditions

Cyanobacterial strains were obtained from the Blue Biotechnology and Ecotoxicology Culture Collection (LEGE-CCB) deposited at the Interdisciplinary Centre of Marine and Environmental Research (CIIMAR), Porto, Portugal (Ramos et al. 2018). *Synechocystis salina* LEGE 00041 (order *Synechococcales*) was originally obtained from a seawater sample, collected on June 2000, at Espinho beach (41.00847 N 8.646958 W) located in the north coast of Portugal (Ramos et al. 2018). *Cyanobium* sp. LEGE 06097 (order *Synechococcales*) was isolated from the intertidal zone, on green macroalga, collected on July 2006, at Martinhal beach (37.01869 N 8.926714 W) located in Vila do Bispo, Portugal (Ramos et al. 2018). Cyanobacterial cells were grown in 750 mL Z8 medium (Kotai 1972) supplemented with 25 g/L of synthetic sea salts (Tropic Marin) and vitamin B12 (Sigma Aldrich, Merck, Saint Louis, MO, USA). Cultures were grown under 14 h light (10‑30 mol photons m^{-2} s^{-1}, λ = 380‑700 nm)/10 h dark cycles at 25 ^{O}C.

3.2.3. Biofilm formation

Biofilm assays were performed on 12-well plates (VWR International, Carnaxide, Portugal) under previously optimized conditions (Romeu et al. 2019). Briefly, transparent double-sided adhesive tape was used to fix the coupons to the wells. The plates were subjected to UV sterilization for 30 min and, then, the sterile coupons were fixed. Each well was incubated with 3 mL of cyanobacterial suspension at a concentration of 1×10^8 cell/mL. Microtiter plates (MTPs) were incubated at 25 ^{O}C in an orbital shaker with a 25 mm orbital diameter (Agitorb 200ICP, Norconcessus, Ermesinde, Portugal) at 40 and 185 rpm and under alternate light cycles of 14 h light (10‑30 mol photons m^{-2} s^{-1})/10 h dark. The selection of the hydrodynamic conditions was based on a previous study describing that a shaking frequency of 185 rpm in this incubator corresponds to an average shear rate of 40 s^{-1} and a

maximum of 120 s^{-1}, while 40 rpm corresponds to an average shear rate of 4 s^{-1} and a maximum of 11 s^{-1} as determined by computational fluid dynamics (CFD) (Romeu et al. 2019). As the shear rate of 50 s^{-1} was estimated for a ship in a harbor (Bakker et al. 2003), and lower shear rates promote marine biofouling (Flemming et al. 2009, Minchin and Gollasch 2003), both hydrodynamic conditions were evaluated.

Biofilm formation was followed for 6 weeks (42 days), every seven days. During the incubation period, the culture medium was replaced twice a week. Biofilm formation experiments were performed with two technical replicates and in two independent assays (biological replicates).

3.2.4. Biofilm analysis

At each sampling point, two coupons of each experimental condition were analyzed concerning i) the number of biofilm cells, ii) biofilm wet weight, iii) biofilm thickness, and iv) chlorophyll *a* content. The biofilm structure was analyzed at day 42 by optical coherence tomography (OCT). Before sampling the culture medium was carefully removed and, then, the coupons were gently rinsed with a sterile sodium chloride (NaCl) solution (8.5 g/L, VWR International, Carnaxide, Portugal) in order to remove loosely attached cyanobacteria.

3.2.4.1. Cyanobacterial cell counting

Cyanobacterial cells were detached from the coupons by dipping each coupon in 2 mL of 8.5 g/L sodium chloride solution and vortexing for 3 min at maximum power. Then, 10 µL of cellular suspension was placed on each side of a Neubauer chamber and observed under the microscope (Nikon Eclipse LV100 microscope, Nikon Corporation, Tokyo, Japan). After vortexing, the coupons were observed by microscopy in order to confirm complete cell detachment.

3.2.4.2. Biofilm wet weight and thickness

To determine the biofilm wet weight, coupons were detached from the wells with a sterile tweezer and weighted. Biofilm wet weight was obtained by the difference between initial coupon weight, determined prior to inoculation, and the weight after sampling.

Biofilm thickness was assessed using a Nikon Eclipse LV100 microscope coupled to a joystick (Prior Scientific Ltd, Cambridge, UK), connected to a camera (Nikon digital sight DS-RI 1, Tokyo, Japan), and analyzed using the NIS-Elements AR (Advanced Research) 4.13.05 software package. This tool features fully automated acquisition and device control through multi-dimensional image acquisition and analysis. For each coupon, a minimum of five representative independent fields were analyzed to obtain accurate and reproducible results.

3.2.4.3. Chlorophyll *a* quantification

Chlorophyll *a* quantification is a common method to estimate the biomass on marine environments because this pigment is unique and predominant in all groups of cyanobacteria (Boyer et al. 2009). Detached cells were harvested by centrifugation (3202 x g, for 5 min at room temperature) and the supernatant discarded. Since chlorophyll pigments are light-sensitive, the following chlorophyll extraction procedures were performed in the dark, as previously reported (Romeu et al. 2019). Briefly, 2 mL of 99.8% methanol (VWR International, Carnaxide, Portugal) was added to the pellet for chlorophyll extraction. Then, cell suspensions were incubated at 4 ^{O} C, during a period of 24 h for a maximal chlorophyll *a* extraction. The absorbance at 750 nm (turbidity), 665 nm (chlorophyll *a*) and 652 nm (chlorophyll *b*) were measured on a V-1200 spectrophotometer (VWR International China Co., Ltd, Shanghai, China). The chlorophyll *a* concentration (µg/cm^2) was calculated using the following Equation (1) (Porra et al. 1989).

$$\text{Chl } a \text{ (µg/mL)} = 16.29 \times A^{665} - 8.54 \times A^{652} \quad (1)$$

3.2.4.4. OCT

On day 42, the biofilms were imaged by OCT using a Thorlabs Ganymede instrument (Thorlabs GmbH, Dachau, Germany) with a central wavelength of 930 nm. After the gentle rinsing, the wells were filled with 3 mL of a sterile NaCl solution (8.5 g/L) and imaged. The captured volume was 3.66 x 1.52 x 2.98 mm^3 (509 x 313 x 1024 pixels). The refractive index was set to 1.40, since this value produced optimal results in a previous study (Romeu et al. 2019). For each coupon, two-dimensional (2D) imaging was performed with a minimum of five fields of view to ensure the accuracy and reproducibility of the results obtained.

3.2.5. Data analysis

Descriptive statistics were used to compute mean and standard deviation for sample parameters (the number of biofilm cells, biofilm wet weight, biofilm thickness, and chlorophyll *a* content). Results were presented as the percentage increase between shear forces (obtained at 40 and 185 rpm).

Data analysis was performed using the GraphPad Prism® for Windows, version 6.01 (GraphPad Software, Inc., San Diego, CA, USA). Since the distribution of some variables was not normal, both parametric and nonparametric tests were used. Student's t-test was used to compare biofilm formation under lower and higher shear forces, either for glass or epoxy-coated glass surfaces. For the determination of the impact of the hydrodynamic conditions and surface hydrophobicity on biofilm formation, the Mann–Whitney test was used (Table 3.1 and Table 3.2). Significant results were considered for *p*-values < 0.05

The impact of the hydrodynamic condition and surface hydrophobicity on biofilm development was estimated for each analyzed parameter (the number of biofilm cells, wet weight, thickness, and chlorophyll *a* content) and represented in radar charts. Radar charts were divided into four quadrants, where each one depicts the average values obtained in each sampling point (days) under the following experimental conditions: Q1) glass at 40 rpm (Gla/40), Q2) epoxy-coated glass at 40 rpm (Epx/40), Q3) epoxy-coated glass at 185 rpm (Epx/185), and Q4) glass at 185 rpm (Gla/185). The impact of the hydrodynamic conditions was calculated by subtracting the values obtained at different shear forces for both glass (Q1

vs. Q4) and epoxy-coated glass (Q2 vs. Q3); whereas the impact of the surface hydrophobicity was determined by subtracting the values obtained for two different surfaces at lower shear (Q1 vs. Q2) and higher shear (Q4 vs. Q3). All positive differences were considered as increments resulting from hydrodynamic condition or surface hydrophobicity and represented by a colored area (hydrodynamic effect−yellow area; surface effect−blue area). The combined effect (green area) has been plotted whenever the surface effect overlapped the hydrodynamic effect.

Table 3.1. *p*-values obtained for the differences between the hydrodynamic conditions (40 vs 185 rpm) on biofilm formation (*p*-values < 0.05 are shown in **bold**).

	***S. salina* 00041**		***Cyanobium* sp. 06097**	
	Glass	Epoxy-coated glass	Glass	Epoxy-coated glass
Biofilm cells	0.091	0.275	0.282	**0.048**
Biofilm wet weight	0.083	0.685	0.698	0.933
Biofilm thickness	**0.018**	**< 0.001**	**0.001**	**0.035**
Chlorophyll *a* content	**< 0.001**	**< 0.001**	0.303	0.751

Table 3.2 *p*-values obtained for the differences between surface hydrophobicity (glass vs epoxy-coated glass) on biofilm formation (*p*-values are shown in **bold**).

	***S. salina* 00041**		***Cyanobium* sp. 06097**	
	Lower shear	Higher shear	Lower shear	Higher shear
Biofilm cells	0.161	0.589	**0.008**	0.137
Biofilm wet weight	0.632	**0.018**	**0.003**	**0.007**
Biofilm thickness	0.053	**< 0.001**	**0.001**	0.202
Chlorophyll *a* content	0.726	0.208	0.079	0.160

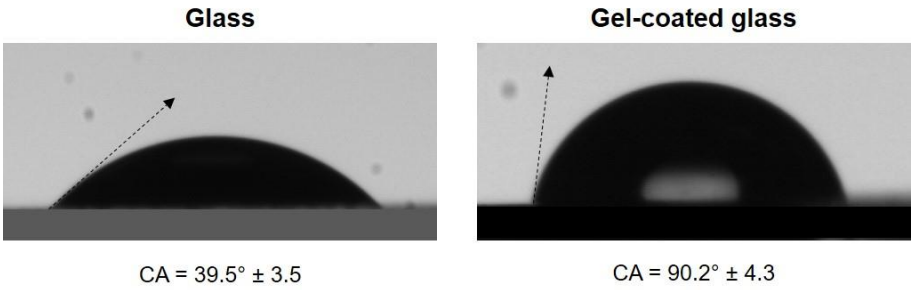

Figure 3.1. A representative image of water contact angle measurement. Pictures of water droplets on glass (left) and epoxy-coated glass (right) surfaces.

3.3. Results

In this study, we investigated the impact of shear forces and surface hydrophobicity on biofilm development by two coccoid cyanobacteria. The different shear forces were obtained by using distinct shaking frequencies (40 and 185 rpm) in an orbital incubator generating average shear rates of 4 and 40 s^{-1}, respectively, as determined by CFD (Romeu et al. 2019). Surface hydrophobicity was evaluated by determining the water contact angle. A value of $39.5^{O} \pm 3.5$ was obtained for glass whereas for the epoxy-coated surface it was $90.2^{O} \pm 4.3$ (Figure 3.1 − A representative image of water contact angle measurement). While glass is clearly hydrophilic, the epoxy-coated surface is slightly hydrophobic (Bayoudh et al. 2006, Ma et al. 2007).

For both *S. salina* (high biofilm former) and *Cyanobium* sp. (low biofilm former), the number of biofilm cells was higher at lower shear for all the time points tested. Biofilms developed on glass at lower shear displayed on average a higher number of cells of *S. salina* (35%, $p < 0.05$ for 44.4% of the time points, Figure 3.2 A) and *Cyanobium* sp. (32%, $p < 0.05$ for 55.6% of the time points, Figure 3.3 A).

In turn, biofilms formed on the epoxy-coated glass surface at lower shear also had on average a higher number of cells of *S. salina* (31%, $p < 0.05$ for 44.4% for the time points, Figure 3.2 E) and *Cyanobium* sp. (14%, $p < 0.05$ for 55.6% for the time points, Figure 3.3 2E).

Biofilms formed on glass at lower shear had, on average, a higher mass for *S. salina* (17%, $p < 0.05$ for 55.6% of the time points, Figure 3.2 B) and *Cyanobium* sp. (12%, $p < 0.05$ for 33.3% of the time points, Figure 3.3 B). On epoxy-coated glass, increased wet weight values were also obtained at low shear for *S. salina* (26%, $p < 0.05$ for 77.8% of the time points, Figure 3.2 F) and *Cyanobium* sp. (10%, $p < 0.05$ for 22.2% of the time points, Figure 3.3 F).

Likewise, biofilms developed on glass at lower shear displayed, on average, a higher thickness for *S. salina* (28%, $p < 0.05$ for 44.4% of the time points, Figure 3.2 C) and *Cyanobium* sp. (41%, $p < 0.05$ for all the time points tested, Figure 3.3 C). On epoxy-coated glass, biofilm thickness was also, on average, higher at lower shear for *S. salina* (52%, $p < 0.05$ for 77.8% of the time points, Figure 3.2 G) and *Cyanobium* sp. (34%, $p < 0.05$ for all the time points tested, Figure 3.3 G).

In addition, biofilms formed on glass at lower shear had, on average, a higher content of chlorophyll *a* for *S. salina* (80%, $p < 0.05$ for 44.4% of the time points, Figure 3.2 D) and *Cyanobium* sp. (73%, $p < 0.05$ for 44.4% of the time points, Figure 3.3 D). Chlorophyll *a* content produced on epoxy coated glass at lower shear was also, on average, higher for *S. salina* (95%, $p < 0.05$ for 66.7% of time points, Figure 3.2 H) and *Cyanobium* sp. (35%, $p < 0.05$ for 44.4% for time points, Figure 3.3 H).

For both *S. salina* and *Cyanobium* sp., biofilms formed on glass displayed a slightly higher number of cells compared to those formed on epoxy-coated glass surfaces. Likewise, increased wet weight, thickness, and chlorophyll *a* content values were observed for biofilms developed on glass (Figure 3.4).

For *S. salina* and for both surfaces, the hydrodynamic conditions had a high impact on the increase of the number of biofilm cells, biofilm wet weight and thickness, and chlorophyll *a* content (Figure 3.4 A‑D), as represented by the yellow area. This increase was observed in all the stages of biofilm formation (from day 1 to 42).

The increase in biofilm wet weight, thickness, and chlorophyll *a* content also resulted from a combined effect between hydrodynamics and surface hydrophobicity (represented by the green area) (Figure 3.4 B‑D). However, the pure effect of hydrodynamics was stronger than the combined effect between surface and hydrodynamics (yellow versus green area).

Conversely, surface hydrophobicity only had an influence on the wet weight and thickness of biofilms developed at higher shear (Figure 3.4 B-C, blue area).

For *Cyanobium* sp. a combined effect resulting from hydrodynamics and surface hydrophobicity was responsible for a higher number of biofilm cells, biofilm wet weight and thickness, and chlorophyll *a* content (Figure 3.4 E‑H, green area). This increment was observed for all sampling points. However, Figures 3.4 E-H show that hydrodynamics had a smaller effect on the increment of these parameters for both glass and epoxy-coated glass surfaces (Figure 3.4 E‑H, yellow area), while surface hydrophobicity only induced an increase on these parameters at lower shear (Figure 3.4 E‑H, blue area).

Biofilm structures were evaluated on day 42 using OCT for *S. salina* and *Cyanobium* sp. (Figure 3.5). For both strains, biofilms developed on glass at 40 rpm were more prominent (Figure 3.5 A and 3.5 E). Moreover, the presence of three-dimensional structures was more noticeable for biofilms formed at lower shear stress for both glass and epoxy-coated glass surfaces (Figure 3.5 A, C, E, G).

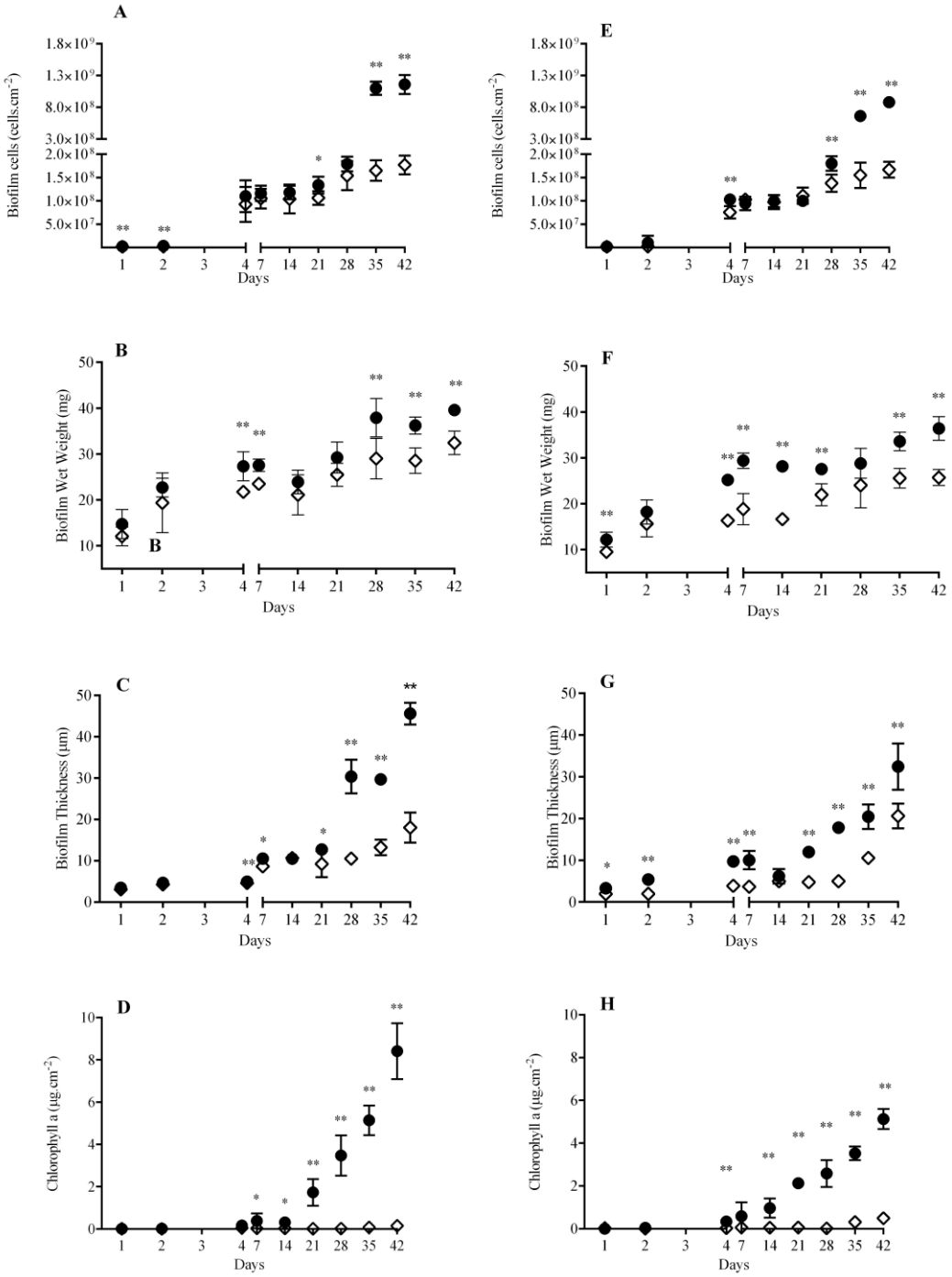

Figure 3.2. Evaluation of the influence of hydrodynamic conditions on biofilm development of *Synechocystic salina* LEGE 00041 for 42 days, on glass (A–D) and epoxy-coated glass (E–H), respectively. The analyzed parameters refer to biofilm cells (A and E), biofilm wet weight (B and F), biofilm thickness (C and G), and chlorophyll *a* (D and H) at two different hydrodynamic conditions (● 40 rpm; ◊ 185 rpm). Symbol * indicates significant results for p-values < 0.05, comparing the two hydrodynamic conditions.

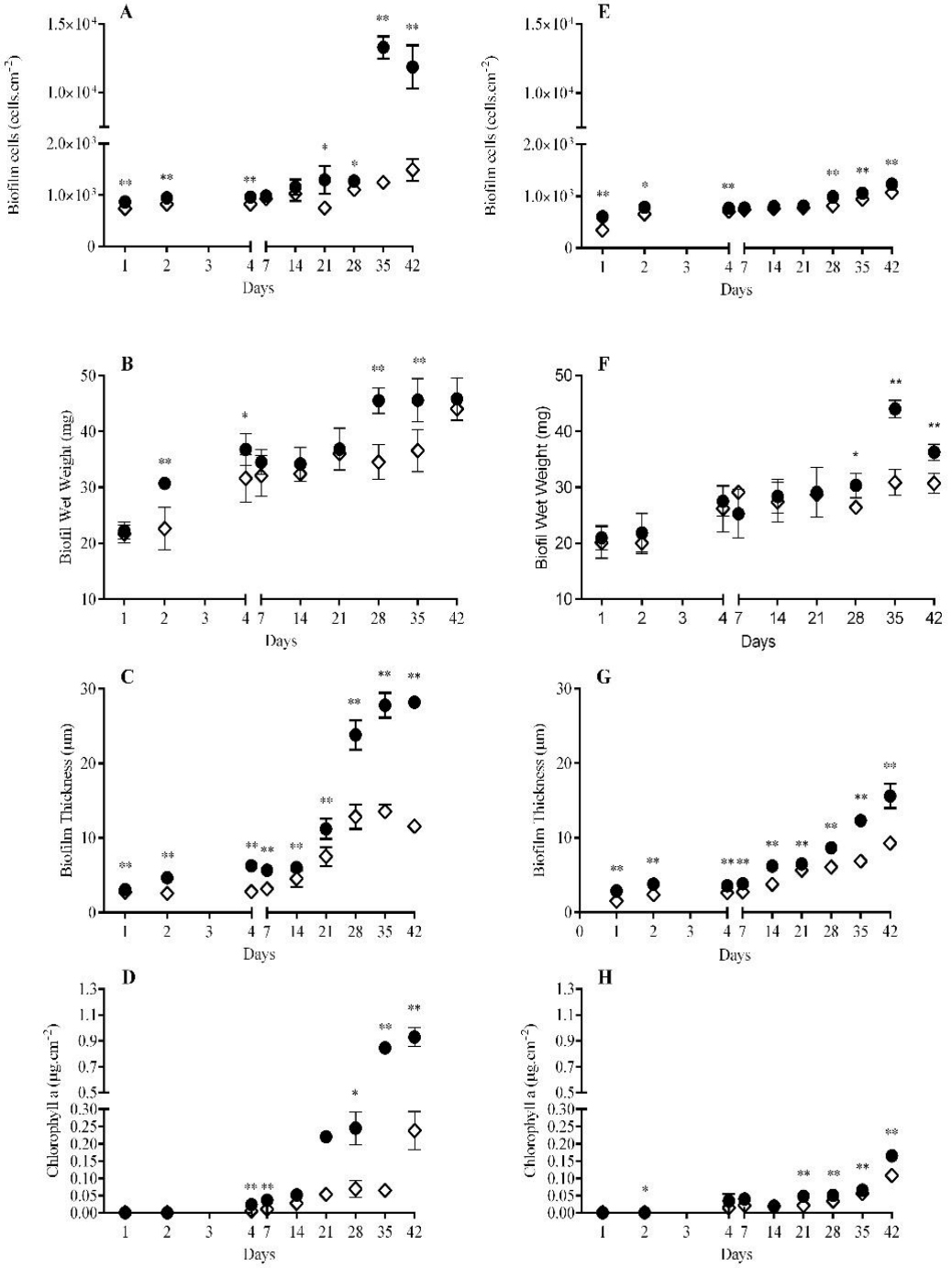

Figure 3.3. Evaluation of the influence of hydrodynamic conditions on biofilm development of *Cyanobium* sp. LEGE 06097 for 42 days, on glass (A–D) and epoxy-coated glass (E–H), respectively. The analyzed parameters refer to biofilm cells (A and E), biofilm wet weight (B and F), biofilm thickness (C and G), and chlorophyll *a* (D and H) at two different hydrodynamic conditions (● 40 rpm; ◊ 185 rpm). Symbol * indicates significant results for p-values < 0.05, comparing the two hydrodynamic conditions.

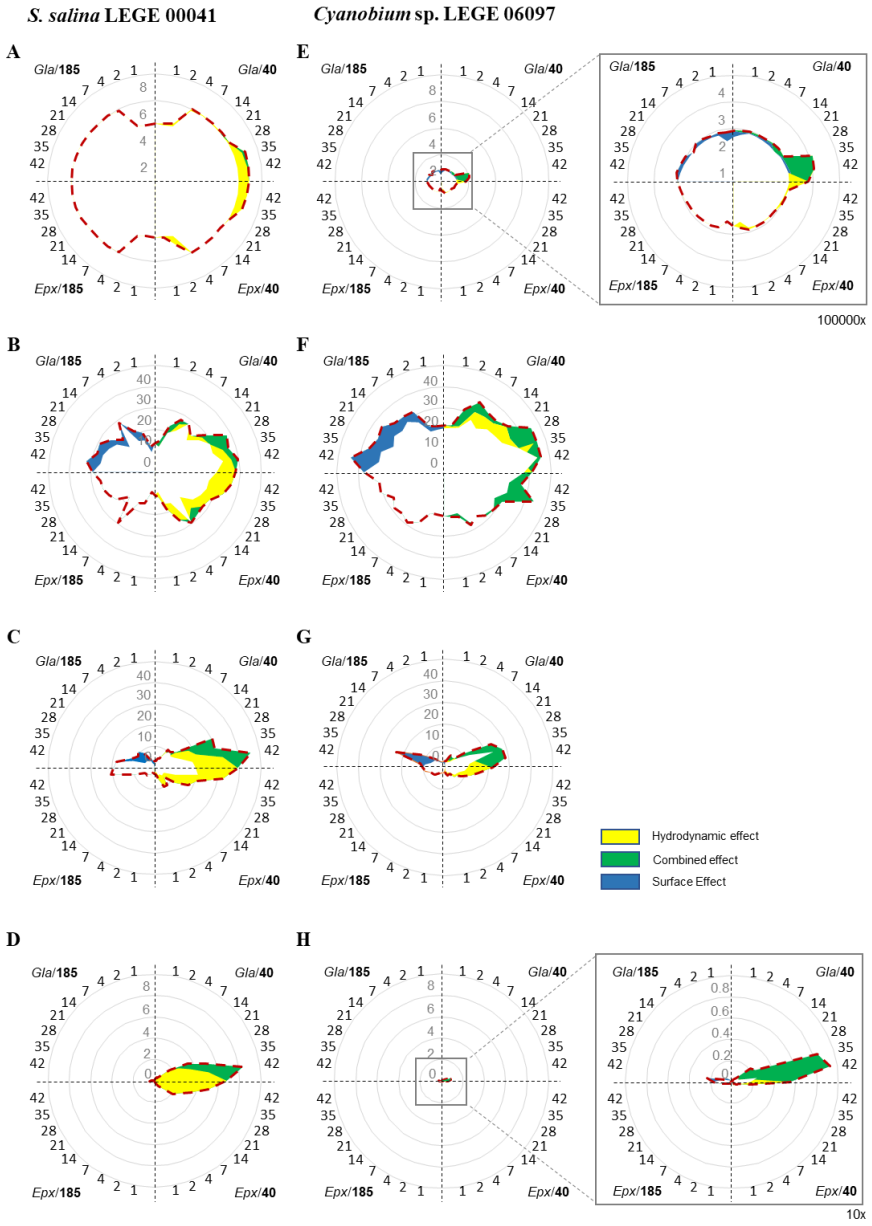

Figure 3.4. Radar charts representing (A and E) the number of biofilm cells (Log cells.cm-2), (B and F) biofilm wet weight (mg), (C and G) biofilm thickness (µm), and (D and H) chlorophyll a content (µg.cm^{-2}), for S. salina LEGE 00041 and Cyanobium sp. LEGE 06097. Average values (previously represented in figures 3.2 and 3.3) are plotted as a dashed line considering the time scale (days) indicated in each quadrant. The following conditions are depicted in each quadrant: Q1: Gla/40 glass at 40 rpm; Q2: Epx/40 epoxy-coated glass at 40 rpm; Q3: Epx/185 epoxy-coated glass at 185 rpm; and Q4: Gla/185 glass at 185 rpm. The hydrodynamic effect calculated by subtracting the values obtained at different shear forces for both glass (Q1 vs. Q4) and epoxy-coated glass (Q2 vs. Q3) is represented by the yellow area. The surface effect determined by subtracting the values obtained for two different surfaces at lower shear (Q1 vs. Q2) and higher shear (Q4 vs. Q3) is represented by the blue area. When these effects overlap, they are represented by the green area. Only positive differences are represented.

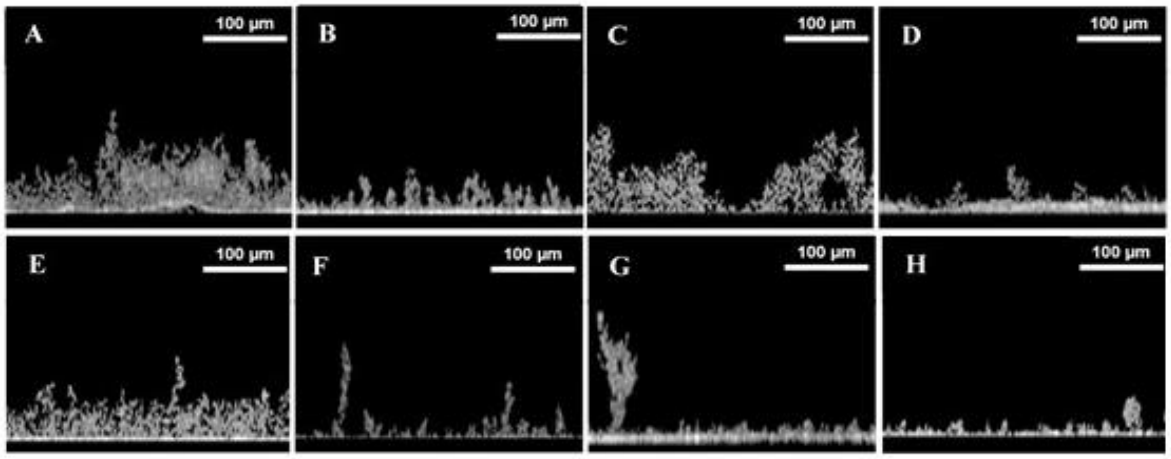

Figure 3.5. Representative images obtained by OCT for S. salina LEGE 00041 biofilm (A–D) and Cyanobium sp. LEGE 06097 biofilm (E–H), on day 42, on glass at 40 (A and E) and 185 rpm (B and F), and on epoxy-coated glass at 40 rpm (C and G) and 185 rpm (D and H).

3.4. Discussion

Our study clearly demonstrated that shear forces and surface properties have a significant impact on biofilm formation by coccoid cyanobacteria, as confirmed by the number of biofilm cells, biofilm wet weight and thickness, and chlorophyll *a* content.

Cyanobacterial biofilms developed at lower shear (obtained at 40 rpm) presented a higher number of biofilm cells when compared to those developed at higher shear (185 rpm), both on glass and epoxy-coated glass surfaces. Similar results were obtained for wet weight and thickness. This later parameter has a strong impact on the performance of underwater devices (Delauney et al. 2010), and therefore, its assessment during biofilm formation is important not only for the development and maintenance of marine devices, but also to better understand the marine biofilm behaviour.

Likewise, several studies have proposed the determination of chlorophyll *a* content as a good indicator of cyanobacterial biofilm growth (Bartram and Chorus 1999, Rees and Bartram 2002). Our results also demonstrated that cyanobacterial biofilms growing at lower shear produced higher amounts of chlorophyll *a*, which is consistent with the higher number

of biofilm cells obtained in this condition. These results are corroborated by a previous study demonstrating that biofilm development by filamentous cyanobacteria is also promoted at low shear forces (Romeu et al. 2019).

Concerning the surface hydrophobicity, results demonstrated that biofilms formed on glass displayed a higher number of cells than on epoxy-coated glass. Similarly, the biofilm wet weight and thickness, and chlorophyll *a* content were higher on glass than on epoxy-coated glass. This result suggests that, in this assay, the hydrophilic surface promoted biofilm formation. Other studies referred that adhesion and consequent biofilm formation may occur to a greater extent on hydrophobic surfaces rather than on hydrophilic surfaces (Cerca et al. 2005). However, according to Mazumder *et al.*, biofilm formation may induce alterations in the hydrophobicity of the substratum surfaces, indicating that bacterial cells already attached can modify the surface properties (Mazumder et al. 2010).

The tendencies verified for the analyzed parameters were validated for both *S. salina* and *Cyanobium* sp. independently of their capacity to form a biofilm. However, our data analysis demonstrated that, for *S. salina*, the increase in biofilm parameters is mainly due to shear forces (yellow shadowed area is greater than blue shadowed area, Figure 3.4 A‑D), whereas for *Cyanobium* sp., a combined effect resulting from the shear force and surface hydrophobicity is responsible for the biofilm development behaviour (green shadowed area prevails over yellow and blue shadowed areas, Figure 3.4 E‑H). Therefore, it was shown that shear forces exert a crucial impact on the development of cyanobacterial biofilms, which is important not only in the early stage of biofilm formation but also during maturation. It is known that lower shear forces promote uniform biofilm formation during all stages of its development, while higher shear forces not only promote uneven biofilm formation but may also induce biofilm detachment and deformation (Thomen et al. 2017). Moreover, it has been reported that higher shear forces cause several functional and morphological changes in biofilms, including quorum-sensing impairment (Kim et al. 2016, Kirisits et al. 2007) and metabolic switching (Liu and Tay 2001), which may hinder their development.

For strains with low biofilm formation capability, although hydrodynamics also play an important role in biofilm development, surface hydrophobicity becomes more important than in high biofilm producers. In this case, a combined effect between hydrodynamics and hydrophobicity becomes relevant. Surface properties such as hydrophobicity may promote

cell/surface interactions that, even in a low magnitude, may facilitate bacterial retention and contribute to biofilm development when combined with lower shear (Thomen et al. 2017). Furthermore, at a higher shear, these cell/surface interactions seem to become crucial for biofilm formation.

OCT analysis highlighted the impact of shear forces on cyanobacterial biofilm development, demonstrating that higher biofilm amounts were obtained at lower shear. It was also possible to observe the presence of three-dimensional structures of streamers in biofilms formed under these conditions on both surfaces. According to Drescher et al., the presence of these structures may contribute to biofilm growth by facilitating the capture of new cells and other components to the biofilm (Drescher et al. 2013).

In ship hulls, epoxy composites are used due to their strong adhesion to the construction material, high strength, and great chemical resistance (Patel et al. 2018). Our results show that the polymeric epoxy resin also has a very good antifouling performance for the specific application that it was designed for. It is known that fouling in ship hulls mainly occurs when the ship is docked due to the lower shear stress when compared to sailing conditions. In this study, we have mimicked the shear forces acting on a ship hull while staying in a port and the results obtained with the polymeric coating suggest that it can decrease biofilm formation. Therefore, it may have the potential to delay hull fouling thus reducing problems associated with frictional drag, fuel consumption, and the introduction of nonindigenous species in different habitats.

3.5. References

Azevedo, N., A. Pacheco, C. Keevil and M. Vieira (2006). "Adhesion of water stressed Helicobacter pylori to abiotic surfaces." Journal of Applied Microbiology **101**(3): 718-724.

Bakker, D., A. Van der Plaats, G. Verkerke, H. Busscher and H. Van Der Mei (2003). "Comparison of velocity profiles for different flow chamber designs used in studies of microbial adhesion to surfaces." Appl Environ Microbiol **69**(10): 6280-6287.

Banerjee, I., R. C. Pangule and R. S. Kane (2011). "Antifouling coatings: recent developments in the design of surfaces that prevent fouling by proteins, bacteria, and marine organisms." Advanced materials **23**(6): 690-718.

Bartram, J. and I. Chorus (1999). Toxic cyanobacteria in water: a guide to their public health consequences, monitoring and management. Boca Raton, FL, USA, CRC Press.

Bayoudh, S., A. Othmane, F. Bettaieb, A. Bakhrouf, H. B. Ouada and L. Ponsonnet (2006). "Quantification of the adhesion free energy between bacteria and hydrophobic and hydrophilic substrata." Materials Science and Engineering: C **26**(2-3): 300-305.

Blain, S., J. Guillou, P. Treguer, P. Woerther, L. Delauney, E. Follenfant, O. Gontier, M. Hamon, B. Leilde and A. Masson (2004). "High frequency monitoring of the coastal marine environment using the MAREL buoy." Journal of Environmental Monitoring **6**(6): 569-575.

Boyer, J. N., C. R. Kelble, P. B. Ortner and D. T. Rudnick (2009). "Phytoplankton bloom status: Chlorophyll a biomass as an indicator of water quality condition in the southern estuaries of Florida, USA." Ecological indicators **9**(6): S56-S67.

Camps, M., J.-F. Briand, L. Guentas-Dombrowsky, G. Culioli, A. Bazire and Y. Blache (2011). "Antifouling activity of commercial biocides vs. natural and natural-derived products assessed by marine bacteria adhesion bioassay." Marine pollution bulletin **62**(5): 1032-1040.

Cao, S., J. Wang, H. Chen and D. Chen (2011). "Progress of marine biofouling and antifouling technologies." Chinese Science Bulletin **56**(7): 598-612.

Cerca, N., G. B. Pier, M. Vilanova, R. Oliveira and J. Azeredo (2005). "Quantitative analysis of adhesion and biofilm formation on hydrophilic and hydrophobic surfaces of clinical isolates of Staphylococcus epidermidis." Research in microbiology **156**(4): 506-514.

Chambers, L. D., K. R. Stokes, F. C. Walsh and R. J. Wood (2006). "Modern approaches to marine antifouling coatings." Surface and Coatings Technology **201**(6): 3642-3652.

de Carvalho, C. C. (2018). "Marine biofilms: a successful microbial strategy with economic implications." Frontiers in Marine Science **5**: 126.

Delauney, L., C. Compere and M. Lehaitre (2010). "Biofouling protection for marine environmental sensors." Ocean Science **6**(2): 503-511.

Donlan, R. M. (2002). "Biofilms: microbial life on surfaces." Emerging infectious diseases **8**(9): 881.

Drescher, K., Y. Shen, B. L. Bassler and H. A. Stone (2013). "Biofilm streamers cause catastrophic disruption of flow with consequences for environmental and medical systems." Proceedings of the National Academy of Sciences **110**(11): 4345-4350.

Essock-Burns, T., A. Wepprich, A. Thompson and D. Rittschof (2016). "Enzymes manage biofilms on crab surfaces aiding in feeding and antifouling." Journal of Experimental Marine Biology and Ecology **479**: 106-113.

Flemming, H.-C., P. S. Murthy, R. Venkatesan and K. Cooksey (2009). Marine and industrial biofouling. Berlin/Heiderberg, Germany, Springer.

Georgiades, E. and D. Kluza (2017). "Evidence-based decision making to underpin the thresholds in New Zealand's craft risk management standard: biofouling on vessels arriving to New Zealand." Marine Technology Society Journal **51**(2): 76-88.

Gomes, L., J. Deschamps, R. Briandet and F. J. Mergulhão (2018). "Impact of modified diamond-like carbon coatings on the spatial organization and disinfection of mixed-biofilms composed of Escherichia coli and Pantoea agglomerans industrial isolates." International journal of food microbiology **277**: 74-82.

Gomes, L., L. Silva, M. Simões, L. Melo and F. Mergulhão (2015). "Escherichia coli adhesion, biofilm development and antibiotic susceptibility on biomedical materials." Journal of Biomedical Materials Research Part A **103**(4): 1414-1423.

Hoge, J. and C. Leach (2016). "Epoxy resin infused boat hulls." Reinforced Plastics **60**(4): 221-223.

Kim, M. K., F. Ingremeau, A. Zhao, B. L. Bassler and H. A. Stone (2016). "Local and global consequences of flow on bacterial quorum sensing." Nature microbiology **1**(1): 1-5.

King, R. K., G. J. Flick, S. A. Smith, M. D. Pierson, G. D. Boardman and C. W. Coale (2006). "Comparison of bacterial presence in biofilms on different materials commonly found in recirculating aquaculture systems." Journal of applied aquaculture **18**(1): 79-88.

Kirisits, M. J., J. J. Margolis, B. L. Purevdorj-Gage, B. Vaughan, D. L. Chopp, P. Stoodley and M. R. Parsek (2007). "Influence of the hydrodynamic environment on quorum sensing in Pseudomonas aeruginosa biofilms." Journal of bacteriology **189**(22): 8357-8360.

Kotai, J. (1972). Instructions for Preparation of Modified Nutrient Solution Z8 for AlgaeNorwegian. Institute for Water Research, Blindern. Blindern, Oslo, Norway.

Lacoursière-Roussel, A., B. M. Forrest, F. Guichard, R. F. Piola and C. W. McKindsey (2012). "Modeling biofouling from boat and source characteristics: a comparative study between Canada and New Zealand." Biological invasions **14**(11): 2301-2314.

Liu, Y. and J. H. Tay (2001). "Metabolic response of biofilm to shear stress in fixed-film culture." Journal of applied microbiology **90**(3): 337-342.

Ma, Y., X. Cao, X. Feng, Y. Ma and H. Zou (2007). "Fabrication of super-hydrophobic film from PMMA with intrinsic water contact angle below 90." Polymer **48**(26): 7455-7460.

Mazumder, S., J. O. Falkinham III, A. M. Dietrich and I. K. Puri (2010). "Role of hydrophobicity in bacterial adherence to carbon nanostructures and biofilm formation." Biofouling **26**(3): 333-339.

McClay, T., C. Zabin, I. Davidson, R. Young and D. Elam (2015). Vessel biofouling prevention and management options report. New London, CT, USA, U. S. Coast Guard R&D Center.

Meireles, A., R. Fulgêncio, I. Machado, F. Mergulhão, L. Melo and M. Simões (2017). "Characterization of the heterotrophic bacteria from a minimally processed vegetables plant." LWT-Food Science and Technology **85**: 293-300.

Minchin, D. and S. Gollasch (2003). "Fouling and ships' hulls: how changing circumstances and spawning events may result in the spread of exotic species." Biofouling **19**(S1): 111-122.

Ministry for Primary Industries. (2018). Craft Risk Management Standard: Biofouling on Vessels Arriving to New Zealand. Wellington, New Zealand, New Zeland Government.

Ministry for Primary Industries.. (2018). The Craft Risk Management Standard for Biofouling: Frquently Asked Questions. Wellington, New Zealand, New Zealand Government.

Nurioglu, A. G. and A. C. C. Esteves (2015). "Non-toxic, non-biocide-release antifouling coatings based on molecular structure design for marine applications." Journal of Materials Chemistry B **3**(32): 6547-6570.

Palmer, J., S. Flint and J. Brooks (2007). "Bacterial cell attachment, the beginning of a biofilm." Journal of industrial microbiology & biotechnology **34**(9): 577-588.

Patel, A., O. Kravchenko and I. Manas-Zloczower (2018). "Effect of curing rate on the microstructure and macroscopic properties of epoxy fiberglass composites." Polymers **10**(2): 125.

Porra, R. J., W. A. Thompson and P. E. Kriedemann (1989). "Determination of accurate extinction coefficients and simultaneous equations for assaying chlorophylls a and b extracted with four different solvents: verification of the concentration of chlorophyll standards by atomic absorption spectroscopy." Biochimica et Biophysica Acta (BBA) - Bioenergetics **975**(3): 384-394.

Ramos, V., J. Morais, R. Castelo-Branco, Â. Pinheiro, J. Martins, A. Regueiras, A. L. Pereira, V. R. Lopes, B. Frazão and D. Gomes (2018). "Cyanobacterial diversity held in microbial biological resource centers as a biotechnological asset: the case study of the newly established LEGE culture collection." Journal of applied phycology **30**(3): 1437-1451.

Rees, G. and J. Bartram (2002). Monitoring bathing waters: a practical guide to the design and implementation of assessments and monitoring programmes. Boca Raton, FL, USA, CRC Press.

Romeu, M. J., P. Alves, J. Morais, J. M. Miranda, E. D. de Jong, J. Sjollema, V. Ramos, V. Vasconcelos and F. J. Mergulhão (2019). "Biofilm formation behaviour of marine filamentous cyanobacterial strains in controlled hydrodynamic conditions." Environmental Microbiology **21**(11): 4411-4424.

Schultz, M., J. Bendick, E. Holm and W. Hertel (2011). "Economic impact of biofouling on a naval surface ship." Biofouling **27**(1): 87-98.

Silva, E., O. Ferreira, P. Ramalho, N. Azevedo, R. Bayón, A. Igartua, J. Bordado and M. Calhorda (2019). "Eco-friendly non-biocide-release coatings for marine biofouling prevention." Science of the Total Environment **650**: 2499-2511.

Takata, L. T., M. B. Falkner and S. Gilmore (2006). Analysis, Evaluation, and Recommendations to Reduce Nonindigenous Species Release from the Non-Ballast Water Vector. Sacramento, CA, USA, California State Lands Commission.

Taylor, D. A. (1996). Introduction to marine engineering. Amsterdam, The Netherlands, Elsevier.

Telegdi, J., L. Trif and L. Románszki (2016). Smart anti-biofouling composite coatings for naval applications. Smart Composite Coatings and Membranes. M. F. Montemos, Woodhead Publishing**:** 123-155.

Thomen, P., J. Robert, A. Monmeyran, A.-F. Bitbol, C. Douarche and N. Henry (2017). "Bacterial biofilm under flow: first a physical struggle to stay, then a matter of breathing." PloS one **12**(4).

4.

Experimental assessment of the performance of two marine coatings to curb biofilm formation of microfoulers[b]

Abstract

Biofilms formed on submerged marine surfaces play a critical role in the fouling process, causing increased fuel consumption, corrosion, and high maintenance costs. Thus, marine biofouling is a major issue and motivates the development of AF coatings. In this study, the performance of two commercial marine coatings, a foul-release silicone-based paint (SilRef) and an epoxy resin (EpoRef), was evaluated regarding their abilities to prevent biofilm formation by *Cyanobium* sp. and *Pseudoalteromonas tunicata* (common microfoulers). Biofilms were developed under defined hydrodynamic conditions to simulate marine settings, and the number of biofilm cells, wet weight, and thickness were monitored

[b] The content of this chapter was adapted from the following publication(s):

Faria, S. I., R. Teixeira-Santos, L. C. Gomes, E. R. Silva, J. Morais, V. Vasconcelos and F. J. Mergulhão (2020). "Experimental assessment of the performance of two marine coatings to curb biofilm formation of microfoulers." Coatings **10**(9): 893.

for 7 weeks. The biofilm structure was analyzed by confocal laser scanning microscopy (CLSM) at the end-point. Results demonstrated that EpoRef surfaces were effective in inhibiting biofilm formation at initial stages (until day 28), while SilRef surfaces showed high efficacy in decreasing biofilm formation during maturation (from day 35 onwards). Wet weight and thickness analysis, as well as CLSM data, indicate that SilRef surfaces were less prone to biofilm formation than EpoRef surfaces. Furthermore, the efficacy of SilRef surfaces may be dependent on the fouling microorganism, while the performance of EpoRef was strongly influenced by a combined effect of surface and microorganism.

4.1. Introduction

In marine environments, aquatic micro and macroorganisms - such as bacteria, algae, and invertebrates - spontaneously colonize submerged surfaces in a process known as biofouling (Silva et al. 2019, Tian et al. 2020). This natural phenomenon has severe economic and environmental implications all over the world (Kuliasha et al. 2019, Silva et al. 2019, Tian et al. 2020). Fouling organisms attached to marine vessel hulls promote surface corrosion and increase frictional drag, leading to higher dry-docking periods and fuel consumption, respectively (Tian et al. 2020). Additionally, biofouling can damage several marine facilities, including oil production platforms, aquaculture systems, and industrial marine water inlet systems, causing substantial economic losses (Tian et al. 2020). Furthermore, marine biofouling promotes the bio-invasion of non-indigenous species traveling with marine vessels (ships, yachts, or sailing boats) between different ecosystems, playing a negative impact on global biodiversity (Lacoursière-Roussel et al. 2012, Mineur et al. 2007, Neves et al. 2020). Therefore, inhibiting biofouling is one of the most important challenges faced by marine industries and environmental agencies.

The biofouling process begins with the colonization of microfoulers (e.g., cyanobacteria, bacteria, algae, and diatoms) and biofilm formation (Gu 2018, Selim et al. 2017). Biofilms formed on marine surfaces protect microorganisms from the action of adverse environmental conditions and allow the occurrence of macrofouling by bryozoans, mollusks, polychaeta, tunicates, coelenterates, or fungi (marine macrofoulers) (Tu et al.

2020). In recent decades, several authors have sought to develop efficient and environmentally friendly marine coatings, aiming to inhibit biofilm formation of microfoulers as a preventive strategy to reduce or delay marine biofouling and its undesirable consequences.

In this chapter, the performance of two commercial marine coatings - a silicone-based paint (SilRef) and an epoxy resin (EpoRef) - was evaluated to prevent biofilm formation by marine microfoulers. The silicone-based paint is a third-generation hydrogel-based FRC, frequently used to coat the ship's hulls, marine water inlet piping, and grids in power stations (Hempel 2016). It combines hydrogel polymers with silicone fouling-release technology to originate PDMS matrices with self-stratifying hydrogel-promoting polymers, conferring, upon water contact, a more hydrophilic character to the hydrophobic polymer matrix and additives. It is thus able to prevent or weaken hydrophobic or hydrophilic interactions, minimizing the adsorption of proteins, bacteria, and complementing the ability of the original FRC approach (Banerjee et al. 2011). In recent years, FRCs - including PDMS-based matrices - have attracted considerable attention because they are biocide-free and hence environmentally friendly, efficient, and have a relatively long life-cycle (Hu et al. 2020, Selim et al. 2017, Tian et al. 2020). Silicone polymers have been widely employed in FRC development due to their ability to provide coating films of low surface tension and porosity, excellent elasticity, heat resistance, and durability against UV irradiation (Selim et al. 2017); as well as proven efficacy against common marine algae, diatoms, tube worms, hydrozoans, barnacles, and mussels (Hu et al. 2020, Krishnan et al. 2008). Additionally, among the most used coating materials, hydrogel polymers combined with diverse other polymers have demonstrated high AF performance against marine organisms, becoming a focus of increasing interest (Murosaki et al. 2012, Zhu et al. 2020). In turn, the polymeric epoxy resin is commonly used to coat the hulls of small recreational vessels (Chambers et al. 2006, Palmer et al. 2007) due to its unique physical, chemical, and mechanical properties, safety issues, and low cost (Mostafaei and Nasirpouri 2013). Epoxy composites also demonstrated high durability and resistance to fatigue and UV irradiation (Hoge and Leach 2016).

Although both commercial coatings are typically used in vessel hulls, the microfoulers' response to these surfaces is not adequately characterized. The present chapter aims to evaluate the long-time performance of a silicone-based paint and an epoxy resin

against biofilm formation by two common microfouling organisms, *Pseudoalteromonas tunicata* and *Cyanobium* sp. LEGE 10375, under defined hydrodynamic conditions in order to predict the antibiofouling response in real marine settings where these surfaces can be used. The fouling behavior of *P. tunicata* has been widely described (Abouelkheir et al. 2020, Rao et al. 2005) and this organism has become one of the preferred test organisms for surface fouling evaluation. *Cyanobium* sp. is distributed in a wide range of habitats like brackish, marine, and freshwater environments around the planet (Komárek and Anagnostidis 1998). Given the fouling potential demonstrated in the current study, it is surprising that only one publication assessed the biofilm formation behavior of a strain from this genus (*Cyanobium* sp. LEGE 06097) in controlled hydrodynamics (Faria et al. 2020). To the best of our knowledge, the present chapter is the first to describe the performance of AF marine coatings against *Cyanobium* sp. LEGE 10375. Understanding how AF surfaces interact with microfoulers can clarify and help to improve their efficacy, leading to the development of new AF coatings to address this challenge.

4.2. Materials and methods

4.2.1. Surface preparation

Two commercial marine coatings, a silicone-based paint (SilRef) and an epoxy resin (EpoRef) were used in this study. Glass coupons (1 cm x 1 cm; Vidraria Lousada, Lda, Lousada, Portugal) were cleaned and disinfected (Faria et al. 2020) before being used as a substrate for coating. The silicone-based paint was provided by Hempel A/S (HEMPASIL X3+ 87500, Copenhagen, Denmark) and it is a two-component system obtained from blending a base resin (Hempasil Base 87509) and curing agent (Hempasil Crosslinker 98951) in a ratio of 17.8/2.2 (v/v). SilRef-coated glass surfaces were prepared using conventional brush painting, following the recommendations of the manufacturer: a prior glass coupons coating with a universal tie-coat (base resin XA17-17310 and curing agent XA18-RD003) and a curing step at room temperature (about 23 °C) for 8 h, followed by a second coating with the HEMPASIL system, and curing step at room temperature (about 23 °C) for 24 h.

Finally, the cured SilRef-coated glass coupons were sterilized with UV radiation for 30 min before use.

The epoxy resin was produced by HB Química (Matosinhos, Porto, Portugal) and consisted of a mixture of HB Eposurf 2 resin and HB Eposurf hardener in a ratio of 10:3 (v/v) (Faria et al. 2020). For the production of EpoRef-coated glass surfaces, 70 µL of epoxy resin was deposited on top of the glass coupons using spin coating (Spin150 PolosTM, Paralab, Porto, Portugal) at 6000 rpm, with increments of 1000 rpm, for 40 s. Then, the surfaces were dried in two steps: (i) 12 h at room temperature (approximately 25 ºC), and (ii) 3 h at 60 ºC, according to the instructions from the manufacturer (Faria et al. 2020), and sterilized by using immersion in 70% (v/v) ethanol (VWR International S.A.S., Fontenay-sous-Bois, France) for 20 min. Before the biofilm formation experiments, the initial weight of each coupon was determined.

4.2.2. Surface characterization

4.2.2.1. Atomic force microscopy (AFM)

AFM studies were carried out using a PicoPlus scanning probe microscope interfaced with a Picoscan 2500 controller (both from Keysight Technologies, Santa Rosa, CA, USA). Each sample was imaged with a 100 x 100 μm^2 piezo-scanner. The surface roughness was determined in 40 x 40 μm^2 scanned areas in three randomly chosen locations per sample (total of three replicates) at room temperature. The SilRef and EpoRef surfaces were analyzed through contact mode, with a v-shape silicon tip, with a spring constant of 0.085 N/m and 0.284 N/m (AppNano, Mountain View, CA, USA), respectively. The scan speed was set at 1.0 L/s. The WSxM5.0 software (Nanotec Electronica, Feldkirchen, Germany) was used to perform the roughness surface measurements and to obtain the 2D images (Horcas et al. 2007). The roughness height parameter calculated was the average roughness (R_a).

4.2.2.2. Hydrophobicity

Surface hydrophobicity was evaluated according to the approach developed by Oss et al. (van Oss 1994). Contact angles were determined at 25 ± 2 ºC by the sessile drop method through a contact angle meter (Dataphysics OCA 15 Plus, Filderstadt, Germany), as fully described by Gomes *et al.* (Gomes et al. 2015) in three independent assays. For each assay, at least 25 measurements were performed for each material.

4.2.3. Marine organisms and growth conditions

Pseudoalteromonas tunicata DSM 14096 (DSMZ, Braunschweig, Germany) and *Cyanobium* sp. LEGE 10375 were used in this study because they have been described as early colonizers (microfoulers) of marine surfaces (Lee et al. 2008, Sekar et al. 2004). Marine *P. tunicata* was stored at -80 ºC in 20% (v/v) glycerol; before experiments, bacteria were spread on the complex marine medium Våatanen Nine Salt Solution (VNSS) prepared according to Holmström *et al.* (Holmstrõm et al. 1998) and supplemented with 15 g/L agar (VWR International S.A.S., Fontenay-sous-Bois, France), and incubated at 25 ºC for 24 h. Then, an overnight culture (16–18 h) of *P. tunicata* was prepared by transferring colonies from the VNSS agar plate to 150 mL of VNSS broth and incubating at 25 ºC, 160 rpm. *Cyanobium* sp. strain was isolated from the intertidal zone, on a marine sponge, collected in October 2010, at São Bartolomeu do Mar beach (41.57378 N 8.798556 W) located in Esposende, Portugal. This cyanobacterial strain belongs to the LEGE-CC deposited at the CIIMAR, Porto, Portugal (Ramos et al. 2018). Cyanobacteria were grown in 750 mL Z8 medium supplemented (Kotai 1972) with 25 g/L of synthetic sea salts (Tropic Marin) and vitamin B12 (Sigma Aldrich, Merck, Saint Louis, MO, USA) under 14 h light (10–30 mol photons/m^2/s, λ = 380–700 nm)/10 h dark cycles at 25 ºC.

4.2.4. Biofilm formation

Biofilm experiments were performed using 12-well MTPs (VWR International, Carnaxide, Portugal) under controlled hydrodynamic conditions. Sterilized SilRef and

EpoRef coupons were fixed to the microplate wells with double-sided adhesive tape (Faria et al. 2020). A *P. tunicata* suspension at an optical density (OD) 610 nm) of 0.1 (which corresponds to 10^8 cells/mL) was prepared from an overnight culture, while the cyanobacterial culture was centrifuged to remove any traces of the supplemented Z8 medium and the pellet was resuspended in fresh VNSS medium to a final concentration of 10^8 cell/mL. Subsequently, 3 mL of each cell suspension was added to the wells, and the plates were incubated at 25 ºC in an orbital shaker with 25 mm diameter (Agitorb 200ICP, Norconcessus, Ermesinde, Portugal) at 185 rpm under alternate light cycles of 14 h light (10–30 mol photons/m^2/s)/10 h dark. According to previous computational fluid dynamic studies performed by the group (Faria et al. 2020, Romeu et al. 2019), the selected shaking frequency of 185 rpm produces an average shear rate of 40 s^{-1} and a maximum of 120 s^{-1} at the plate bottom, including for instance the shear rate estimated for a ship in a harbor (50 s^{-1}) (Bakker et al. 2003). Biofilm formation was monitored for seven weeks (49 days) and sampled every seven days. During the incubation period, the culture medium was replaced twice a week. Three independent biofilm formation experiments (biological replicates) were performed with two technical replicates each (two coupons of SilRef or EpoRef).

4.2.5. Biofilm analysis

Every seven days, the culture medium was carefully removed, and the coupons were gently washed with 3 mL of 0.85% (v/v) sterile saline solution to remove loosely attached microorganisms. Two coupons from each experimental condition were analyzed regarding (i) the number of biofilm cells, (ii) biofilm wet weight, and (iii) biofilm thickness. Additionally, the biofilm structure was analyzed at day 49 using CLSM.

4.2.5.1. Biofilm cell counting and wet weight

For cell counting, coupons were taken out of the wells, dipped in 2 mL of 0.85% (v/v) sterile saline solution and vortexed for 3 min at maximum power to release biofilm cells. Then, 10 µL of each cell suspension was placed on each side of a Neubauer chamber and

observed in a bright field microscope (Nikon Eclipse LV100 microscope, Nikon Corporation, Tokyo, Japan).

To assess the wet weight of biofilms, coupons were removed from the wells with a tweezer and weighted on an analytical balance. The biofilm wet weight was determined by the difference between the initial weight of coupon (before inoculation) and the weight measured on the sampling day.

4.2.5.2. Biofilm thickness

Biofilm thickness was assessed through OCT (Thorlabs Ganymede Spectral Domain Optical Coherence Tomography system, Thorlabs GmbH, Dachau, Germany) with a central wavelength of 930 nm. Before biofilms were imaged, the culture medium was carefully removed from the microplate wells, the coupons were gently washed, and the wells were filled with 3 mL of 8.5 g/L NaCl sterile solution. Since biofilms are essentially composed of water (Telegdi et al. 2016), the established refractive index was 1.40, close to the refractive index of water (1.33). At each sampling day, a minimum of five different fields of view (2D images) per material and microorganism were analyzed and captured. Image analysis was performed using a routine developed in the Image Processing Toolbox from MATLAB 8.0 and Statistics Toolbox 8.1 (The MathWorks, Inc., Natick, MA, USA), as described by Romeu et al. (Romeu et al. 2020).

4.2.5.3. CLSM

At day 49, coupons containing the biofilms were removed from the microplates, washed with saline solution, and stained with 6 µM Syto9 (Thermo Fisher Scientific, Waltham, MA, USA) - a green cell-permeant nucleic acid marker - for 10 min at room temperature. Each stained sample was mounted on a microscopic slide and image acquisition was performed using a Leica TCS SP5 II Confocal Laser Scanning Microscope (Leica Microsystems, Wetzlar, Germany). All biofilms were scanned at 400 Hz using a 40x water objective lens (LEICA HCX PL APO CS 40.0x/1.10WATER UV) with a 488-nm argon laser set at 25% intensity. The emitted fluorescence was recorded within the range of 500–600 nm.

A minimum of five stacks of horizontal-plane images (512 x 512 pixels, corresponding to 387.5 µm x 387.5 µm) with a z-step of 1 µm were acquired per sample.

Three-dimensional (3D) projections of the biofilms were constructed from the CLSM acquisitions using the "Easy 3D" function of the IMARIS 9.1 software (Bitplane, Zurich, Switzerland). Quantitative structural parameters (biovolume and surface coverage) were extracted from confocal image series with the plug-in COMSTAT2 (Heydorn et al. 2000) run in ImageJ 1.48v software (Schneider et al. 2012). While the biovolume provides an estimate of the biomass in the biofilm ($\mu m^3/\mu m^2$), the surface coverage corresponds to the percentage of surface area covered on the biofilm base.

4.2.6. Data analysis

Descriptive statistics were used to calculate the mean and standard deviation for the different biofilm parameters (number of biofilm cells, wet weight, thickness, biovolume, and surface coverage).

Data analysis was performed using the GraphPad Prism® for Windows, version 8 (GraphPadSoftware, Inc., San Diego, CA, USA). Since the variable distribution was normal, Student's *t-test* was used to compare biofilm formation between the two marine surfaces tested (SilRef and EpoRef) for both *P. tunicata* and *Cyanobium* sp. LEGE 10375 strains. The same statistical test was used to compare the biovolume and surface coverage of *P. tunicata* and *Cyanobium* sp. LEGE 10375 biofilms between the two tested surfaces at the end of the experiment (day 49). Significant results were considered for p-values < 0.1.

In order to ascertain the performance of SilRef and EpoRef marine coatings to curb biofilm formation of main microfoulers, the surface and microorganism influence were estimated for each parameter monitored over time (number of biofilm cells, wet weight, and thickness) and represented in radar charts. Radar charts were split into four quadrants and each one represents the average values obtained in each sampling point (days) for the following assays: *P. tunicata* biofilm formation on SilRef (Ps/SilR, top right quadrant); *P. tunicata* biofilm formation on EpoRef (Ps/EpoR, bottom right quadrant); *Cyanobium* sp. biofilm formation on EpoRef (Cya/EpoR, bottom left quadrant); and *Cyanobium* sp. biofilm formation on SilRef (Cya/SilR, top left quadrant). The influence of the microorganism on

biofilm development was calculated by subtracting the values obtained for the two microfoulers for both SilRef (Ps/SilR vs. Cya/SilR) and EpoRef (Ps/EpoR vs. Cya/EpoR) surfaces, whereas the influence of the surface on biofilm development was determined by subtracting the values obtained for two different surfaces for *P. tunicata* (Ps/SilR vs. Ps/EpoR) and *Cyanobium* sp. (Cya/SilR vs. Cya/EpoR) microfoulers. All positive differences were considered as increments resulting from the microorganism or surface effect and represented by a colored area (microorganism effect - orange area; surface effect - red area). The combined effect (blue area) has been plotted whenever the surface effect overlapped the microorganism effect.

4.3. Results

In this study, the antibiofilm efficacy of two commercial marine coatings, a silicone-based paint (SilRef) and an epoxy resin (EpoRef), was determined through the analysis of *Cyanobium* sp. and *P. tunicata* biofilms developed on SilRef- and EpoRef-coated glass substrates for 49 days under hydrodynamic conditions that mimic the marine environment.

The SilRef and EpoRef surfaces were first analyzed concerning their hydrophobicity and roughness (Table 4.1.). Both water contact angles (θ_w) and degree of hydrophobicity (ΔG) indicated that the SilRef is more hydrophobic than the EpoRef surface (θ_w EpoRef = 69.4º, vs. θ_w SilRef = 108.4º Figure 4.1.; ΔG_{EpoRef} = -26.7 mJ/m^2 vs. ΔG_{SilRef} = -55.8 mJ/m^2).

The surface topography of SilRef and EpoRef surfaces was examined by AFM in contact mode (Figure 4.2.). The topography images revealed that both coatings are homogeneous and very smooth. In fact, the roughness of both surfaces is at a nanoscale, suggesting that there are no features in the surfaces to act as niches for the microfoulers. Nevertheless, the SilRef surface displayed higher roughness with an average value (R_a) of 49.7 nm, in opposition to R_a = 12.9 nm for the EpoRef surface (Table 4.1.).

Table 4.1. Contact angles with water (θ_w), formamide (θ_F) and α-bromonaphthalene (θ_B), hydrophobicity (ΔG) and roughness (R_a) determined for the SilRef and EpoRef surfaces. Values are presented as means ± standard deviations.

Surface	Contact angles (°)			Hydrophobicity (mJ/m^2)	Roughness (nm)
	θ_w	θ_F	θ_B	ΔG	R_a
EpoRef	69.4 ± 3.0	56.8 ± 3.0	23.3 ± 2.2	-26.7	12.9 ± 2.9
SilRef	108.4 ± 3.5	104.0 ± 1.9	70.0 ± 2.0	-55.8	49.7 ± 8.3

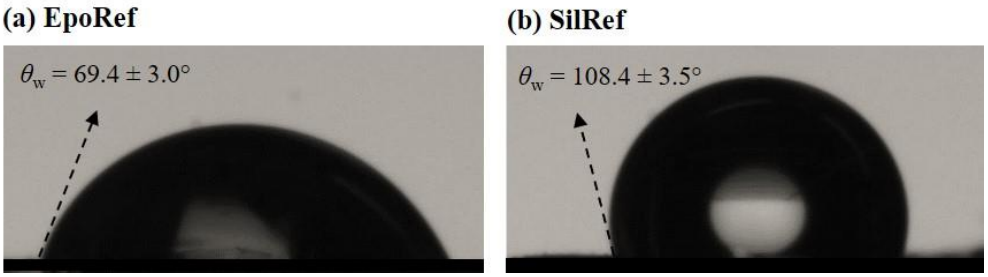

Figure 4.1. Representative images of water contact angle (θ_w) measurements on EpoRef (a) and SilRef (b) coatings.

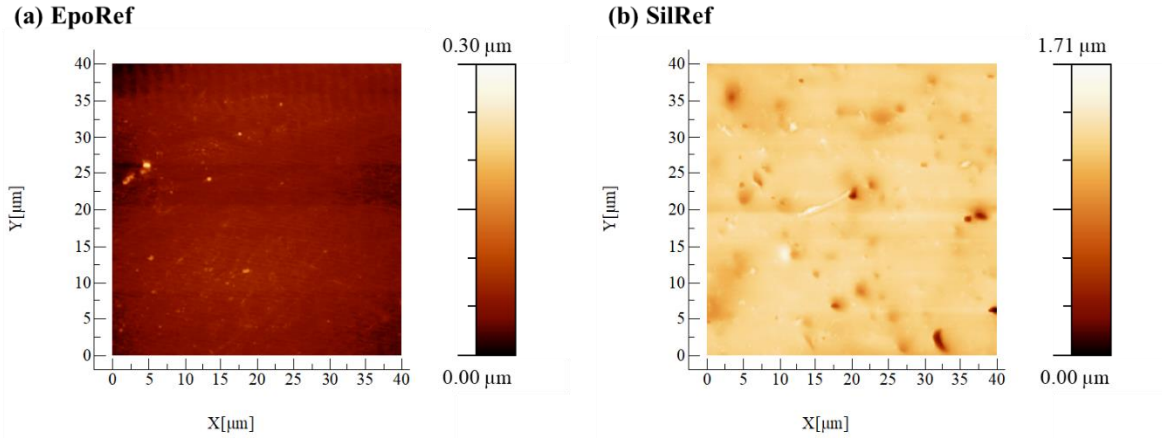

Figure 4.2. AFM images of EpoRef **(a)** and SilRef **(b)** surfaces with a scan range of 40 µm x 40 µm (contact mode). The color bar corresponds to the z-range of the respective image.

Results of biofilm analysis - including the number of biofilm cells, wet weight, and thickness - are presented in Figure 4.3. In general, regardless of the surface material, the cyanobacterial strain has higher biofilm-forming capacity than *P. tunicata*. This is

particularly evident in the last two weeks of the experiment (between days 35 and 49), in which the wet weight and mean thickness values obtained for the cyanobacterial biofilms (Figure 4.3.b,c) were about 26% higher than those of bacterial biofilms (Figure 4.3.e,f). On the other hand, it is possible to globally observe that, while the biofilm parameters for cyanobacteria (in particular, the wet weight and thickness) followed an increasing tendency over time, there was a certain stagnation of the biofilm values for the marine bacteria, regardless of the surface (Figure 4.3.).

Looking at the cell number of *Cyanobium* sp. biofilms (Figure 4.3.a), there was a growing trend for EpoRef surfaces from day 7 (with 8.39 x 10^7 cells/cm^2) to the end of the experiment (with 1.25 x 10^9 cells/cm^2). The beneficial effect of the SilRef surfaces was particularly evident towards the end of the experimental period, when a reduction in the cell number of about 26% was registered compared to EpoRef surfaces for day 49 ($p < 0.05$, Figure 4.3.a). For *P. tunicata* biofilms (Figure 4.3.d), the number of cells increased until day 21 and then kept more or less constant for both surfaces (on average, 7.66 x 10^8 cells/cm^2). Again, at day 49, the SilRef-coated surfaces presented 17% less cells than the EpoRef surfaces ($p < 0.1$, Figure 4.3.b).

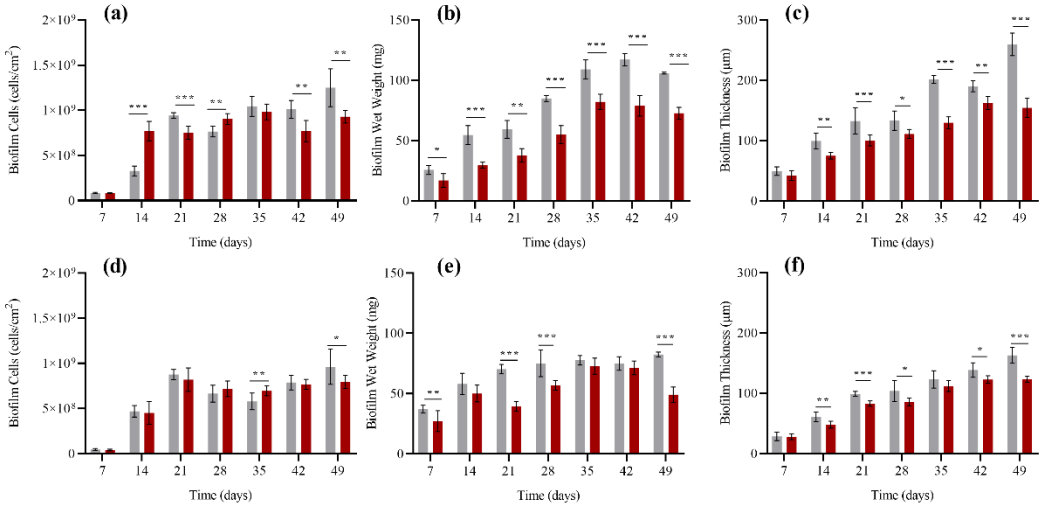

Figure 4.3. Effect of two commercial coatings (■ EpoRef; ■ SilRef) on biofilm development of *Cyanobium* sp. LEGE 10375 (a–c) and *Pseudoalteromonas tunicata* (d–f) for 49 days. The analyzed parameters refer to the number of biofilm cells (a,d), biofilm wet weight (b,e), and biofilm thickness (c,f). Statistical analysis was performed by paired t-test, and significant differences between the two surfaces are indicated with *** ($p < 0.01$), ** ($p < 0.05$), and * ($p < 0.1$).

The wet weight of *Cyanobium* sp. biofilms developed either on SilRef or EpoRef surfaces (Figure 4.3.b) increased until day 35. In all sampling points, statistically significant differences were found between the wet weight of biofilms developed on EpoRef and SilRef surfaces. Indeed, on SilRef surfaces, *Cyanobium* sp. biofilms weighted, on average, 33% less than the biofilms formed on EpoRef surfaces.

The wet weight of *P. tunicata* biofilms (Figure 4.3.e) increased on both surfaces until day 35 and then remained constant, with exception of biofilms formed on SilRef surfaces whose wet weight decreased on day 49. An average wet weight reduction of 35% was obtained for biofilms developed on SilRef compared to those formed on EpoRef surfaces (Figure 4.3.e).

The mean thickness of *Cyanobium* sp. biofilms generally increased until day 49 (Figure 4.3.c) and biofilms formed on SilRef surfaces had, on average, 27% lower thickness than those developed on EpoRef surfaces throughout the experiment. This difference was particularly visible on day 49, when the biofilm formed on SilRef had almost half the mean thickness of the biofilm grown on EpoRef surfaces ($p < 0.01$, Figure 4.3.c). The thickness of *P. tunicata* biofilms also increased over time (Figure 4.3.f), stabilizing on day 42 for biofilms developed on SilRef surfaces. On average, *P. tunicata* biofilms developed on SilRef surfaces were approximately 15% thinner than those developed on EpoRef surfaces.

The relative importance of surface properties and microorganism type on biofilm formation was estimated for each analyzed parameter (Figure 4.3.) and graphically represented in Figure 4.4 where only increases in the assayed parameters are depicted. For *Cyanobium* sp. biofilms developed on SilRef surfaces (top left quadrant), the microfouler organism had a strong influence on the increase of biofilm cells, wet weight, and thickness (Figure 4.4.a–c), as represented by the orange area. Additionally, a subtle combined effect was observed between the surface and microorganism (blue area) that contributed to a higher number of cells at an early stage of *Cyanobium* sp. biofilm formation (between day 7 and 28) (Figure 4.4.a). For *Cyanobium* sp. biofilms formed on EpoRef surfaces (bottom left quadrant), a combined effect between the surface and microorganism (blue area) was responsible for a higher number of biofilm cells, wet weight, and thickness (Figure 4.4.a–c). This effect was more noticeable from day 35 of biofilm formation. Although the

microorganism type affected biofilm formation, the combined effect was stronger (blue area > orange area) (Figure 4.4.a–c). Moreover, the surface effect (red area) contributed to an increase of *Cyanobium* sp. biofilm wet weight at an early stage of its development (Figure 4.4.b).

For *P. tunicata* biofilms formed on SilRef surfaces (top right quadrant), an increase in the assayed parameters is not seen due to the effect of the microorganism type (orange area) as only a slight increase in wet weight can be seen in Figure 4.4.b. In turn, for *P. tunicata* biofilms formed on EpoRef surfaces (bottom right quadrant), a strong influence of the surface (red area) was visible, contributing to a higher number of biofilm cells, wet weight, and thickness (Figure 4.4.a–c). Additionally, the combined effect between the surface and microorganism had a small influence on the biofilm wet weight at an early development stage (days 7 and 14) (Figure 4.4.a).

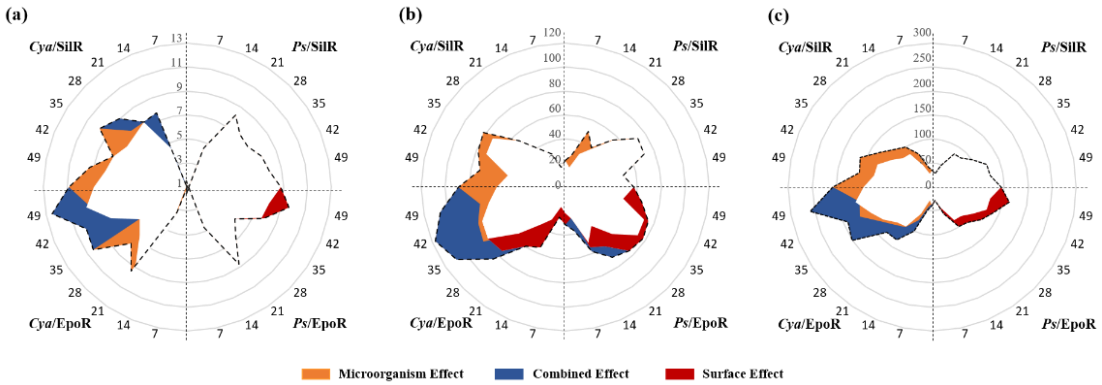

Figure 4.4. Radar charts representing **(a)** the number of cells (108 cells/cm2), **(b)** wet weight (mg), and **(c)** thickness (µm) for *Pseudoalteromonas tunicata* (Ps, right side) and *Cyanobium* sp. LEGE 10375 (Cya, left side) biofilms developed on SilRef (upperside) and EpoRef (downside) surfaces. Average values (previously represented in Figure 4.3) are plotted as a dashed line considering the time scale (days) indicated in each quadrant. The following conditions are depicted in each quadrant: Ps/SilR (top right quadrant), *P. tunicata* on SilRef; Ps/EpoR (bottom right quadrant), *P. tunicata* on EpoRef; Cya/EpoR (bottom left quadrant), *Cyanobium* sp. on EpoRef; Cya/SilR (bottom right quadrant), *Cyanobium* sp. on SilRef. Colored areas represent the microorganism or surface effect, which are equivalent to all positive differences observed in each parameter (biofilm cell number, wet weight, and thickness), when subtracting the results obtained at the same microorganism (surface effect) or with the same surface (microorganism effect). Overlap areas are also highlighted, indicating a combined effect of the microorganism and surface.

The structural differences between the *Cyanobium* sp. and *P. tunicata* single-species biofilms formed on the two tested surfaces at the end of the experiment (49 days) were evaluated using CLSM. Examples of 3D biofilm reconstructions are presented in Figure 4.5. It is possible to observe that denser and thicker biofilms grew on the epoxy resin, regardless of the microorganism (Figure 4.5.a,c), which confirms the results of the biofilm cell number (Figure 4.3.a,b) and thickness (Figure 4.3.c,d) obtained by bright field microscopy and OCT, respectively. On the contrary, biofilms formed on the silicone-based coating were thinner and did not cover the entire surface area (Figure 4.5.b,d) due to the formation of large cell aggregates, which are particularly visible in the *P. tunicata* biofilm (Figure 4.5.d). In fact, while in the EpoRef surfaces, both *Cyanobium* sp. and *P. tunicata* biofilms displayed a surface coverage above 70%, it was only around 45% in the SilRef surfaces ($p < 0.01$, Figure 4.6.b,d). With regard to biovolumes (Figure 4.6.a,c), they were also significantly higher for the EpoRef surfaces when compared to the SilRef surfaces. In the case of cyanobacteria, the biovolume determined for the EpoRef surfaces was about 3 times higher than that found for the SilRef surfaces after 49 days of biofilm development. This is correlated to the higher cell density and weight of cyanobacterial biofilms on the EpoRef coating at the experimental end-point (Figure 4.3.a,b).

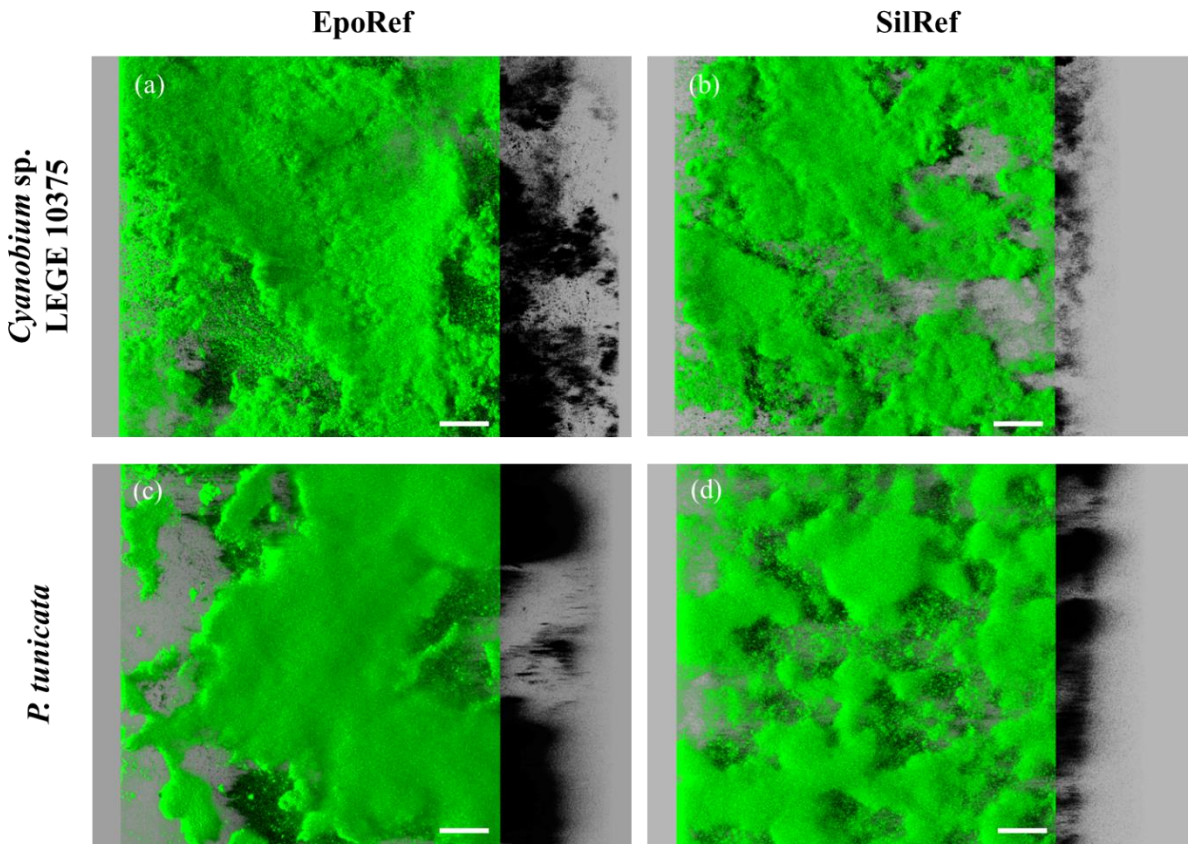

Figure 4.5. Representative biofilm structures of (a) *Cyanobium* sp. LEGE 10375 on EpoRef surface, (b) *Cyanobium* sp. LEGE 10375 on SilRef surface, (c) *Pseudoalteromonas tunicata* on EpoRef surface, and (d) *Pseudoalteromonas tunicata* on SilRef surface after 49 days of biofilm formation. These images were obtained from confocal z-stacks using IMARIS software and present an aerial, 3D view of the biofilms (shadow projection on the right). The scale bar is 50 µm.

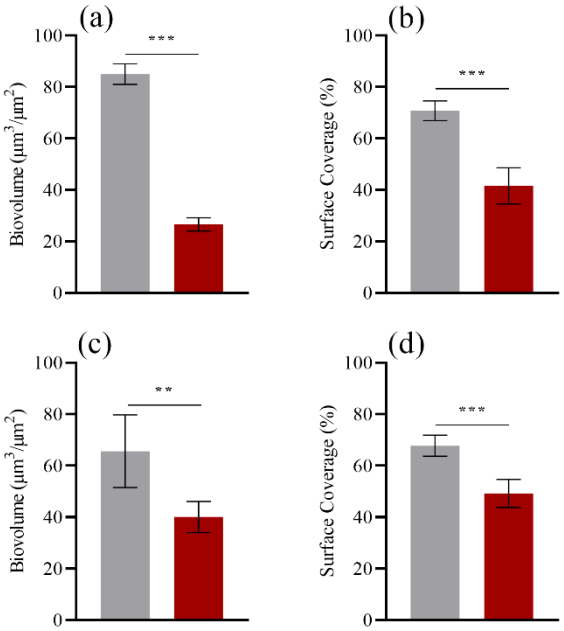

Figure 4.6. Biofilm structural parameters obtained from the z-stacks acquired at the confocal laser scanning microscopy (CLSM) after 49 days: biovolume **(a, c)** and surface coverage **(b,d)**. *Cyanobium* sp. LEGE 10375 **(a, b)** and *Pseudoalteromonas tunicata* **(c, d)** biofilms formed on EpoRef (■) and SilRef (■) surfaces. Standard deviations for three independent experiments are presented. Statistical analysis was performed by using paired t-test, and significant differences between two surfaces are indicated with *** ($p < 0.01$) and ** ($p < 0.05$).

4.4. Discussion

In this chapter, the long-term performance of two commercial marine coatings, a silicone-based paint and an epoxy resin, to prevent biofilm formation by common microfoulers was demonstrated through the kinetic evaluation of different biofilm parameters, including the number of biofilm cells, wet weight, and thickness. For this purpose, *Cyanobium* sp. and *P. tunicata* biofilms were developed on both surfaces for seven weeks under controlled hydrodynamic conditions that mimic those found in some marine

settings. As the hydrodynamic forces bring a strong impact on marine biofilm development (Ali et al. 2020, Fang et al. 2020, Faria et al. 2020, Romeu et al. 2019), the experiments were performed under specific shear forces that include the shear rate estimated for a ship in a harbor (50/s) (Bakker et al. 2003) in order to increase the predictive value of the results.

At an initial development stage (until day 28), *Cyanobium* sp. biofilms formed on SilRef-coated surfaces presented, on average, a higher number of cells compared to biofilms formed on EpoRef surfaces. However, from day 35 onwards, the number of biofilm cells stabilized on SilRef surfaces, while on EpoRef surfaces this number increased up to day 49. A similar biofouling response was detected for *P. tunicata* biofilms. Until day 28, the number of cells of biofilms formed on SilRef surfaces was slightly higher than those obtained for biofilms formed on EpoRef. However, on SilRef surfaces, the biofilm cell number was maintained, while on EpoRef surfaces, it increased up to day 49. Based on this parameter, the EpoRef surfaces effectively inhibited biofilm formation at initial stages (until day 28), while SilRef surfaces showed higher AF activity during biofilm maturation (from day 35 onwards). Indeed, surface characterization analysis demonstrated that the EpoRef surface is less hydrophobic and rough, which may explain its higher performance at initial stages of biofilm formation. In opposition, the higher hydrophobicity and roughness of SilRef may have hindered their initial AF activity. However, despite several studies reporting a correlation between the surface hydrophobicity and roughness and cell attachment (De-la-Pinta et al. 2019, Ozkan and Berberoglu 2013), there is evidence that the biofilm formation induces changes in the surface properties (Mazumder et al. 2010, Moreira et al. 2017). These findings corroborate the higher AF activity of SilRef surfaces during the biofilm maturation stages.

SilRef is a commercial coating, and accordingly with its technical properties, is based on a dual-mode of action, a ‘non-stick’ ability and a foul-release effect, allied to its relative higher elasticity (Young’s modulus). These properties may contribute to decreasing fouling settlements and cell cohesion interactions (Bakker et al. 2003, Hempel 2016, Selim et al. 2017), as confirmed by using confocal microscopy for both studied marine strains. Besides, this dual-action has improved the FRC original properties by the hydrogel contribution in its singular hydrogel-PDMS polymeric matrix, which acquires a more hydrophilic character upon contact with water. Thus, it can prevent either weaker hydrophobic or hydrophilic

interactions, which can delay the adsorption of proteins, bacteria, and subsequent fouling (Banerjee et al. 2011, Hu et al. 2020, Murosaki et al. 2012).

Recently, Faria *et al.* demonstrated the impact of the surface properties on marine biofilm formation under controlled hydrodynamic conditions (Faria et al. 2020). Indeed, surface properties may promote cell–surface interactions that, even in a low magnitude, may facilitate microfouler retention and contribute to biofilm development (Thomen et al. 2017).

Although there was a shift between the number of cells of biofilms formed on SilRef and EpoRef surfaces that may be dependent on the biofilm age, wet weight and thickness analysis revealed that, in all development stages, *Cyanobium* sp. and *P. tunicata* biofilms formed on SilRef surfaces showed lower weight and were thinner than those developed on EpoRef surfaces. These results should be interpreted considering that a biofilm is an organized community of aggregated cells, living at an interface between a surface and a liquid phase, and embedded in a self-produced organic polymeric matrix (Tu et al. 2020) whose behavior is driven by cell–cell, cell–extracellular polymer, and cell–surface interactions (Di Martino 2018). As a consequence of these dynamic interactions, biofilm size, matrix composition, architecture, and cellular physiology can change during biofilm development (Serra et al. 2013, Vidakovic et al. 2018). Thus, the discrepancy initially observed between the number of biofilm cells and biofilm weight and thickness may be an indirect effect of the cell–surface interactions. Nevertheless, both biofilm wet weight and thickness analysis also suggested that SilRef-coated surfaces had a better performance in preventing *Cyanobium* sp. and *P. tunicata* biofilm formation than EpoRef surfaces. Moreover, CLSM analysis revealed that the biovolume and surface coverage of 49-old-biofilms grown on SilRef surfaces were lower than on EpoRef surfaces. These results can be explained by the foul release properties of this coating that prevent fouling settlements and provide extremely smooth and self-cleaning surfaces (Banerjee et al. 2011, Gittens et al. 2013, Hempel 2016, Murosaki et al. 2012, Selim et al. 2017).

The properties of the fouling surfaces, together with the features of the fouling microorganisms, are the main factors that govern the fouling impact and strength of the biofouling interface (Kuliasha et al. 2019). The results demonstrated that the efficacy of SilRef-coated surfaces may be compromised by the microorganism. Indeed, for *Cyanobium* sp. biofilms, the increase observed in all biofilm parameters was mainly due to the

microorganism features. Accordingly, SilRef surfaces displayed higher activity against *P. tunicata* than *Cyanobium* sp. biofilms. For *Cyanobium* sp. biofilms formed on EpoRef surfaces, a combined effect between the surface and microorganism features played a considerable role in biofilm development at the maturation stage. The microfoulers features also determined, to a lower extent, the biofilm formation. In addition, the properties of EpoRef surfaces contributed to a higher biofilm weight at the initial biofilm development stage. Lastly, the surface properties exerted a significant effect on *P. tunicata* biofilm development, contributing to a higher number of cells, wet weight, and thickness, especially in the biofilm maturation stage.

4.5. Conclusion

This chapter suggests that the dynamic behavior of biofilms developed on the different marine coatings is affected by the properties of the coatings, the microfoulers' features, and the interactions that are established between them in the different stages of biofilm development. Furthermore, it was shown that the SilRef marine coating is an effective, non-toxic commercial alternative to toxic biocide AF paints to control biofilm formation of common microfoulers.

4.6. References

Abouelkheir, S. S., E. A. A. H. A. Ghozlan and S. A. Sabry (2020). "Characterization of Biofilm Forming Marine Pseudoalteromonas spp." Journal of Marine Science **2**(01).

Ali, A., M. I. Jamil, J. Jiang, M. Shoaib, B. U. Amin, S. Luo, X. Zhan, F. Chen and Q. Zhang (2020). "An overview of controlled-biocide-release coating based on polymer resin for marine antifouling applications." Journal of Polymer Research **27**(4): 1-17.

Bakker, D., A. Van der Plaats, G. Verkerke, H. Busscher and H. Van Der Mei (2003). "Comparison of velocity profiles for different flow chamber designs used in studies of microbial adhesion to surfaces." Appl Environ Microbiol **69**(10): 6280-6287.

Banerjee, I., R. C. Pangule and R. S. Kane (2011). "Antifouling coatings: recent developments in the design of surfaces that prevent fouling by proteins, bacteria, and marine organisms." Advanced materials **23**(6): 690-718.

Chambers, L. D., K. R. Stokes, F. C. Walsh and R. J. Wood (2006). "Modern approaches to marine antifouling coatings." Surface and Coatings Technology **201**(6): 3642-3652.

De-la-Pinta, I., M. Cobos, J. Ibarretxe, E. Montoya, E. Eraso, T. Guraya and G. Quindós (2019). "Effect of biomaterials hydrophobicity and roughness on biofilm development." Journal of Materials Science: Materials in Medicine **30**(7): 77.

Di Martino, P. (2018). "Extracellular polymeric substances, a key element in understanding biofilm phenotype." AIMS microbiology **4**(2): 274.

Fang, H., L. Huang, H. Zhao, W. Cheng, Y. Chen, M. Fazeli and Q. Shang (2020). Biofilm Growth and the Impacts on Hydrodynamics. Mechanics of Bio-Sediment Transport. Berlin/Heidelberg, Germany, Springer**:** 153-208.

Faria, S. I., R. Teixeira-Santos, M. J. Romeu, J. Morais, V. Vasconcelos and F. J. Mergulhão (2020). "The Relative Importance of Shear Forces and Surface Hydrophobicity on Biofilm Formation by Coccoid Cyanobacteria." Polymers **12**(3): 653.

Gittens, J. E., T. J. Smith, R. Suleiman and R. Akid (2013). "Current and emerging environmentally-friendly systems for fouling control in the marine environment." Biotechnology advances **31**(8): 1738-1753.

Gomes, L., L. Silva, M. Simões, L. Melo and F. Mergulhão (2015). "Escherichia coli adhesion, biofilm development and antibiotic susceptibility on biomedical materials." Journal of Biomedical Materials Research Part A **103**(4): 1414-1423.

Gu, J.-D. (2018). Microbial Biofilms, Fouling, Corrosion, and Biodeterioration of Materials. Handbook of Environmental Degradation of Materials. Oxford, UK, Elsevier**:** 273-298.

Hempel (2016). Product Data HEMPASIL X3+ 87500. Hempel.

Heydorn, A., A. T. Nielsen, M. Hentzer, C. Sternberg, M. Givskov, B. K. Ersbøll and S. Molin (2000). "Quantification of biofilm structures by the novel computer program COMSTAT." Microbiology **146**(10): 2395-2407.

Hoge, J. and C. Leach (2016). "Epoxy resin infused boat hulls." Reinforced Plastics **60**(4): 221-223.

Holmstrõm, C., S. James, B. A. Neilan, D. C. White and S. Kjelleberg (1998). "Pseudoalteromonas tunicata sp. nov., a bacterium that produces antifouling agents." International Journal of Systematic and Evolutionary Microbiology **48**(4): 1205-1212.

Horcas, I., R. Fernández, J. Gomez-Rodriguez, J. Colchero, J. Gómez-Herrero and A. Baro (2007). "WSXM: a software for scanning probe microscopy and a tool for nanotechnology." Review of scientific instruments **78**(1): 013705.

Hu, P., Q. Xie, C. Ma and G. Zhang (2020). "Silicone-based fouling-release coatings for marine antifouling." Langmuir **36**(9): 2170-2183.

Komárek, J. and K. Anagnostidis (1998). Cyanoprokaryota, part 1: Chroococcales, Gustav Fischer Verlag Stuttgart, Germany.

Kotai, J. (1972). Instructions for Preparation of Modified Nutrient Solution Z8 for AlgaeNorwegian. Institute for Water Research. Oslo, Norway.

Krishnan, S., C. J. Weinman and C. K. Ober (2008). "Advances in polymers for anti-biofouling surfaces." Journal of Materials Chemistry **18**(29): 3405-3413.

Kuliasha, C. A., R. L. Fedderwitz, J. A. Finlay, S. C. Franco, A. S. Clare and A. B. Brennan (2019). "Engineered Chemical Nanotopographies: Reversible Addition–Fragmentation Chain-Transfer Mediated Grafting of Anisotropic Poly (acrylamide) Patterns on Poly (dimethylsiloxane) To Modulate Marine Biofouling." Langmuir **36**(1): 379-387.

Lacoursière-Roussel, A., B. M. Forrest, F. Guichard, R. F. Piola and C. W. McKindsey (2012). "Modeling biofouling from boat and source characteristics: a comparative study between Canada and New Zealand." Biological invasions **14**(11): 2301-2314.

Lee, J.-W., J.-H. Nam, Y.-H. Kim, K.-H. Lee and D.-H. Lee (2008). "Bacterial communities in the initial stage of marine biofilm formation on artificial surfaces." The journal of microbiology **46**(2): 174-182.

Mazumder, S., J. O. Falkinham III, A. M. Dietrich and I. K. Puri (2010). "Role of hydrophobicity in bacterial adherence to carbon nanostructures and biofilm formation." Biofouling **26**(3): 333-339.

Mineur, F., M. P. Johnson, C. A. Maggs and H. Stegenga (2007). "Hull fouling on commercial ships as a vector of macroalgal introduction." Marine biology **151**(4): 1299-1307.

Moreira, J., L. Gomes, K. Whitehead, S. Lynch, L. Tetlow and F. Mergulhão (2017). "Effect of surface conditioning with cellular extracts on Escherichia coli adhesion and initial biofilm formation." Food and Bioproducts Processing **104**: 1-12.

Mostafaei, A. and F. Nasirpouri (2013). "Preparation and characterization of a novel conducting nanocomposite blended with epoxy coating for antifouling and antibacterial applications." Journal of Coatings Technology and Research **10**(5): 679-694.

Murosaki, T., N. Ahmed and J. P. Gong (2012). "Antifouling properties of hydrogels." Science and Technology of Advanced Materials.

Neves, A. R., J. R. Almeida, F. Carvalhal, A. Câmara, S. Pereira, J. Antunes, V. Vasconcelos, M. Pinto, E. R. Silva and E. Sousa (2020). "Overcoming environmental problems of biocides: Synthetic bile acid derivatives as a sustainable alternative." Ecotoxicology and environmental safety **187**: 109812.

Ozkan, A. and H. Berberoglu (2013). "Cell to substratum and cell to cell interactions of microalgae." Colloids and surfaces B: Biointerfaces **112**: 302-309.

Palmer, J., S. Flint and J. Brooks (2007). "Bacterial cell attachment, the beginning of a biofilm." Journal of industrial microbiology & biotechnology **34**(9): 577-588.

Ramos, V., J. Morais, R. Castelo-Branco, Â. Pinheiro, J. Martins, A. Regueiras, A. L. Pereira, V. R. Lopes, B. Frazão, D. Gomes, C. Moreira, M. S. Costa, S. Brûle, S. Faustino, R. Martins, M. Saker, J. Osswald, P. N. Leão and V. M. Vasconcelos (2018). "Cyanobacterial diversity held in microbial biological resource centers as a biotechnological asset: the case study of the newly established LEGE culture collection." Journal of Applied Phycology **30**(3): 1437-1451.

Rao, D., J. S. Webb and S. Kjelleberg (2005). "Competitive interactions in mixed-species biofilms containing the marine bacterium Pseudoalteromonas tunicata." Applied and environmental microbiology **71**(4): 1729-1736.

Romeu, M. J., P. Alves, J. Morais, J. M. Miranda, E. D. de Jong, J. Sjollema, V. Ramos, V. Vasconcelos and F. J. Mergulhão (2019). "Biofilm formation behaviour of marine

filamentous cyanobacterial strains in controlled hydrodynamic conditions." Environmental Microbiology **21**(11): 4411-4424.

Romeu, M. J., D. Domınguez-Pérez, D. Almeida, J. Morais, A. Campos, V. Vasconcelos and F. J. Mergulhão (2020). "Characterization of planktonic and biofilm cells from two filamentous cyanobacteria using a shotgun proteomic approach." Biofouling.

Schneider, C. A., W. S. Rasband and K. W. Eliceiri (2012). "NIH Image to ImageJ: 25 years of image analysis." Nature methods **9**(7): 671-675.

Sekar, R., V. Venugopalan, K. Satpathy, K. Nair and V. Rao (2004). Laboratory studies on adhesion of microalgae to hard substrates. Asian Pacific Phycology in the 21st Century: Prospects and Challenges. Amsterdam, The Netherlands, Springer**:** 109-116.

Selim, M. S., M. Shenashen, S. A. El-Safty, S. Higazy, M. M. Selim, H. Isago and A. Elmarakbi (2017). "Recent progress in marine foul-release polymeric nanocomposite coatings." Progress in Materials Science **87**: 1-32.

Serra, D. O., A. M. Richter, G. Klauck, F. Mika and R. Hengge (2013). "Microanatomy at cellular resolution and spatial order of physiological differentiation in a bacterial biofilm." MBio **4**(2).

Silva, E., O. Ferreira, P. Ramalho, N. Azevedo, R. Bayón, A. Igartua, J. Bordado and M. Calhorda (2019). "Eco-friendly non-biocide-release coatings for marine biofouling prevention." Science of the Total Environment **650**: 2499-2511.

Telegdi, J., L. Trif and L. Románszki (2016). Smart anti-biofouling composite coatings for naval applications. Smart Composite Coatings and Membranes. Amsterdam, The Netherlands, Elsevier**:** 123-155.

Thomen, P., J. Robert, A. Monmeyran, A.-F. Bitbol, C. Douarche and N. Henry (2017). "Bacterial biofilm under flow: first a physical struggle to stay, then a matter of breathing." PloS one **12**(4): e0175197.

Tian, L., Y. Yin, H. Jin, W. Bing, E. Jin, J. Zhao and L. Ren (2020). "Novel marine antifouling coatings inspired by corals." Materials Today Chemistry **17**: 100294.

Tu, C., T. Chen, Q. Zhou, Y. Liu, J. Wei, J. J. Waniek and Y. Luo (2020). "Biofilm formation and its influences on the properties of microplastics as affected by exposure time and depth in the seawater." Science of The Total Environment: 139237.

van Oss, C. (1994). Interfacial forces in aqueous media. Marcel Dekker. New York, NY, USA.

Vidakovic, L., P. K. Singh, R. Hartmann, C. D. Nadell and K. Drescher (2018). "Dynamic biofilm architecture confers individual and collective mechanisms of viral protection." Nature microbiology **3**(1): 26-31.

Zhu, H.-W., J.-N. Zhang, P. Su, T. Liu, C. He, D. Feng and H. Wang (2020). "Strong adhesion of poly (vinyl alcohol)–glycerol hydrogels onto metal substrates for marine antifouling applications." Soft Matter(16): 709-717.

5.

Unveiling the antifouling performance of different marine surfaces and their effect on the development and structure of cyanobacterial biofilms[c]

Abstract

Since biofilm formation by microfoulers significantly contributes to the fouling process, it is important to evaluate the performance of marine surfaces to prevent biofilm formation, as well as understand their interactions with microfoulers and how these affect biofilm development and structure. In this study, the long-term performance of five surface materials - glass, perspex, polystyrene, epoxy-coated glass, and a silicone hydrogel coating - in inhibiting biofilm formation by cyanobacteria was evaluated. For this purpose, cyanobacterial biofilms were developed under controlled hydrodynamic conditions typically found in marine environments, and the biofilm cell number, wet weight, chlorophyll *a* content, and biofilm thickness and structure were assessed after 49 days. In order to obtain more insight into the effect of surface properties on biofilm formation, they were characterized concerning their hydrophobicity and roughness. Results demonstrated that

[c] The content of this chapter was adapted from the following publication(s):

Faria, S. I., R. Teixeira-Santos, M. J. Romeu, J. Morais, E. d. Jong, J. Sjollema, V. Vasconcelos and F. J. Mergulhão (2021). "Unveiling the Antifouling Performance of Different Marine Surfaces and Their Effect on the Development and Structure of Cyanobacterial Biofilms." Microorganisms **9**(5): 1102.

silicone hydrogel surfaces were effective in inhibiting cyanobacterial biofilm formation. In fact, biofilms formed on these surfaces showed a lower number of biofilm cells, chlorophyll *a* content, biofilm thickness, and percentage and size of biofilm empty spaces compared to remaining surfaces. Additionally, our results demonstrated that the surface properties, together with the features of the fouling microorganisms, have a considerable impact on marine biofouling potential.

5.1. Introduction

Marine biofouling is the attachment of undesirable molecules and micro- and macroorganisms to submerged surfaces, posing serious economic and environmental implications. Biofouling on ship hulls causes an increase in frictional drag, which leads to higher fuel consumption, maintenance costs, and downtimes (Rajeev et al. 2020, Tian et al. 2020, Zecher et al. 2018). Moreover, submerged marine facilities and equipment can be damaged by biofouling, representing additional costs for marine industries (Tian et al. 2020). Furthermore, this natural process allows the bio-invasion of exotic species whenever fouling organisms travel in vessel hulls (ships, yachts, or sailing boats) across different geographic areas, compromising the conservation of marine ecosystems (Lacoursière-Roussel et al. 2016, Neves et al. 2020). For these reasons, there is a clear need to develop more efficient AF coatings and understand their interactions with microfouling organisms during biofilm formation, since this is the initial colonization stage.

Biofouling occurs spontaneously via the adhesion of microfouling organisms (e.g., cyanobacteria and diatoms) to underwater surfaces with consequent biofilm formation, which builds the basis for the later settlement of macrofouling organisms (e.g., bryozoans, mollusks, polychaeta, tunicates, coelenterates, or fungi) (Arrhenius et al. 2014). This is a dynamic process that involves several consecutive steps and is modulated by different factors, such as the surface properties, hydrodynamic conditions, and microbial composition (Faria et al. 2020). At the initial stages of biofouling, the physicochemical properties of marine surfaces, including surface free energy, roughness, and hydrophobicity may have a significant impact

on the rate and extent of microorganisms adhesion and biofilm formation (Donlan 2002, Jindal et al. 2016). Moreover, microorganisms live in microenvironments subject to external factors that condition local nutrient transport and chemical gradients, creating specialized niches and shaping the biofilm structure (Aufrecht et al. 2019). The spatial organization of microorganisms can influence emergent phenomena like QS, intracellular communication, and biofilm formation, conferring them greater resistance to mechanical and chemical stresses (e.g., fluid shear, detergents, and AF compounds) (Hou et al. 2019).

Although it is known that microbial biofilms are complex systems that shape, and are shaped by, their local microenvironments (Aufrecht et al. 2019), there are few studies about how marine surfaces influence microfouler attachment and biofilm formation (Kanematsu and Barry 2020).

In this study, the long-term performance of five surface materials - glass, perspex, polystyrene, epoxy-coated glass, and a silicone hydrogel coating - in inhibiting or delaying biofilm formation by microfoulers was evaluated. Glass, perspex, and polystyrene materials are commonly found on different marine facilities and equipment, including underwater windows of boats, aquaculture systems, flotation spheres, moored buoys, underwater cameras, measuring devices or sensors, pontoons, and floating docks (Romeu et al. 2019, Turner 2020). In turn, polymer epoxy resin and silicone hydrogel are two commercial marine coatings; the first is used to coat the hulls of small recreation vessels (e.g., powerboats, yachts, and sailing boats) (Blain et al. 2004, Taylor 1996), while the second is frequently used to coat ship hulls, marine water inlet piping, and grids in power stations (Faria et al. 2020).

Although the presented materials are typically found in marine environments, the microfouler response to these surfaces is not adequately characterized, and their effect on the development and structure of marine biofilms is unexplored. Hence, the present study aimed to evaluate the long-time performance of these surface materials against biofilm formation by one of the most common microfouling organisms (Angelova et al. 2019, de Carvalho 2018), cyanobacteria, under defined hydrodynamic conditions, to estimate their AF performance and to assess their effects on biofilm architecture in conditions mimicking marine settings.

5.2. Material and methods

5.2.1. Surface preparation

Cyanobacterial biofilm formation was studied using five different marine surfaces, glass, perspex, polystyrene, epoxy-coated glass, and a silicone hydrogel coating.

Glass, perspex, and polystyrene surfaces were cut into squares (1 x 1 cm) designated by coupons. The epoxy resin and silicone hydrogel coatings were prepared using glass coupons as a substrate, as described below.

Glass (Vidraria Lousada Lda, Lousada, Portugal), perspex (Neves & Neves Lda, Porto, Portugal), and polystyrene (VWR, International, Carnaxide, Portugal) coupons were cleaned and disinfected by immersion in a 2% (v/v) TEGO 2000® solution (an amphoteric disinfectant; JohnsonDiversey, Northampton, United Kingdom), for 20 min under agitation (150 rpm) (Gomes et al. 2018, Meireles et al. 2017). Subsequently, coupons were washed with sterile distilled water to remove possible remains of the disinfectant solution, air-dried, and sterilized by autoclaving at 121° for 15 min (glass) or UV radiation for 30 min (perspex and polystyrene).

Epoxy resin- and silicone hydrogel-coated surfaces were prepared using glass as a substrate following the protocol described by Faria et al. (Faria et al. 2020). Briefly, 70 µL of epoxy resin (HB Química, Porto, Portugal) was deposited on the top of glass coupons by spin coating (Spin150 PolosTM, Paralab, Portugal) at 6000 rpm, with increments of 1000 rpm, for 40 s. Afterward, surfaces were dried in two sequential steps (12 h at room temperature and 3 h at 60 °C) and sterilized by immersion in 70% (v/v) ethanol (VWR International S.A.S., Fontenay-sous-Bois, France) for 20 min (Faria et al. 2020). The silicone hydrogel surfaces (HEMPASIL X3+ 87500, Copenhagen, Denmark) were prepared using conventional brush painting following the recommendations of the manufacturer and sterilized by UV radiation for 30 min (Faria et al. 2020).

Before the biofilm formation experiments, the initial weight of each coupon was determined.

5.2.2. Surface characterization

5.2.2.1. AFM

AFM studies were performed using a Bruker Catalyst microscope in contact mode with a DNP-D cantilever with a spring constant of 0.06 N/m (Bruker Billerica, Massachusetts, USA). The surface roughness was determined from three random areas (75 x 75 µm) on three samples at room temperature. The scan speed was set to 1 Hz. Surface roughness calculations and 2D images were made using the Nanoscope Analysis Software from Bruker. The roughness height parameter determined was the average roughness (R*a*).

5.2.2.2. Thermodynamic analysis

The hydrophobicity of the surfaces and cyanobacteria cells was determined by contact angle measurement (Ma et al. 2007) and, subsequently, estimated using the van Oss approach (Van Oss 1994).

Cyanobacterial substrata were prepared by filtering cell suspensions containing 1 x 10^9 cells/mL using cellulose membranes following the protocol developed by Busscher et al. (Busscher et al. 1984). The contact angles of materials and cyanobacteria cells were determined automatically at 25 ± 2 °C by the sessile drop method in a contact angle meter (Dataphysics OCA 15 Plus, Filderstadt, Germany) using water, formamide, and α-bromonaphthalene as reference liquids, in three independent assays. For each experiment, at least 25 measurements were performed.

Water contact angles (θ_w) indicate the surface hydrophobicity ($\theta_w < 90°$ indicates that a surface is hydrophilic, while $\theta_w > 90°$ indicates that it is hydrophobic) (Ma et al. 2007).

In turn, based on the van Oss approach (Van Oss 1994), the total surface free energy (γ^{TOT}) of a pure substance results from the sum of the apolar Lifshitz–van der Waals component of the surface free energy (γ^{LW}) and the polar Lewis acid–base component (γ^{AB}).

$$\gamma^{TOT} = \gamma^{LW} + \gamma^{AB} \quad (1)$$

The polar AB component comprises the electron acceptor, γ^+, and electron donor, γ^-, parameters and is given by

$$\gamma^{AB} = 2\sqrt{\gamma^+\gamma^-} \quad (2)$$

The surface free energy components of a solid surface (*s*) are obtained by measuring the contact angles (θ) with three different liquids (*l*) with known surface tension components (Janczuk et al. 1993), followed by the simultaneous resolution of three equations of the following type:

$$(1 + \cos\theta)\gamma_l = 2\left(\sqrt{\gamma_s^{LW}\gamma_l^{LW}} + \sqrt{\gamma_s^+\gamma_l^-} + \sqrt{\gamma_s^+\gamma_l^-}\right) \quad (3)$$

The degree of hydrophobicity of a given surface is expressed as the free energy of interaction (ΔG, mJ.m^{-2}) between two entities of that surface immersed in polar liquid (such as water (*w*) as a model solvent). Therefore, ΔG is calculated using the following equation:

$$\Delta G = -2\left(\sqrt{\gamma_s^{LW}} - \sqrt{\gamma_w^{LW}}\right)^2 - 4\left(\sqrt{\gamma_s^+\gamma_w^-} + \sqrt{\gamma_s^-\gamma_w^+} - \sqrt{\gamma_s^+\gamma_s^-} - \sqrt{\gamma_w^+\gamma_w^-}\right) \quad (4)$$

According to this approach, if the interaction between the two entities is stronger than the interaction of each one with water ($\Delta G < 0$ mJ/m^2), the material is considered hydrophobic (free energy of interaction is attractive); contrarily, if $\Delta G > 0$ mJ/m^2, the material is hydrophilic (free energy of interaction is repulsive) (Bayoudh et al. 2006).

When studying the interaction (free energy of adhesion) between the surface (*s*) and cyanobacteria cells (*b*), the total interaction energy, ΔG^{Adh}, can be expressed as:

$$\Delta G^{Adh} = \gamma_{sb}^{Lw} - \gamma_{sw}^{Lw} - \gamma_{bw}^{Lw} + 2\left[\sqrt{\gamma_w^+}\left(\sqrt{\gamma_s^-} + \sqrt{\gamma_b^-} - \sqrt{\gamma_w^-}\right) + \sqrt{\gamma_w^-}\left(\sqrt{\gamma_s^+} + \sqrt{\gamma_b^+} - \sqrt{\gamma_w^+}\right) - \sqrt{\gamma_s^+\gamma_b^-} - \sqrt{\gamma_s^-\gamma_b^+}\right] \quad (5)$$

Thermodynamically, if $\Delta G^{Adh} < 0$ mJ/m^2, the adhesion of cyanobacteria to the material is favored; on the other hand, the adhesion is thermodynamically not favorable when $\Delta G^{Adh} > 0$ mJ/m^2.

5.2.3. Marine organisms and growth conditions

Three coccoid cyanobacteria isolates, *Synechocystis salina* LEGE 00041, *Cyanobium* sp. LEGE 06098, and *Cyanobium* sp. LEGE 10375, from the LEGE-CC, deposited at the CIIMAR, Matosinhos, Portugal, were used in this study.

S. salina LEGE 00041 was isolated from a tide pool, on the intertidal zone, in June 2000, at Espinho beach (41.00847 N 8.646958 W) located on the north coast of Portugal. *Cyanobium* sp. LEGE 06098 was originally obtained from an intertidal zone, in a green macroalga, collected in July 2006, at Martinhal beach (37.01869 N 8.926714 W) located in Vila do Bispo, Portugal. *Cyanobium* sp. LEGE 10375 was isolated from the intertidal zone, in a marine sponge, collected in October 2010, at São Bartolomeu do Mar beach (41.57378 N 8.798556 W) located in Esposende, Portugal (Ramos et al. 2018). The organisms used in this study comprise cyanobacterial isolates from different geographical locations and taxonomic genera with the aim of assessing the influence of different genotypic and phenotypic profiles on surface material performance.

Cyanobacterial isolates were grown in Z8 medium (Kotai 1972) supplemented with 25 g·L^{-1} of synthetic sea salts (Tropic Marin) and vitamin B12 (Sigma Aldrich, Merck, Saint Louis, MO, USA), under 14 h light (10‑30 mol photons m^{-2} s^{-1}, λ = 380–700 nm)/10 h dark cycles at 25 °C (Faria et al. 2020).

5.2.4. Biofilm formation assays

Cyanobacterial biofilm formation assays were performed using 12-well plates (VWR International, Carnaxide, Portugal) under controlled hydrodynamic conditions. Sterilized coupons of glass, perspex, polystyrene, epoxy-coated glass, and silicone hydrogel coating were fixed to the microplate wells using transparent double-sided adhesive tape. Then, 3 mL of cyanobacterial suspension at a final concentration of 1×10^8 cells/mL was added to each well, and plates were incubated at 25 °C in an orbital shaker with a 25 mm diameter (Agitorb 200ICP, Norconcessus, Ermesinde, Portugal) at 185 rpm, under alternate light cycles of 14 h light (10‑30 mol photons m^{-2} s^{-1})/10 h dark. According to previous computational fluid dynamic studies using this type of incubator (Romeu et al. 2019), a shaking frequency of 185 rpm corresponds to an average shear rate of 40 s^{-1} and a maximum of 120 s^{-1}, which encompasses the shear rate estimated for a ship in a harbor (50 s^{-1}) (Bakker et al. 2003).

Biofilm formation experiments were monitored for 7 weeks (49 days) since this period corresponds on average to half of the minimal economically viable interval accepted for the maintenance of underwater systems (Blain et al. 2004) and hull cleaning (Akinfijevs et al. 2007, Schultz et al. 2011). During this period, the culture medium was replaced twice a week. On day 49, two coupons of each material were removed and gently rinsed in a sterile NaCl solution (8.5 mg/mL) to remove loosely attached cyanobacteria. Subsequently, coupons were analyzed concerning the number of biofilm cells, biofilm wet weight, chlorophyll a content, and biofilm thickness and structure.

Biofilm experiments were performed in duplicate and in three independent assays.

5.2.4.1. Biofilm cell counting

The biofilm cell counting was performed as described in chapter 3, section 3.2.4.1

5.2.4.2. Biofilm wet weight

To evaluate the biofilm wet weight, coupons were removed from the microplate wells using a sterile tweezer and weighted. The biofilm wet weight was determined by the difference between the initial weight of coupons (before inoculation) and the weight measured on day 49.

5.2.4.3. Chlorophyll *a* content

The chlorophyll *a* content was performed as described in chapter 3, section 3.2.4.3.

5.2.4.4. Biofilm thickness and structure

The evaluation of biofilm thickness and structure was performed on day 49 through OCT using a Thorlabs Ganymede Spectral Domain Optical Coherence Tomography system with a central wavelength of 930 nm (Thorlabs GmbH, Dachau, Germany). Before biofilm analysis, the culture medium was carefully removed from the microplate wells, coupons were washed once, and wells filled with 3 mL of 8.5 g/L NaCl sterile solution. Images from cyanobacterial biofilms developed on studied surfaces were captured and analyzed as previously described by Romeu et al. (Romeu et al. 2019). For each coupon, 2D and 3D imaging were performed with a minimum of three fields of view, to ensure the accuracy and reliability of the obtained results. For image analysis, the bottom of the biofilm was determined as the best-fitting parabole and hyperboloid, in 2D and 3D images, respectively, that connected the white pixels resulting from light reflection on the substratum surface. A gray-value threshold that separates the biofilm from the background was calculated on the basis of the gray-value histogram of the entire image (Otsu 1979). The upper contour line of the biofilm was defined as those pixels in the image that have a gray value just higher than the gray-value threshold and are connected to the biofilm bottom. Objects not connected to the bottom were rejected from the biofilm structure, and the mean biofilm thickness was

calculated as a function of the number of pixels between the bottom of the biofilm and the upper contour line for each vertical line in the image.

5.2.5. Statistical analysis

Descriptive statistics were used to calculate the mean and standard deviation for the contact angles, surface roughness, number of biofilm cells, biofilm wet weight, chlorophyll *a* content, biofilm thickness, and percentage and size of biofilm empty spaces.

Differences in the number of biofilm cells, biofilm wet weight, chlorophyll *a* content, biofilm thickness, and biofilm empty spaces obtained for tested surfaces (glass, perspex, polystyrene, epoxy-coated glass, and silicone hydrogel coating) were evaluated using Kruskal–Wallis and Mann–Whitney tests since the variables were not normally distributed.

Statistically significant differences were considered for p-values <0.05. Letters were assigned in alphabetic order from the highest to the lowest value (from *a* to *e*) for each surface. These assignments were made as long as statistically significant differences existed between the biofilms.

Data analysis was performed using the IBM SPSS Statistics version 24.0 for Windows (IBM SPSS, Inc., Chicago, IL, USA).

5.3. Results

In this study, the AF performance of five different marine surface materials, glass, perspex, polystyrene, epoxy-coated glass, and a silicone hydrogel coating, was evaluated through the analysis of cyanobacterial biofilms formation on those substrates for 49 days under controlled hydrodynamic conditions.

5.3.1. Surface characterization of materials and cyanobacterial isolates

Since it is known that surface properties influence cell adhesion and subsequent biofilm formation (Spengler et al. 2019, Zheng et al. 2021), surface materials were first analyzed regarding their hydrophobicity, topography, and roughness. Table 5.1. presents the contact angles, hydrophobicity, and roughness values for the tested materials.

The hydrophobicity was evaluated by contact angle measurement and based on the van Oss approach (Van Oss 1994). Considering that water contact angles (θ_w) values <90° and free energy of interaction (ΔG) values >0 $mJ \cdot m^{-2}$ indicate that a surface is hydrophilic, both measures showed that glass is the most hydrophilic material (θ_w = 27.8° ± 4.0°; ΔG = 32.5 mJ/m^2) followed by epoxy-coated glass (θ_w = 69.4° ± 3.0°; ΔG = −6.7 mJ/m^2), perspex (θ_w = 72.6° ± 3.2°; ΔG = −42.7 mJ/m^2), and polystyrene (θ_w = 77.9° ± 3.6°; ΔG = −43.8 mJ/m^2). Moreover, the hydrophobic behavior of the silicone hydrogel coating was also demonstrated by the water contact angle (θ_w = 108.4° ± 3.5°; $\theta_w > 90°$), as well as the degree of hydrophobicity (ΔG = −55.8 mJ/m^2; $\Delta G < 0$ mJ/m^2).

The surface topography and roughness of the five materials were evaluated by AFM in contact mode as these parameters are directly related to cell adhesion (Crawford et al. 2012, Dantas et al. 2016). The topography images revealed that perspex and glass are the most homogeneous and smooth materials (Figure 5.1.a,d). In fact, these surfaces displayed, on average, a lower roughness value (R_a = 6.2 nm) compared to the other surfaces. The polystyrene and epoxy-coated glass showed R_a values of 10.1 and 13.4 nm, respectively (Table 5.1.). In opposition, the silicone hydrogel coating registered the highest R_a value (49.7 nm).

Because cell adhesion and biofilm formation are also influenced by the physicochemical properties of the microorganisms (Wang et al. 2011, Zhang et al. 2015), the water contact angles and degree of hydrophobicity of cells were also assessed (Table 5.2.).

Table 5.1. The contact angles with water (θ_w), formamide (θ_F), and α-bromonaphthalene (θ_B), hydrophobicity (according to Equation (4)) (ΔG), and roughness (R_a) determined for the tested surfaces. Values are presented as the mean ± standard deviation.

Surface	Contact Angle (°)			ΔG (mJ/m^2)	R_a (nm)
	θ_w	θ_F	θ_B		
Perspex	72.6 ± 3.2	52.2 ± 3.2	22.4 ± 1.7	−42.7	6.2 ± 1.7
Silicone hydrogel	108.4 ± 3.5	104.0 ± 1.9	70.0 ± 2.0	−55.8	49.7 ± 8.3
Polystyrene	77.9 ± 3.6	62.1 ± 2.3	28.4 ± 2.6	−43.8	10.1 ± 2.2
Glass	27.8 ± 4.0	36.5 ± 3.9	44.3 ± 4.0	32.5	6.2 ± 0.9
Epoxy-coated glass	69.4 ± 3.0	56.8 ± 3.0	23.3 ± 2.2	−26.7	13.4 ± 4.1

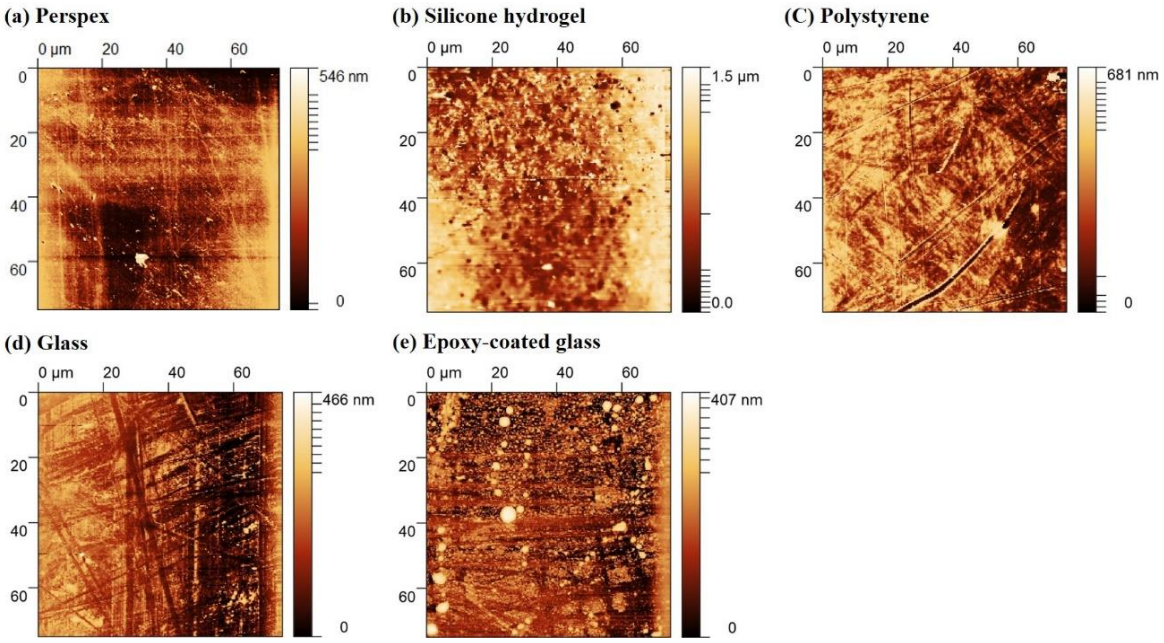

Figure 5.1. Two-dimensional AFM images of perspex (**a**), silicone hydrogel coating (**b**), polystyrene (**c**), glass (**d**), and epoxy-coated glass (**e**) surfaces with a scan range of 75 x 75 µm (contact mode). The color bar corresponds to the z-range (surface height range) of the respective image.

Cyanobium sp. LEGE 10375 showed the highest ΔG value and, thus, this strain is relatively more hydrophilic ($\Delta G > 0$ mJ/m^2) than the other cyanobacteria (ΔG_{10375} = 63.2 mJ.m^{-2} > ΔG_{06098} = 53.1 mJ/m^2 > ΔG_{00041} = 42.6 mJ/m^2).

As the free energy of the interaction between cyanobacterial isolates and tested surfaces can estimate the extent of cell adhesion (Zhang et al. 2015), it was calculated and

the results are presented in Table 5.3. The values of free energy of adhesion (ΔG^{Adh}) obtained for the different cyanobacteria strains were similar for the same material and indicated that cell adhesion on the silicone hydrogel coating and perspex (lower ΔG^{Adh} values) is thermodynamically more favorable compared to other materials, particularly to glass.

Table 5.2. The contact angles with water (θ_w), formamide (θ_F), and *a*-bromonaphthalene (θ_B) and the hydrophobicity (ΔG) for cyanobacterial strains, calculated according to Equation (4).

Microorganism	Contact Angle (°)			ΔG (mJ/m^2)
	θ_w	θ_F	θ_B	
S. salina LEGE 00041	32.3 ± 4.5	43.2 ± 5.1	45.5 ± 5.5	42.6
Cyanobium sp. LEGE 06098	23.4 ± 3.1	39.8 ± 5.3	36.0 ± 5.4	53.1
Cyanobium sp. LEGE 10375	41.7 ± 3.9	63.9 ± 3.9	33.3 ± 4.0	63.2

Table 5.3. Free energy of the interaction between cyanobacterial strains and tested surfaces (according to Equation (5)).

Microorganism	ΔG^{Adh} (mJ/m^2)				
	Perspex	Silicone Hydrogel	Polystyrene	Glass	Epoxy-Coated Glass
S. salina LEGE 00041	2.4	0.5	4.5	38.5	12.3
Cyanobium sp. LEGE 06098	4.8	4.3	7.4	42.2	14.4
Cyanobium sp. LEGE 10375	6.8	6.4	9.7	46.6	18.3

ΔG^{Adh} - free energy of adhesion.

5.3.2. Quantification of biofilms developed on tested surfaces

Cyanobacterial biofilm formation on the tested surfaces was assessed on day 49 through an analysis of the number of biofilm cells, biofilm wet weight, chlorophyll *a* content, and biofilm thickness (Figure 5.2.) in order to evaluate the performance of tested surface materials. Regardless of surface material, *S. salina* LEGE 00041 had a lower biofilm-forming capacity than the other cyanobacteria, as demonstrated by the low number of adhered cells.

Concerning the number of biofilm cells (Figure 5.2.a), the glass and epoxy-coated glass surfaces showed, on average, a higher number of attached cells for *S. salina* LEGE 00041 ($3.83 \times 10^8 \pm 1.27 \times 10^7$ and $3.55 \times 10^8 \pm 3.24 \times 10^7$ cells/cm^2, respectively; Figure

5.2.(1a)) and *Cyanobium* sp. LEGE 06098 ($2.82 \times 10^9 \pm 4.72 \times 10^8$ and $3.12 \times 10^9 \pm 3.49 \times 10^8$ cells/cm^2, respectively; Figure 5.2.(2a)). *Cyanobium* sp. LEGE 10375 displayed, on average, a higher number of biofilm cells on epoxy-coated glass surfaces ($1.76 \times 10^9 \pm 2.08 \times 10^8$ cells/cm^2; Figure 5.2.(3a)). Conversely, the silicone hydrogel-coated surfaces registered, on average, a lower number of biofilm cells for *Cyanobium* sp. LEGE 06098 ($5.24 \times 10^8 \pm 4.65 \times 10^8$ cells/cm^2; Figure 5.2.(2a)) and *Cyanobium* sp. LEGE 10375 ($5.49 \times 10^8 \pm 1.34 \times 10^8$ cells/cm^2; Figure 5.2.(3a)). For *S. salina* LEGE 00041, the lowest number of biofilm cells was registered for the perspex ($3.61 \times 10^7 \pm 3.13 \times 10^6$ cells/cm^2) and silicone hydrogel ($4.11 \times 10^7 \pm 3.81 \times 10^6$ cells/cm^2) surfaces (Figure 5.2.(1a)). These results suggested that silicone hydrogel is among the surfaces with fewer adhered cells.

Considering the biofilm wet weight (Figure 5.2.b), *S. salina* LEGE 00041 showed no significant differences across the tested surfaces, with biofilms weighing about 30 mg on average (Figure 5.2.(1b)). For *Cyanobium* sp. LEGE 06098, biofilms formed on epoxy-glass surfaces showed, on average, lower wet weight (28.6 ± 5.5 mg; Figure 5.2.(2b)). In turn, *Cyanobium* sp. LEGE 10375 biofilms displayed, on average, lower wet weight when formed on glass (52.9 ± 4.3 mg; Figure 5.2.(3b)).

Regarding the chlorophyll *a* production (Figure 5.2.c), *S. salina* LEGE 00041 biofilms showed, on average, lower chlorophyll *a* content when formed on the silicone hydrogel (0.07 ± 0.04 µg/cm^2) than the rest of surfaces (Figure 5.2.(1c)). Likewise, *Cyanobium* sp. LEGE 06098 and *Cyanobium* sp. LEGE 10375 biofilms (Figure 5.2.(2c) and 5.2(3c)) produced, on average, a lower chlorophyll *a* amount on silicone hydrogel surfaces (0.48 ± 0.10 and 0.56 ± 0.25 µg/cm^2, respectively). These results are consistent with the number of biofilm cells.

Lastly, the thickness of *S. salina* LEGE 00041 biofilms (Figure 5.2.(1d)) was equal for the tested surfaces. *Cyanobium* sp. LEGE 06098 biofilms showed lower thickness when formed on silicone hydrogel surfaces (41.3 ± 7.9 µm; Figure 5.2.(2d)), while *Cyanobium* sp. LEGE 10375 biofilms were thinner on glass (74.1 ± 10.6 µm) and silicone hydrogel surfaces (84.8 ± 7.7 µm) (Figure 5.2.(3d)).

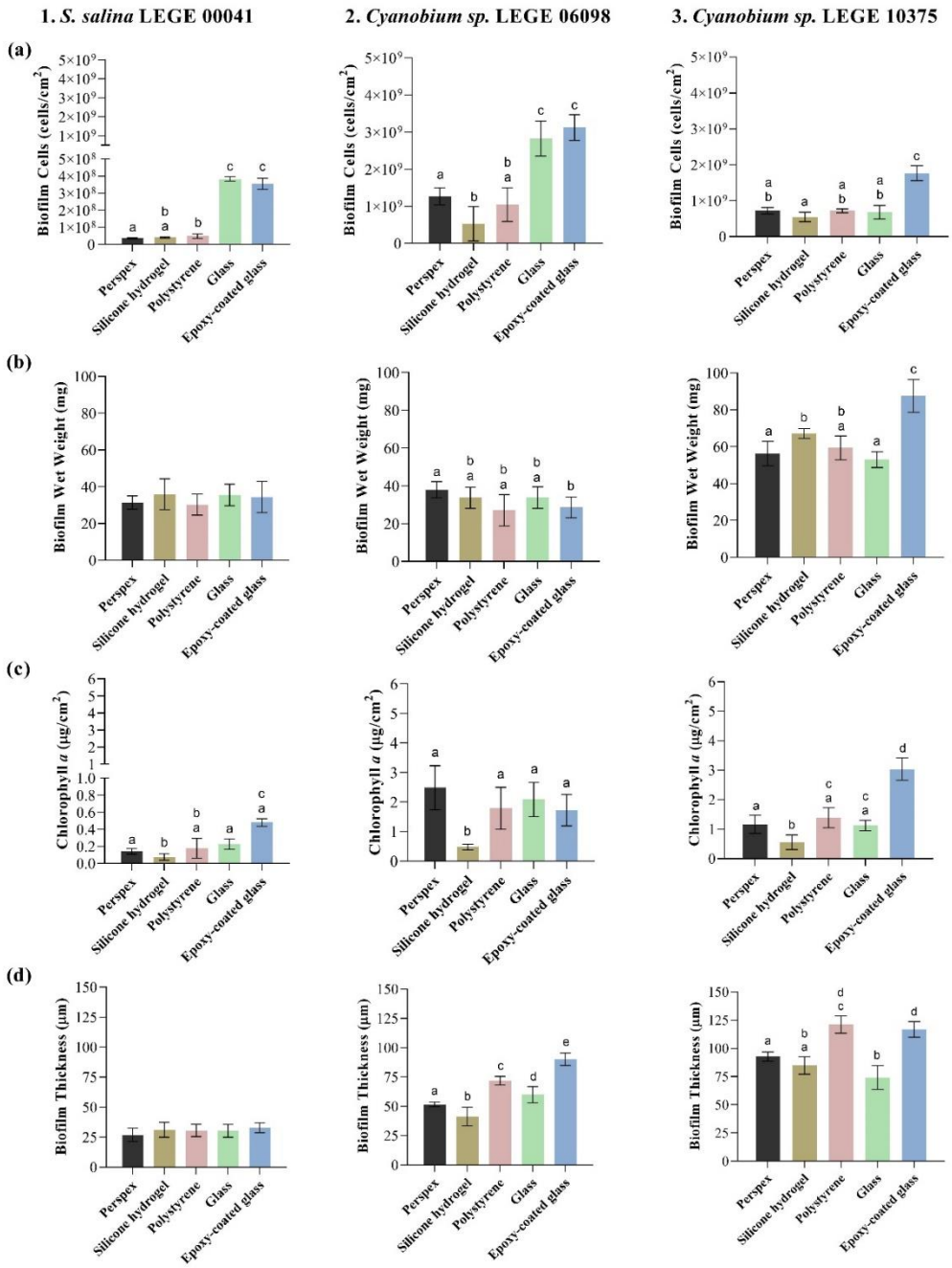

Figure 5.2. Biofilm development of S. salina LEGE 00041 (**1**), Cyanobium sp. LEGE 06098 (**2**), and Cyanobium sp. LEGE 10375 (**3**) on perspex ■, silicone hydrogel coating ■, polystyrene ■, glass ■, and epoxy-coated glass ■ surfaces after 49 days. The analyzed parameters refer to the number of biofilm cells (**a**), biofilm wet weight (**b**), chlorophyll *a* content (**c**), and biofilm thickness (**d**). Error bars indicate the standard error of the mean. For each cyanobacterial isolate, different lowercase letters indicate significant differences between surfaces with a confidence level greater than 95% ($p < 0.05$).

5.3.3. Structure analysis of biofilms developed on tested surfaces

The study of biofilm structure deserves special attention since it indicates how cells interact with surfaces. Figure 5.3. shows representative 3D cross-sectional images obtained by OCT for cyanobacterial biofilms developed on the five surface materials. Cyanobacterial biofilms presented visible differences in their structure, while *S. salina* LEGE 00041 biofilms were more homogenous, *Cyanobium* sp. LEGE 06098 and *Cyanobium* sp. LEGE 10375 biofilms presented more heterogeneous contours, suggesting that cell - surface interactions depend on cyanobacterial isolates. Moreover, at the biofilm bottom of *S. salina* LEGE 00041, a uniform cell layer was observed, while *Cyanobium* sp. LEGE 10375 biofilms showed different shapes, and the uniform cell layer at the biofilm bottom was not detected.

Concerning the tested materials, biofilms formed on glass, epoxy-coated glass, or polystyrene surfaces presented a more developed structure for all cyanobacteria isolates than those developed on silicone hydrogel surfaces. This result is supported by the thickness of *Cyanobium* sp. LEGE 06098 and *Cyanobium* sp. LEGE 10375 biofilms.

As the spatial confinement of microorganisms can influence biofilm formation (Aufrecht et al. 2019), the percentage and the size of biofilm empty spaces were also determined. Figure 5.4a shows the mean percentage of empty spaces obtained for the different cyanobacterial biofilms formed on each surface. The mean percentage of empty spaces ranged from 1.8% (obtained from *S. salina* LEGE 00041 biofilm formed on silicone hydrogel) to 12.1% (obtained from *Cyanobium* sp. LEGE 10375 biofilm formed on polystyrene). The lowest values of empty spaces were observed for *S. salina* LEGE 00041 biofilms, whereas, in *Cyanobium* sp. LEGE 10375 biofilms, a higher percentage of empty spaces was detected. Additionally, a similar percentage of empty spaces was observed for *S. salina* LEGE 00041 biofilms formed on the different surfaces, from 1.8% to 3.7%. For *Cyanobium* sp. LEGE 06098 biofilms these values changed from 2.6% to 5.5%, and, for *Cyanobium* sp. LEGE 10375 biofilms, they changed from 7.9% to 12.1%. For *S. salina* LEGE 00041, biofilms formed on perspex and silicone hydrogel surfaces showed a lower percentage of empty spaces compared to other materials. *Cyanobium* sp. LEGE 06098 biofilms developed on perspex, silicone hydrogel, and glass surfaces revealed a lower

percentage of empty spaces than on polystyrene and epoxy-coated glass surfaces, while *Cyanobium* sp. LEGE 10375 biofilms formed on the silicone hydrogel presented a lower percentage of empty spaces compared to perspex and polystyrene surfaces.

Figure 5.4.b shows the mean size of empty spaces obtained for the different cyanobacterial biofilms. In addition, a graphical representation of the biofilm empty spaces for each surface and cyanobacteria strain is presented in Figure 5.5. The mean size of empty spaces ranged from 24 μm^2 (obtained from *S. salina* LEGE 00041 biofilm formed on polystyrene) to 119 μm^2 (obtained from *Cyanobium* sp. LEGE 10375 biofilm also formed on polystyrene). Regardless of the surface, the lower values of mean size of empty spaces were observed for *S. salina* LEGE 00041, and the higher values were observed for *Cyanobium* sp. LEGE 10375. In addition, *S. salina* LEGE 00041 biofilms displayed similar values of mean size of empty spaces (around 30 μm^2) for glass, epoxy-coated glass, and silicone hydrogel surfaces (Figure 5.4.b). In turn, *Cyanobium* sp. LEGE 06098 and *Cyanobium* sp. 10375 biofilms developed on silicone hydrogel surfaces showed, on average, a smaller size of empty spaces compared to glass, epoxy-coated glass, and polystyrene surfaces.

These results suggested that biofilm structure is not only dependent on the surface but also on the cyanobacterial isolate, as previously shown by Zheng et al. (Zheng et al. 2021).

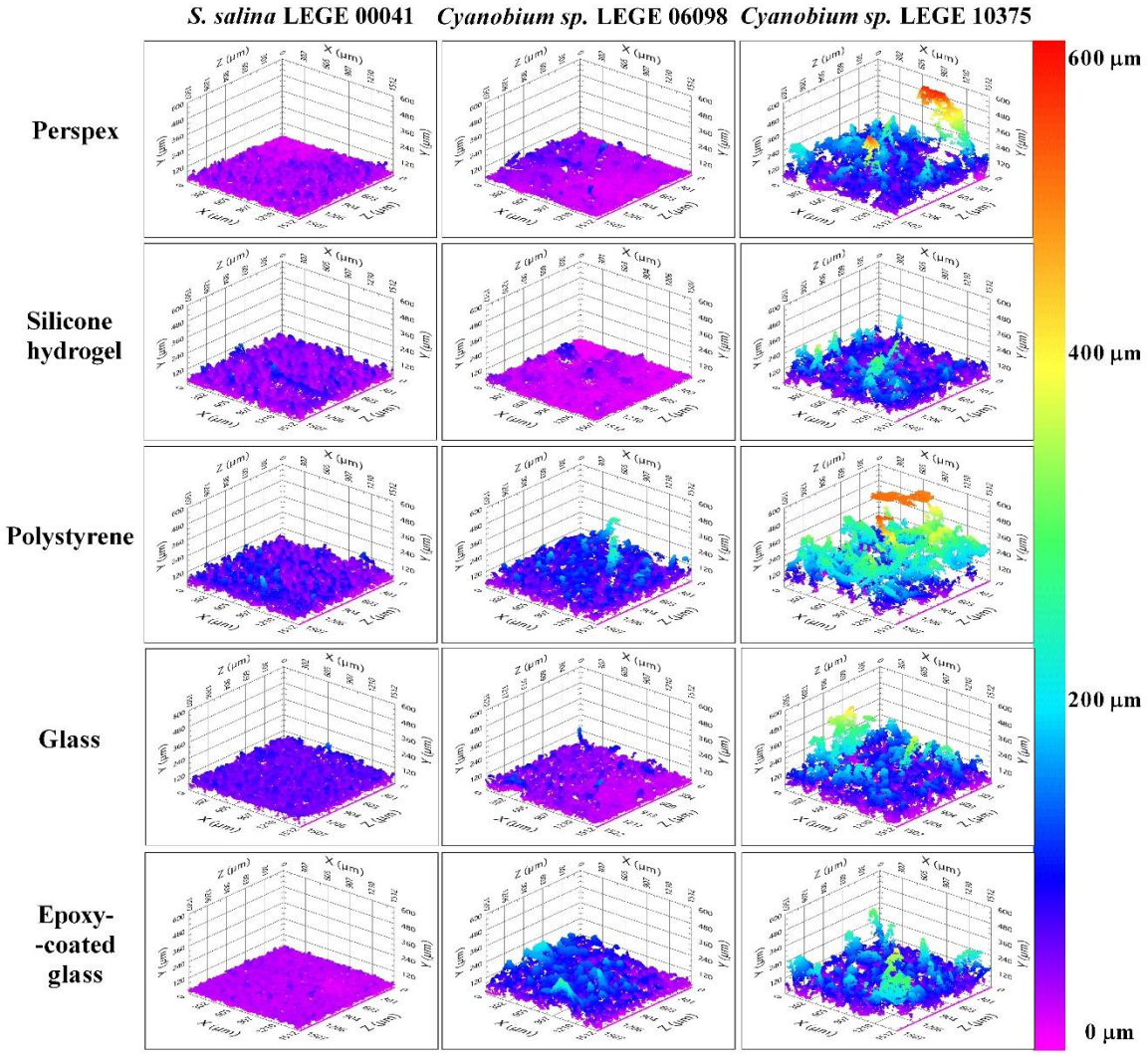

Figure 5.3. Representative 3D OCT images obtained for *S. salina* LEGE 00041, *Cyanobium* sp. LEGE 06098, and *Cyanobium* sp. LEGE 10375 biofilms formed on perspex, silicone hydrogel, polystyrene, glass, and epoxy-coated glass surfaces after 49 days. The color scale shows the range of biofilm thickness.

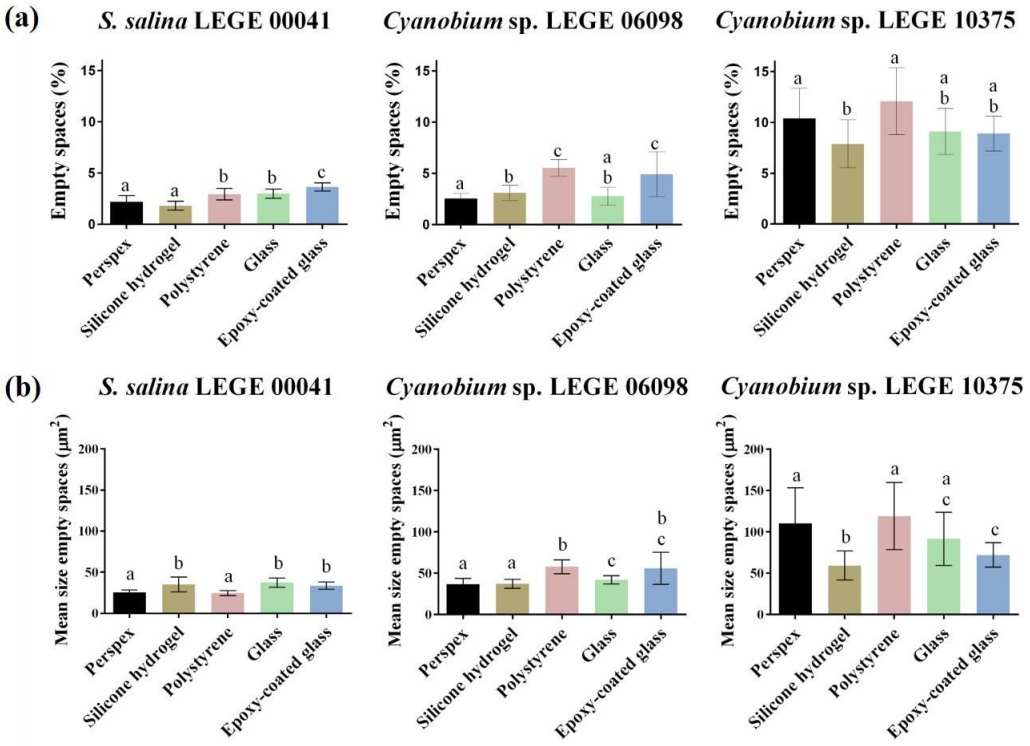

Figure 5.4. Mean percentage (**a**) and size (**b**) of empty spaces obtained for *S. salina* LEGE 00041, *Cyanobium* sp. LEGE 06098, and *Cyanobium* sp. LEGE 10375 biofilms developed on perspex ■, silicone hydrogel coating ■, polystyrene ■, glass ■, and epoxy-coated glass ■ surfaces after 49 days. For each cyanobacterial isolate, different lowercase letters indicate significant differences between surfaces with a confidence level greater than 95% ($p < 0.05$).

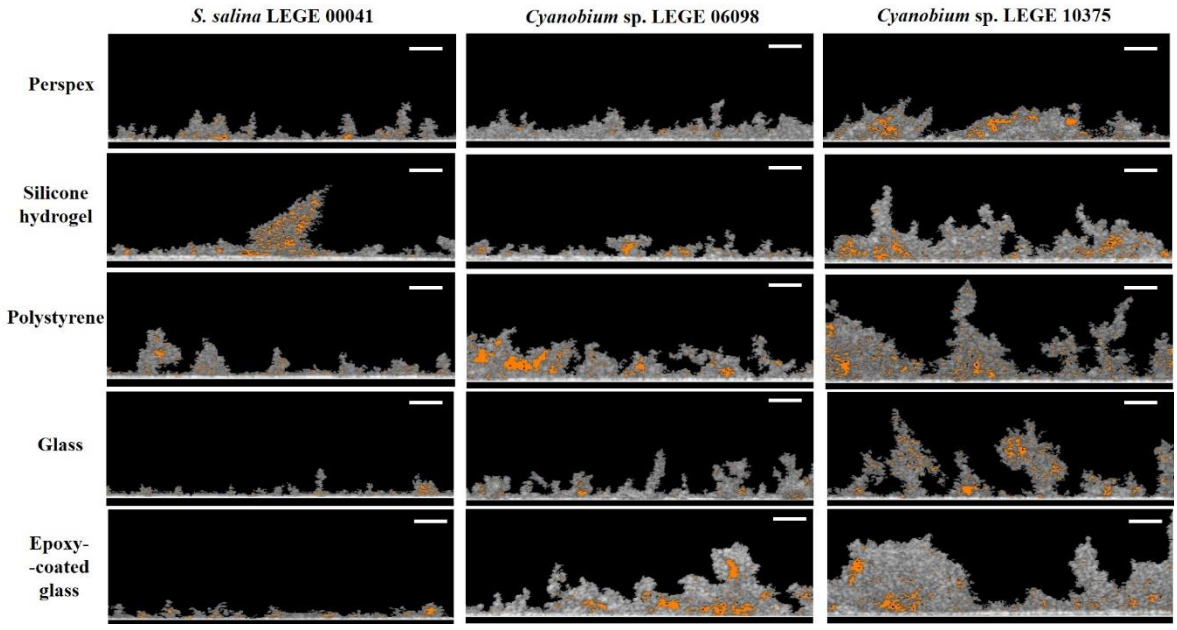

Figure 5.5. Representative 2D cross-sectional OCT images obtained for *S. salina* LEGE 00041, *Cyanobium* sp. LEGE 06098, and *Cyanobium* sp. LEGE 10375 biofilms formed on perspex, silicone hydrogel coating, polystyrene, glass, and epoxy-coated glass surfaces after 49 days. The empty spaces are indicated in orange (scale bars = 100 µm).

5.4. Discussion

In this study, the long-term performance of five different material surface characteristics in inhibiting biofilm formation by coccoid cyanobacteria was evaluated under hydrodynamic conditions found in marine environments, through an analysis of biofilm cell number, biofilm wet weight, chlorophyll *a* content, and biofilm thickness and architecture.

Since marine biofilm formation is influenced by several factors, including the surface properties and microfouler type (Faria et al. 2020, Telegdi et al. 2016), an extensive characterization of the surface materials and microorganisms was also performed in order to obtain more insight into the tested surfaces and their interactions with cyanobacterial isolates.

It is known that surface properties, including hydrophobicity and roughness, influence cell adhesion and subsequent biofilm formation (Spengler et al. 2019, Zhang et al. 2015). In this study, the results from thermodynamic analysis classified glass as the most

hydrophilic material, followed by epoxy-coated glass, perspex, and polystyrene surfaces (Table 5.1.). Conversely, the silicone hydrogel surface was characterized as hydrophobic. These results are in accordance with previous studies (Faria et al. 2020, Romeu et al. 2019, Thukkaram et al. 2014). In addition, the calculation of the free energy of adhesion indicates that cyanobacterial cell adhesion to glass and epoxy-coated glass is thermodynamically less favorable than to the silicone hydrogel coating, perspex, and polystyrene surfaces (Table 5.3.). Concerning AFM analysis, results revealed that glass and perspex are the smoothest tested materials, displaying a lower R_a value, followed by polystyrene and epoxy-coated glass surfaces (Table 5.1.). In opposition, the silicone hydrogel surface showed higher roughness, as found in a previous study (Faria et al. 2020). According to Dantas et al. (Dantas et al. 2016), a reduction in surface roughness is directly related to a decrease in bacterial adhesion. Thus, both hydrophobicity and roughness results suggest that glass and epoxy-coated glass surfaces may be more efficient materials in controlling cyanobacteria biofilm formation than silicone hydrogel surfaces. Nevertheless, in general, the analysis of biofilm parameters indicated that cyanobacterial biofilms formed on glass and epoxy-coated glass surfaces were more developed than those formed on the silicone hydrogel coated surfaces (Figure 5.2.(1–2a), (c), and (2d)). In fact, this adds to the debate on whether surfaces displaying higher degrees of hydrophobicity and roughness favor bacterial adhesion (Cerca et al. 2005, De-la-Pinta et al. 2019, Ozkan and Berberoglu 2013). It has been shown, in particular for cyanobacterial adhesion, that it is not always possible to correlate surface hydrophobicity and roughness with cell attachment (Faria et al. 2020, Irving and Allen 2011, Mazumder et al. 2010, Talluri et al. 2020). Furthermore, there is evidence that biofilm formation induces changes in the substratum surfaces since already attached cells modify surface properties (De-la-Pinta et al. 2019, Mazumder et al. 2010, Moreira et al. 2017, Ozkan and Berberoglu 2013).

The discrepancy observed between the material characterization and biofilm analysis may be explained by the formation of conditioning films resulting from the adsorption of molecules on the substrates that change the adhesion conditions for microorganisms (Hwang et al. 2012, Lorite et al. 2011). The nature of formed films depends on the material type, surrounding environment, and microorganisms (Lorite et al. 2011, Talluri et al. 2020). It is known that these conditioning films play an important role in cyanobacterial adhesion and

subsequent biofilm formation (Talluri et al. 2020). Therefore, despite surface properties being of extreme importance, particularly during the adhesion phase (Zhang et al. 2015), our results suggest that biofilm formation may also be modulated by other factors.

According to Zhang et al. (Zhang et al. 2015), biofilm formation is also influenced by the physicochemical properties of the microorganisms. Indeed, the thermodynamic analysis of cyanobacterial cells indicated that *S. salina* LEGE 00041 is relatively more hydrophilic than *Cyanobium* sp. LEGE 06098 and *Cyanobium* sp. LEGE 10375 (Table 5.2). Moreover, the free energy of adhesion revealed that there is a tendency for *S. salina* LEGE 00041 to adhere more to all tested surfaces (Table 5.3.). These results are corroborated by the biofilm parameter analysis, i.e., number of cells, chlorophyll *a* content, and biofilm thickness, which demonstrated that *S. salina* LEGE 00041 had a lower biofilm-forming capacity on these surfaces than the other cyanobacteria (Figure 5.2.).

Concerning the performance of surface materials, the biofilm analysis indicated that cyanobacterial biofilms formed on glass and epoxy glass surfaces showed, on average, a higher number of *S. salina* LEGE 00041 and *Cyanobium* sp. LEGE 06098 cells compared to perspex, silicone hydrogel, and polystyrene surfaces. *Cyanobium* sp. LEGE 10375 biofilms formed on epoxy-coated glass exhibited a higher number of cells than the other surfaces, whereas the performance of perspex and polystyrene was different between cyanobacterial isolates. Furthermore, silicone hydrogel surfaces were among the surfaces that exhibited a low number of adhered cells (Figure 5.2.a). Although these results were dependent on cyanobacterial isolates, they are supported by the literature. Glass, perspex, and polystyrene are not considered AF surfaces and are frequently used as positive fouling controls in several studies (Jain et al. 2007, Lou et al. 2021, Sekar et al. 2004). Likewise, epoxy resin coatings have not completely emerged in marine applications, especially where high fouling resistance is needed (Qu and Zhang 2012). Lastly, silicone hydrogel surfaces are among the most successful AF coatings to prevent marine biofouling (Nurioglu et al. 2015). The commercial silicone hydrogel coating exerts a dual-mode of action, a ‘nonstick’ ability and a fouling-release effect, associated with relative higher elasticity. These features may decrease fouling settlements and cell cohesion interactions (Faria et al. 2020, Selim et al. 2017). Additionally, this is a third-generation hydrogel-based FRC, which acquires a more hydrophilic behavior upon contact with water (Tulcidas et al. 2015, Xie et al. 2011). Thus, it can prevent either

hydrophobic or hydrophilic interactions, delaying the adsorption of proteins, bacteria, and subsequent fouling (Banerjee et al. 2011, Hu et al. 2020, Murosaki et al. 2012, Sjollema et al. 2017).

Our results indicated that *S. salina* LEGE 00041 biofilms presented, on average, a similar wet weight for all tested surfaces, while *Cyanobium* sp. LEGE 06098 and *Cyanobium* sp. LEGE 10375 biofilms, formed on epoxy-coated glass and glass surfaces, respectively, exhibited a lower weight (Figure 5.2.b). Indeed, once adhered, cells express different QS-related signaling molecules that stimulate or block EPS formation (Nahar et al. 2018), which may justify the observed differences in wet weight concerning other biofilm parameters.

Regarding the chlorophyll *a* content, results were consistent with the number of biofilm cells (Figure 5.2.a,c), which would be expected since several authors have proposed pigment quantification as a good indicator of cyanobacterial biofilm growth (Bartram and Chorus 1999, Rees and Bartram 2002). On the other hand, *S. salina* LEGE 00041 biofilms presented, on average, similar thickness values for all tested surfaces, while *Cyanobium* sp. LEGE 06098 biofilms formed on silicone hydrogel surfaces were thinner (supporting the biofilm cell number and chlorophyll *a* content) (Figure 5.2.d). *Cyanobium* sp. LEGE 10375 biofilms developed on glass and silicone hydrogel surfaces showed a lower thickness than on the remaining surfaces (Figure 5.2.d). Results demonstrated that there was no direct association between the number of biofilm cells and biofilm thickness. In fact, biofilm thickness, analogous to biofilm wet weight, is linked to several features of biofilm architecture, such as density, shape, and porosity, and cannot easily be isolated from environmental factors (e.g., flow, nutrient conditions, development age of the biofilm, carbon–nitrogen ratios, and temperature) (Suarez et al. 2019).

Considering that heterogeneous structures may influence the biofilm resistance to mechanical and chemical challenges, such as fluid shear, detergents, and AF compounds (Hou et al. 2019), the study of biofilm architecture deserves special attention. Microorganisms often live in heterogeneous microenvironments with conditions that modulate local nutrient transport and chemical gradients, creating specialized niches for them. The spatial confinement of microorganisms can influence emergent phenomena, including QS, intracellular communication, and biofilm. In fact, these microenvironment factors shape the structure of microbial communities and contribute to their phenotype

diversity and synergism (Aufrecht et al. 2019, Boedicker et al. 2009, Kim et al. 2008). Our OCT analysis demonstrated that cyanobacterial biofilms presented visible differences in their structure; while *S. salina* LEGE 00041 biofilms were more homogenous, *Cyanobium* sp. LEGE 06098 and *Cyanobium* sp. LEGE 10375 biofilms presented more heterogeneous contours (Figure 5.3.). Indeed, biofilms of *Cyanobium* sp. LEGE 10375 showed a higher biofilm wet weight and thickness when compared with *S. salina* LEGE 00041 (Figure 5.2.b,d). Moreover, biofilms formed on the glass, epoxy-coated glass and polystyrene surfaces presented more developed structures, contrary to silicone hydrogel surfaces (Figure 5.3.). These results are corroborated by the biofilm cell density.

In addition, the analysis of biofilm empty spaces demonstrated that *S. salina* LEGE 00041 biofilms showed lower percentage and mean size values of empty spaces compared to *Cyanobium* sp. LEGE 10375 (Figure 5.4.). *S. salina* LEGE 00041 and *Cyanobium* sp. LEGE 06098 biofilms formed on silicone hydrogel surfaces showed, on average, a lower percentage of empty spaces compared to polystyrene and epoxy-glass surfaces (Figure 5.4.a). Furthermore, *Cyanobium* sp. LEGE 10375 biofilms formed on silicone hydrogel surfaces showed, on average, a lower percentage of empty spaces compared to polystyrene (Figure 5.4.a). While there were no significant differences in the size of empty spaces of *S. salina* LEGE 00041 biofilms formed on the glass, epoxy-coated glass, and silicone hydrogel surfaces, *Cyanobium* sp. LEGE 06098 and *Cyanobium* sp. LEGE 10375 biofilms developed on silicone hydrogel surfaces showed, on average, a lower size of empty spaces compared to polystyrene, glass, and epoxy-coated glass surfaces (Figure 5.4.b). Overall, results from OCT analysis suggest that the biofilms formed on silicone hydrogel surfaces show, in general, a less developed and heterogeneous structure compared to polystyrene, glass, and epoxy-coated glass surfaces, while also presenting a low percentage and size of empty spaces. However, these results should be interpreted with caution as they vary among cyanobacterial isolates. According to Aufrecht et al. (Aufrecht et al. 2019), the spatial distribution of microorganisms in their heterogenous network is determined by the EPS production ability and biofilm expansion over the biofilm formation process. In fact, biofilms developed on silicone hydrogel surfaces exhibited lower biofilm thickness, which may be related to their lower cellular growth and expansion.

5.5. Conclusions

Our results demonstrated high AF performance of the silicone hydrogel coating in inhibiting or delaying cyanobacterial biofilm formation. Additionally, the comprehensive analysis carried out in this study revealed that the surface material properties, together with the features of the fouling microorganisms, play a considerable role in marine biofouling.

5.6. References

Akinfijevs, T., A. Janvaevskis and E. Lavendelis (2007). A Brief Survey of Ship Hull Cleaning Devices. RTU. Riga, Latvia. **24:** 133-146.

Angelova, A. G., G. A. Ellis, H. W. Wijesekera and G. J. Vora (2019). "Microbial Composition and Variability of Natural Marine Planktonic and Biofouling Communities From the Bay of Bengal." Frontiers in Microbiology **10**(2738).

Arrhenius, A., T. Backhaus, A. Hilvarsson, I. Wendt, A. Zgrundo and H. Blanck (2014). "A novel bioassay for evaluating the efficacy of biocides to inhibit settling and early establishment of marine biofilms." Mar Pollut Bull **87**(1-2): 292-299.

Aufrecht, J. A., J. D. Fowlkes, A. N. Bible, J. Morrell-Falvey, M. J. Doktycz and S. T. Retterer (2019). "Pore-scale hydrodynamics influence the spatial evolution of bacterial biofilms in a microfluidic porous network." PLoS One **14**(6): e0218316.

Bakker, D., A. Van der Plaats, G. Verkerke, H. Busscher and H. Van der Mei (2003). "Comparison of velocity profiles for different flow chamber designs used in studies of microbial adhesion to surfaces." Applied and environmental microbiology **69**(10): 6280-6287.

Banerjee, I., R. C. Pangule and R. S. Kane (2011). "Antifouling coatings: recent developments in the design of surfaces that prevent fouling by proteins, bacteria, and marine organisms." Advanced materials **23**(6): 690-718.

Bartram, J. and I. Chorus (1999). Toxic cyanobacteria in water: a guide to their public health consequences, monitoring and management. Boca Raton, FL, USA, CRC Press.

Bayoudh, S., A. Othmane, F. Bettaieb, A. Bakhrouf, H. B. Ouada and L. Ponsonnet (2006). "Quantification of the adhesion free energy between bacteria and hydrophobic and hydrophilic substrata." Materials Science and Engineering: C **26**(2-3): 300-305.

Blain, S., J. Guillou, P. Tréguer, P. Woerther, L. Delauney, E. Follenfant, O. Gontier, M. Hamon, B. Leildé, A. Masson, C. Tartu and R. Vuillemin (2004). "High frequency monitoring of the coastal marine environment using the MAREL buoy." Journal of Environmental Monitoring **6**(6): 569-575.

Boedicker, J. Q., M. E. Vincent and R. F. Ismagilov (2009). "Microfluidic confinement of single cells of bacteria in small volumes initiates high-density behavior of quorum sensing and growth and reveals its variability." Angew Chem Int Ed Engl **48**(32): 5908-5911.

Busscher, H. J., A. H. Weerkamp, H. C. van der Mei, A. W. van Pelt, H. P. de Jong and J. Arends (1984). "Measurement of the surface free energy of bacterial cell surfaces and its relevance for adhesion." Applied and environmental microbiology **48**(5): 980-983.

Cerca, N., G. B. Pier, M. Vilanova, R. Oliveira and J. Azeredo (2005). "Quantitative analysis of adhesion and biofilm formation on hydrophilic and hydrophobic surfaces of clinical isolates of Staphylococcus epidermidis." Res Microbiol **156**(4): 506-514.

Crawford, R. J., H. K. Webb, V. K. Truong, J. Hasan and E. P. Ivanova (2012). "Surface topographical factors influencing bacterial attachment." Advances in Colloid and Interface Science **179-182**: 142-149.

Dantas, L. C. d. M., J. P. da Silva-Neto, T. S. Dantas, L. Z. Naves, F. D. das Neves and A. S. da Mota (2016). "Bacterial Adhesion and Surface Roughness for Different Clinical Techniques for Acrylic Polymethyl Methacrylate." International journal of dentistry: 8685796-8685796.

De-la-Pinta, I., M. Cobos, J. Ibarretxe, E. Montoya, E. Eraso, T. Guraya and G. Quindós (2019). "Effect of biomaterials hydrophobicity and roughness on biofilm development." Journal of Materials Science: Materials in Medicine **30**(7): 77.

de Carvalho, C. C. C. R. (2018). "Marine Biofilms: A Successful Microbial Strategy With Economic Implications." Frontiers in Marine Science **5**(126).

Donlan, R. M. (2002). "Biofilms: microbial life on surfaces." Emerg Infect Dis **8**(9): 881-890.

Faria, S. I., R. Teixeira-Santos, L. C. Gomes, E. R. Silva, J. Morais, V. Vasconcelos and F. J. M. Mergulhão (2020). "Experimental Assessment of the Performance of Two Marine Coatings to Curb Biofilm Formation of Microfoulers." Coatings **10**(9).

Faria, S. I., R. Teixeira-Santos, M. J. Romeu, J. Morais, V. Vasconcelos and F. J. Mergulhão (2020). "The Relative Importance of Shear Forces and Surface Hydrophobicity on Biofilm Formation by Coccoid Cyanobacteria." Polymers **12**(3).

Gomes, L. C., J. Deschamps, R. Briandet and F. J. Mergulhao (2018). "Impact of modified diamond-like carbon coatings on the spatial organization and disinfection of mixed-biofilms composed of Escherichia coli and Pantoea agglomerans industrial isolates." Int J Food Microbiol **277**: 74-82.

Hou, J., C. Wang, R. T. Rozenbaum, N. Gusnaniar, E. D. de Jong, W. Woudstra, G. I. Geertsema-Doornbusch, J. Atema-Smit, J. Sjollema, Y. Ren, H. J. Busscher and H. C. van der Mei (2019). "Bacterial Density and Biofilm Structure Determined by Optical Coherence Tomography." Scientific Reports **9**(1): 9794.

Hu, P., Q. Xie, C. Ma and G. Zhang (2020). "Silicone-based fouling-release coatings for marine antifouling." Langmuir **36**(9): 2170-2183.

Hwang, G., S. Kang, M. G. El-Din and Y. Liu (2012). "Impact of conditioning films on the initial adhesion of Burkholderia cepacia." Colloids Surf B Biointerfaces **91**: 181-188.

Irving, T. E. and D. G. Allen (2011). "Species and material considerations in the formation and development of microalgal biofilms." Appl Microbiol Biotechnol **92**(2): 283-294.

Jain, A., K. K. Nishad and N. B. Bhosle (2007). "Effects of DNP on the cell surface properties of marine bacteria and its implication for adhesion to surfaces." Biofouling **23**(3): 171-177.

Janczuk, B., E. Chibowski, J. M. Bruque, M. L. Kerkeb and F. G. Caballero (1993). "On the Consistency of Surface Free Energy Components as Calculated from Contact Angles of Different Liquids: An Application to the Cholesterol Surface." Journal of Colloid and Interface Science **159**(2): 421-428.

Jindal, S., S. Anand, K. Huang, J. Goddard, L. Metzger and J. Amamcharla (2016). "Evaluation of modified stainless steel surfaces targeted to reduce biofilm formation by common milk sporeformers." J Dairy Sci **99**(12): 9502-9513.

Kanematsu, H. and D. M. Barry (2020). "Biofilm on Materials' Surfaces in Marine Environments." Monitoring Artificial Materials and Microbes in Marine Ecosystems: Interactions and Assessment Methods **2**: 177-187.

Kim, H. J., J. Q. Boedicker, J. W. Choi and R. F. Ismagilov (2008). "Defined spatial structure stabilizes a synthetic multispecies bacterial community." Proceedings of the National Academy of Sciences **105**(47): 18188.

Kotai, J. (1972). Instructions for Preparation of Modified Nutrient Solution Z8 for AlgaeNorwegian. Institute for Water Research. Blindern, Oslo, Norway.

Lacoursière-Roussel, A., D. G. Bock, M. E. Cristescu, F. Guichard and C. W. McKindsey (2016). "Effect of shipping traffic on biofouling invasion success at population and community levels." Biological Invasions **18**(12): 3681-3695.

Lorite, G. S., C. M. Rodrigues, A. A. de Souza, C. Kranz, B. Mizaikoff and M. A. Cotta (2011). "The role of conditioning film formation and surface chemical changes on Xylella fastidiosa adhesion and biofilm evolution." Journal of Colloid and Interface Science **359**(1): 289-295.

Lou, T., X. Bai, X. He and C. Yuan (2021). "Antifouling performance analysis of peptide-modified glass microstructural surfaces." Applied Surface Science **541**: 148384.

Ma, Y., X. Cao, X. Feng, Y. Ma and H. Zou (2007). "Fabrication of super-hydrophobic film from PMMA with intrinsic water contact angle below 90°." Polymer **48**(26): 7455-7460.

Mazumder, S., J. O. Falkinham, A. M. Dietrich and I. K. Puri (2010). "Role of hydrophobicity in bacterial adherence to carbon nanostructures and biofilm formation." Biofouling **26**(3): 333-339.

Meireles, A., R. Fulgêncio, I. Machado, F. Mergulhão, L. Melo and M. Simões (2017). "Characterization of the heterotrophic bacteria from a minimally processed vegetables plant." LWT - Food Science and Technology **85**: 293-300.

Moreira, J., L. Gomes, K. Whitehead, S. Lynch, L. Tetlow and F. Mergulhão (2017). "Effect of surface conditioning with cellular extracts on Escherichia coli adhesion and initial biofilm formation." Food and Bioproducts Processing **104**: 1-12.

Murosaki, T., N. Ahmed and J. P. Gong (2012). "Antifouling properties of hydrogels." Science and Technology of Advanced Materials **12**.

Nahar, S., M. F. R. Mizan, A. J.-w. Ha and S.-D. Ha (2018). "Advances and Future Prospects of Enzyme-Based Biofilm Prevention Approaches in the Food Industry." Comprehensive Reviews in Food Science and Food Safety **17**(6): 1484-1502.

Neves, A. R., J. R. Almeida, F. Carvalhal, A. Câmara, S. Pereira, J. Antunes, V. Vasconcelos, M. Pinto, E. R. Silva, E. Sousa and M. Correia-da-Silva (2020). "Overcoming environmental problems of biocides: Synthetic bile acid derivatives as a sustainable alternative." Ecotoxicology and Environmental Safety **187**: 109812.

Nurioglu, A. G., A. C. C. Esteves and G. de With (2015). "Non-toxic, non-biocide-release antifouling coatings based on molecular structure design for marine applications." Journal of Materials Chemistry B **3**(32): 6547-6570.

Otsu, N. (1979). "A Threshold Selection Method from Gray-Level Histograms." IEEE Transactions on Systems, Man, and Cybernetics **9**(1): 62-66.

Ozkan, A. and H. Berberoglu (2013). "Cell to substratum and cell to cell interactions of microalgae." Colloids and Surfaces B: Biointerfaces **112**: 302-309.

Qu, Y.-Y. and S.-F. Zhang (2012). "Preparation and characterization of novel waterborne antifouling coating." Journal of Coatings Technology and Research **9**(6): 667-674.

Rajeev, M., T. J. Sushmitha, K. G. Prasath, S. R. Toleti and S. K. Pandian (2020). "Systematic assessment of chlorine tolerance mechanism in a potent biofilm-forming marine bacterium Halomonas boliviensis." International Biodeterioration & Biodegradation **151**: 104967.

Ramos, V., J. Morais, R. Castelo-Branco, Â. Pinheiro, J. Martins, A. Regueiras, A. L. Pereira, V. R. Lopes, B. Frazão, D. Gomes, C. Moreira, M. S. Costa, S. Brûle, S. Faustino, R. Martins, M. Saker, J. Osswald, P. N. Leão and V. M. Vasconcelos (2018). "Cyanobacterial diversity held in microbial biological resource centers as a biotechnological asset: the case

study of the newly established LEGE culture collection." Journal of Applied Phycology **30**(3): 1437-1451.

Rees, G. and J. Bartram (2002). Monitoring bathing waters: a practical guide to the design and implementation of assessments and monitoring programmes. Boca Raton, FL, USA, CRC Press.

Romeu, M. J., P. Alves, J. Morais, J. M. Miranda, E. D. de Jong, J. Sjollema, V. Ramos, V. Vasconcelos and F. J. M. Mergulhão (2019). "Biofilm formation behaviour of marine filamentous cyanobacterial strains in controlled hydrodynamic conditions." Environ Microbiol **21**(11): 4411-4424.

Schultz, M. P., J. A. Bendick, E. R. Holm and W. M. Hertel (2011). "Economic impact of biofouling on a naval surface ship." Biofouling **27**(1): 87-98.

Sekar, R., V. P. Venugopalan, K. K. Satpathy, K. V. K. Nair and V. N. R. Rao (2004). "Laboratory studies on adhesion of microalgae to hard substrates." Hydrobiologia **512**(1): 109-116.

Selim, M. S., M. A. Shenashen, S. A. El-Safty, S. A. Higazy, M. M. Selim, H. Isago and A. Elmarakbi (2017). "Recent progress in marine foul-release polymeric nanocomposite coatings." Progress in Materials Science **87**: 1-32.

Sjollema, J., H. Keul, H. van der Mei, R. Dijkstra, M. Rustema-Abbing, J. de Vries, T. Loontjens, T. Dirks and H. Busscher (2017). "A Trifunctional, Modular Biomaterial Coating: Nonadhesive to Bacteria, Chlorhexidine-Releasing and Tissue-Integrating." Macromolecular Bioscience **17**(4): 1600336.

Spengler, C., F. Nolle, J. Mischo, T. Faidt, S. Grandthyll, N. Thewes, M. Koch, F. Müller, M. Bischoff, M. A. Klatt and K. Jacobs (2019). "Strength of bacterial adhesion on nanostructured surfaces quantified by substrate morphometry." Nanoscale **11**(42): 19713-19722.

Suarez, C., M. Piculell, O. Modin, S. Langenheder, F. Persson and M. Hermansson (2019). "Thickness determines microbial community structure and function in nitrifying biofilms via deterministic assembly." Scientific Reports **9**(1): 5110.

Talluri, S. N. L., R. M. Winter and D. R. Salem (2020). "Conditioning film formation and its influence on the initial adhesion and biofilm formation by a cyanobacterium on photobioreactor materials." Biofouling **36**(2): 183-199.

Taylor, D. A. (1996). Introduction to Marine Engineering. Oxford, UK, Butterworth-Heinemann.

Telegdi, J., L. Trif and L. Románszki (2016). 5 - Smart anti-biofouling composite coatings for naval applications. Smart Composite Coatings and Membranes. M. F. Montemor. Sawston, Cambridge, Woodhead Publishing**:** 123-155.

Thukkaram, M., S. Sitaram, S. k. Kannaiyan and G. Subbiahdoss (2014). "Antibacterial Efficacy of Iron-Oxide Nanoparticles against Biofilms on Different Biomaterial Surfaces." International Journal of Biomaterials **2014**: 716080.

Tian, L., Y. Yin, H. Jin, W. Bing, E. Jin, J. Zhao and L. Ren (2020). "Novel marine antifouling coatings inspired by corals." Materials Today Chemistry **17**: 100294.

Tulcidas, A. V., R. Bayón, A. Igartua, J. C. M. Bordado and E. R. Silva (2015). "Friction reduction on recent non-releasing biocidal coatings by a newly designed friction test rig." Tribology International **91**: 140-150.

Turner, A. (2020). "Foamed Polystyrene in the Marine Environment: Sources, Additives, Transport, Behavior, and Impacts." Environmental Science & Technology **54**(17): 10411-10420.

Van Oss, C. J. (1994). Interfacial forces in aqueous media. Marcel Dekker Inc. New York, USA.

Wang, H., M. Sodagari, Y. Chen, X. He, B.-m. Z. Newby and L.-K. Ju (2011). "Initial bacterial attachment in slow flowing systems: Effects of cell and substrate surface properties." Colloids and Surfaces B: Biointerfaces **87**(2): 415-422.

Xie, L., F. Hong, C. He, C. Ma, J. Liu, G. Zhang and C. Wu (2011). "Coatings with a self-generating hydrogel surface for antifouling." Polymer **52**(17): 3738-3744.

Zecher, K., V. P. Aitha, K. Heuer, H. Ahlers, K. Roland, M. Fiedel and B. Philipp (2018). "A multi-step approach for testing non-toxic amphiphilic antifouling coatings against marine microfouling at different levels of biological complexity." J Microbiol Methods **146**: 104-114.

Zhang, X., Q. Zhang, T. Yan, Z. Jiang, X. Zhang and Y. Y. Zuo (2015). "Quantitatively predicting bacterial adhesion using surface free energy determined with a spectrophotometric method." Environmental science & technology **49**(10): 6164-6171.

Zheng, S., M. Bawazir, A. Dhall, H.-E. Kim, L. He, J. Heo and G. Hwang (2021). "Implication of Surface Properties, Bacterial Motility, and Hydrodynamic Conditions on Bacterial Surface Sensing and Their Initial Adhesion." Frontiers in Bioengineering and Biotechnology **9**(82).

6.

Developing new marine antifouling surfaces: learning from single-strain laboratory tests[d]

Abstract

The development of AF technology for marine environments is an area of intense research given the severe economic and ecological effects of marine biofouling. Preliminary data from *in vitro* assays is frequently used to screen the performance of AF coatings. It is intuitive that the microbial composition plays a major role in surface colonization. The rationale behind this study is to investigate whether using a mixed population for the *in vitro* tests yields substantially different results than using single-strains during initial screening. A polymeric coating was tested against single- and dual-species cultures of two common microfouler organisms for 49 days. A bacterium (*Pseudoaltermonas tunicata*) and a cyanobacterium (*Cyanobium* sp. LEGE 10375) were used in this chapter. Linear regression analysis revealed that *Cyanobium* sp. biofilms were significantly associated with a higher number of cells, wet weight, thickness, and biovolume compared to dual-species biofilms. *P. tunicata* alone had a biofilm growth kinetics similar to dual-species biofilms, although the *P. tunicata* - *Cyanobium* sp. mixture developed less dense and thinner biofilms compared to

[d] The content of this chapter was adapted from the following publication(s):

Faria, S. I., L. C. Gomes, R. Teixeira-Santos, J. Morais, V. Vasconcelos and F. J. Mergulhão (2021). "Developing New Marine Antifouling Surfaces: Learning from Single-Strain Laboratory Tests." Coatings **11**(1): 90.

both single-species biofilms. *Cyanobium* sp. LEGE 10375 biofilms provided the worst-case scenario, *i.e.*, the conditions that caused higher biofilm amounts on the surface material under test. Therefore, it is likely that assessing the AF performance of new coatings using the most stringent conditions may yield more robust results than using a mixed population, as competition between microfouler organisms may reduce the biofilm formation capacity of the consortium.

6.1.Introduction

Marine biofouling is a colonization process that starts when a surface material is immersed in seawater and leads to the development of complex biological communities called biofilms (Caruso 2020). This undesirable attachment of molecules and fouling organisms to submerged surfaces causes economic losses to human activities in the sea, including maritime transport, water desalination, aquaculture, and oil and gas industries (de Carvalho 2018). Indeed, the main problems of biofouling on marine vessels are related to the corrosion and increased frictional effects created by the presence of organisms on the vessel surface (Tian et al. 2020). This can reduce the maneuverability of ships due to their increased weight and reduced speed, resulting in increased fuel consumption (Brooks and Waldock 2009, Tian et al. 2020). High levels of biofouling activity can also lead to increased frequency of dry-docking operations and an overall reduction of the integrity of the ship hulls, factors that have significant financial impacts to the vessel owners (Brooks and Waldock 2009). Additionally, biofouling communities have the potential to transport invasive non-native species across geographical niches, which can have disastrous effects on native populations and communities (Lacoursière-Roussel et al. 2016). Therefore, the need to protect submerged surfaces from biofouling organisms is of economic and environmental importance.

The scientific community has been focusing its efforts on overcoming these problems by developing AF coatings (Miller et al. 2020). The most well-consolidated and commercially established AF coatings are biocide-containing paints (Silva et al. 2019), typically employing copper or zinc as the active ingredient (Amara et al. 2018, Miller et al. 2020). However, alternative protective AF coatings are being developed taking into account

new rigid international regulations and consumer environmental concerns. At present, there are two major environmental-friendly AF strategies, which are foul release coatings (Faria et al. 2020a, Silva et al. 2019) and bioinspired coatings that prevent the settlement of organisms through their surface properties (e.g., micro- or nano-structured "self-cleaning" surfaces) (Li and Guo 2019, Salta et al. 2010).

For testing the performance of novel AF coatings, these should be first screened under laboratory conditions that mimic the marine environment since the direct evaluation of coatings in the ocean would be very expensive due to the large quantities of test products and prolonged immersion times that are required. Additionally, field tests have their own drawbacks, like the ecotoxicity of some biocide-release coatings (Zecher et al. 2018).

Several factors may influence the efficacy of an AF coating, including the water temperature and salinity, available nutrients, hydrodynamics, and organisms that can vary significantly depending on the sea site (Caruso 2020, Romeu et al. 2019). It is described that marine biofilms are mainly composed of different species of bacteria and diatoms (de Carvalho 2018). The most studied biofilm communities are those established in the euphotic zones of aquatic habitats, comprising photoautotrophic microorganisms, such as diatoms, green algae, and cyanobacteria, which produce the organic carbon that fuels the life of heterotrophic microorganisms, such as bacteria (Buhmann et al. 2012). Although diatom-bacteria co-cultures under photoautotrophic conditions would be more realistic than single monocultures, there are only a few test systems at a laboratory scale using such mixed cultures (Buhmann et al. 2012, Zecher et al. 2018). The study of multispecies biofilms may be limited by the complexity of each community and the lack of knowledge regarding the identity and abundance of each biofilm resident, which makes it difficult to select the organisms for the *in vitro* assays, as well as by some technical limitations associated with different biofilm setups (Magana et al. 2018). Furthermore, although it is described that the physiology and function of these complex communities differ from those of the individual species when examined as monocultures (Burmølle et al. 2014, Røder et al. 2016), it has recently been proven that increasing culture diversity beyond a threshold has little effect on interspecies interactions and biomass production (Azevedo et al. 2020, Yu et al. 2019). The rationale behind the present chapter is whether there are benefits in varying the degree of complexity of marine cultures when the goal is to get the first indications about the AF

materials´ performance. A polymeric coating commonly used to coat the hulls of small recreational vessels and with known antibiofilm activity (Faria et al. 2020b) was tested against single mono-species (*Pseudoalteromonas tunicata* or *Cyanobium* sp. LEGE 10375) and dual-species cultures (*P. tunicata* - *Cyanobium* sp. LEGE 10375) in order to identify which culture conditions generate the worst-case scenario, and thus the most appropriate *in vitro* experiments for the initial screening of the performance of novel AF marine surfaces.

6.2. Materials and methods

6.2.1. Surface preparation

A glass surface coated with a polymer epoxy resin was tested for single- and dual-species biofilm formation. Epoxy resins are typically used to coat the hulls of small recreation vessels (e.g. powerboats, yachts, sailing boats) (Blain et al. 2004, Taylor 1996) since they contribute to the production of stiffer, stronger, lighter hulls with improved structural stability and hydrodynamic performance (Hoge and Leach 2016). Furthermore, they can have AF activity (Faria et al. 2020b). Glass coupons (1 x 1 cm^2; Vidraria Lousada, Lda, Lousada, Portugal) were firstly washed and sterilized as fully described in Faria el al. 2020 (Faria et al. 2020b), and then coated with 70 µL of a polymer epoxy resin (HB Química company, Matosinhos, Portugal) by spin coating (Spin150 Polos^{TM} , Paralab, Porto, Portugal) at 6000 rpm for 40 s, with ascends of 1000 rpm. Coated surfaces were dried in two different steps (12 h at room temperature and 3 h at 60 °C) as previously described (Faria et al. 2020b). Surfaces were sterilized by immersion in 70% (v/v) ethanol (VWR International S.A.A., Fontenay-sous-Bois, France) for 20 min and air-dried inside a flow chamber to maintain sterility. The initial weight of each coupon was determined before experiments.

6.2.2. Marine organisms and culture conditions

One marine bacteria - *Pseudoalteromonas tunicata* DSM 14096 - and one cyanobacteria - *Cyanobium* sp. LEGE 10375 - were the microorganisms chosen for this study

since they are recognized as early colonizers in the fouling process (de Carvalho 2018). Additionally, they are typically present in the euphotic zone of a marine ecosystem, where the best characterized multispecies biofilms are developed (Buhmann et al. 2012).

P. tunicata (DSMZ, Braunschweig, Germany) was stored at -80 °C in 20% (v/v) glycerol (Fisher Scientific, Geel, Belgium). Before the experiments, bacteria were subcultured twice on the complex marine medium Våatanen Nine Salt Solution (VNSS) (Holmström et al. 1998) supplemented with 15 g/L agar (VWR International S.A.A., Fontenay-sous-Bois, France) for 24 h at 25 °C. An overnight culture was then prepared by transferring colonies from a VNSS agar plate to 150 mL of VNSS medium and incubating at 25 °C with agitation.

Cyanobium sp. LEGE 10375 was isolated from an intertidal zone, on a marine sponge, at São Bartolomeu do Mar beach (Esposende, Braga, Portugal) (41.57378 N 8.798556 W). This cyanobacteria was obtained from LEGE-CC, located at the CIIMAR, Matosinhos, Portugal (Ramos et al. 2018). Cyanobacteria were growth in 750 mL of Z8 medium supplemented with 25 g/L of synthetic sea salts (Tropic Marin, Montague, MA, USA) and vitamin B12 (Sigma Aldrich, Merck, Saint Louis, MO, USA), at 25 °C under 14 h light (10 - 30 mol photons/m^2 s, λ = 380 - 700 nm)/10 h dark cycles (Faria et al. 2020b).

6.2.3. Single- and dual-species biofilm formation

The ability of *P. tunicata* and *Cyanobium* sp. alone and in co-culture to colonize the coated surface was monitored for 7 weeks (49 days) using 12-well microplates (VWR International, Carnaxide, Portugal) under controlled hydrodynamic conditions. Biofilm development was followed for 49 days because this period corresponds to approximately half of the minimal economically viable interval accepted for the maintenance of underwater systems (Blain et al. 2004) and hull cleaning (Schultz et al. 2011). Biofilms were grown in an orbital shaker with a 25 mm diameter (Agitorb 200ICP, Norconcessus, Ermesinde, Portugal) at 185 rpm, which corresponds to an average shear rate of 40 s^{-1} and a maximum of 120 s^{-1} (Faria et al. 2020a, Romeu et al. 2019), comprising the shear rate value of 50 s^{-1} estimated for a ship in a harbour (Bakker et al. 2003).

P. tunicata DSM 14096 and *Cyanobium* sp. LEGE 10375 suspensions at a final concentration of 1 x 10^8 CFU/mL were prepared in VNSS medium from the corresponding overnight cultures. For *Cyanobium* sp., a 1 x 10^8 CFU/mL cell suspension was also prepared in Z8 medium as a growth control (Figure 6.1.) since this is the recommended medium for the cultivation of these species of cyanobacteria (Faria et al. 2020b). For dual-species biofilms of *P. tunicata* and *Cyanobium* sp., both cell suspensions were mixed at a 1:1 ratio (Gomes et al. 2018) in order to obtain a final concentration of 1 x 10^8 CFU/mL. The coated glass coupons were first fixed to the plate wells using double-sided adhesive tape UV-sterilized for 30 min (Faria et al. 2020b). Then, 3 mL of each single- and dual-species culture were added to the wells, and the microplates were incubated with the alternate light cycles of 14 h light/10 h dark cycles, at 25 °C for 49 days. Additionally, 3 mL of VNSS medium were added to the wells containing coated glass coupons in order to control the surfaces´ sterility throughout the 49 days of the experiment (negative control). Two coupons for each experimental condition were removed every 7 days for biofilm analysis. During the incubation period, the culture medium was carefully replaced twice a week. Three independent biofilm formation assays, with two technical replicates each, were performed.

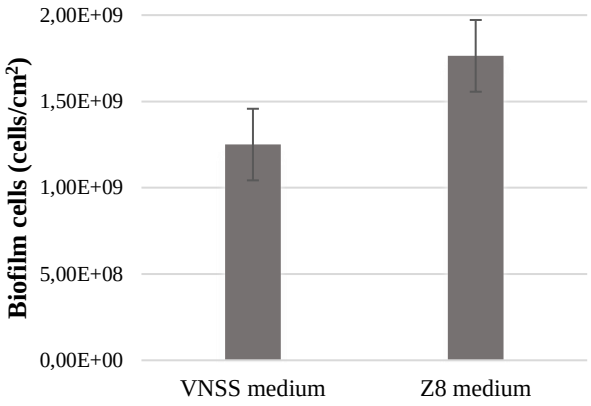

Figure 6.1. Number of *Cyanobium* sp. cells growing in Våatanen nine salt solution (VNSS) and Z8 medium attached on polymer epoxy resin after 49 days of incubation.

6.2.4. Biofilm analysis

The removed coupons were gently washed with 3 mL of 0.85 % (v/v) sterile saline solution to remove non-attached microorganisms (Faria et al. 2020a) and analyzed regarding the number of biofilm cells, biofilm wet weight, and biofilm thickness. The biofilm architecture was also evaluated through CLSM after 21, 35 and 49 days.

6.2.4.1. Cell density and wet weight

The cell counting and biofilm wet weight determination was performed as was described in chapter 4, section 4.2.5.1.

6.2.4.2. Thickness

The biofilm thickness analysis was performed as was described in chapter 4, section 4.2.5.2.

6.2.4.3. CLSM

Single- and dual-species biofilms of *P. tunicata* and *Cyanobium* sp. were imaged using a Leica TCS SP5 II Confocal Laser Scanning Microscope (Leica Microsystems, Wetzlar, Germany) after 21, 35 and 49 days of biofilm formation. Biofilm samples were counter-stained with Syto9 (Thermo Fisher Scientific, Waltham, MA, USA), a green cell-permeant nucleic acid marker, for 10 min at room temperature, and then scanned at 40x magnitude with a HCX PL APO CS 40x/1.10 CORR water objective lens at an excitation wavelength of 488 nm (argon laser). The emitted fluorescence was recorded within the range of 460 to 575 nm. A minimum of five stacks of horizontal plane images (512 x 512 pixels, corresponding to 387.5 µm x 387.5 µm) with a *z*-step of 1 µm were acquired for each biofilm sample.

3D projections of biofilm structures were reconstructed from the CLSM acquisitions using the blend mode of the "Easy 3D" function of the IMARIS 9.1 software (Bitplane, Zurich, Switzerland). Biofilm biovolume ($\mu m^3/\mu m^2$) was extracted from confocal image

series with the plug-in COMSTAT2 run in ImageJ 1.48v software, as previously described (Heydorn et al. 2000). Biovolume represents the total amount of biofilm (μm^3) in the substratum area of the image stack (μm^2).

6.2.5. Statistical analysis

Descriptive statistics were used to compute mean and standard deviation for all parameters evaluated in single- and dual-species biofilms: the total cell number (Figure 6.1.A), wet weight (Figure 6.1.B), thickness (Figure 6.1C) and biovolume (Figure 6.2.A). Since the variable distribution was normal, one-way ANOVA analysis was used to compare biofilm formation between single- (*P. tunicata* or *Cyanobium* sp.) and dual-species biofilms (*P. tunicata* - *Cyanobium* sp.) on each experimental day. For each time point, letters were assigned in alphabetic order from the highest to the lowest value (from a to c) as long as statistically significant differences exist between the biofilms with a confidence level greater than 95% ($p < 0.05$).

Linear regression models (LRM) were applied between the biofilm cells, wet weight, thickness and biovolume, and single- and dual-species biofilms (Figure 6.1.D, E and F, and Figure 6.2B). Models were adjusted for incubation days. For all LRMs, dual-species biofilms were used as the reference condition. Results were presented as beta estimates (β) and the corresponding 95% confidence intervals (95% CI).

Data analysis was performed using the IBM SPSS Statistics version 24.0 for Windows (IBM SPSS, Inc., Chicago, IL, USA).

6.3. Results

In this study, the ability of two common microfouler organisms, a marine bacterium and a cyanobacterium (*P. tunicata* and *Cyanobium* sp.) to develop single- and dual-species biofilms in epoxy-coated surfaces was analysed. The importance of conducting multispecies biofilm assays for initial screening of the AF potential of novel surface coatings for marine settings was assessed.

Figure 6.2 presents the number of biofilm cells, wet weight and thickness determined for single- (*P. tunicata* or *Cyanobium* sp. LEGE 10375) and dual-species biofilms (*P. tunicata* - *Cyanobium* sp. LEGE 10375) grown for 49 days under hydrodynamic conditions that mimic the aquatic environment.

In general, the cell number of *Cyanobium* sp. LEGE 10375 biofilms was higher than for *P. tunicata* and dual-species biofilms (on average 33% and 27%, respectively), with significant statistical differences in almost all sampling points ($p < 0.05$, Figure 6.2.A). While single-species biofilms of *P. tunicata* and dual-species biofilms grew markedly between days 7 and 14 (approximately 1 log cells/cm^2), tending towards similar growth kinetics and stabilization by the end of the experiment, the cell number in cyanobacterial biofilms increased exponentially until day 21, reaching $9.4 \times 10^8 \pm 3.3 \times 10^5$ cells/cm^2, which is 52% and 28% higher than the value for *P. tunicata* biofilms and dual-species biofilms, respectively, at the same time point ($p < 0.05$).

The wet weight of *P. tunicata* single-species biofilms and mixed biofilms increased to an average value of 76 mg on day 21 (Figure 6.2.B). This biofilm parameter remained practically constant in the following two weeks for both types of biofilm. However, its behavior changed with the gradual increase of the wet weight of dual-species biofilms until day 49, and the abrupt reduction of the weight of *P. tunicata* biofilms (to about half at the end of the experiment). With regard to cyanobacterial biofilms, their wet weight increased linearly until day 35, exceeding by 26% the wet weight of bacterial and bacteria - cyanobacteria biofilms ($p < 0.01$).

Concerning biofilm thickness, there was a linear increase during the 7-week assay in the three types of analyzed biofilms, *P. tunicata* and *Cyanobium* sp. single-species biofilms and *P. tunicata* - *Cyanobium* sp. biofilms (Figure 6.2.C). Moreover, cyanobacterial biofilms were significantly thicker than *P. tunicata* biofilms (on average 31%, $p < 0.05$ for five out of seven time points) and dual-species biofilms (on average 42%, $p < 0.05$ for all time points). This difference between *Cyanobium* sp. biofilms and both *P. tunicata* single- and dual-species biofilms was particularly noticeable from day 28 onwards when the thickness of cyanobacterial biofilms increased from about 100 µm to the maximum value of 260 µm at day 49 (37% and 53% higher than *P. tunicata* single- and dual-species biofilms, respectively, $p < 0.01$). It is also possible to observe that the thickness profile of *P. tunicata* biofilms was

similar to the mixed biofilms, although slightly higher thickness values were obtained for the single-species biofilms (on average 17%; $p < 0.05$ for three of the seven experimental points).

Regarding the biovolume obtained from the CLSM data acquired (Figure 6.3.A), cyanobacterial biofilms displayed 50% more biomass accumulation than axenic *P. tunicata* biofilms and dual-species biofilms, regardless of the sampling day ($p < 0.05$).

In an attempt to clarify the relationship between the biofilm parameter (number of biofilm cells, weight, thickness, or biovolume) and the community complexity (single- or dual-species biofilms), linear regression models were used (Figure 6.2.D-F, and Figure 6.3.B). The results from the LRMs have positive or negative results whenever a giver condition generated an increase or decrease, respectively, in the analysis parameter (β) in comparison with the reference condition (in this case, the dual-species biofilms). In general, *Cyanobium* sp. biofilms formed on gel-coated glass surfaces were significantly associated with a large number of cells ($\beta = 2.32 \times 10^8$ cells/cm^2, 95% CI = [7.84×10^7: 3.85×10^8]), thickness ($\beta = 61.89$ µm, 95% CI = [46.07: 77.71]) and biovolume ($\beta = 36.01$ µm^3/µm^2, 95% CI = [28.38: 43.64]) when compared to dual-species biofilms (Figure 6.2.D, F, and Figure 6.3.B). Likewise, the wet weight of *Cyanobium* sp. biofilms was higher than dual-species biofilms (β = 3.64 mg, 95% CI = [- 7.13: 14.4]) (Figure 6.2.E). Considering *P. tunicata* biofilms, only the biofilm thickness was significantly higher than dual-species biofilms ((β = 22.27 µm, 95% CI = [8.12: 36.42]) (Figure 6.2.F). *P. tunicata* biofilms were significantly associated with a lower biofilm wet weight (β = -10.63 mg, 95% CI = [- 20.27: - 1.00]) and biovolume (β = -7.87 µm^3/µm^2, 95% CI = [-15.80: 0.00]) when compared to dual-species biofilms (Figure 6.2.E and 6.3.B).

The spatial distribution of single- and dual-species biofilms developed on gel-coated surfaces was evaluated by CLSM (Figure 6.4.). Regardless of incubation day, cyanobacterial biofilms exhibited more biomass and thickness than *P. tunicata* biofilms and dual-species biofilms. Confocal microscopic images corroborate the results presented in Figures 6.2. and 6.3. by showing that *Cyanobium* sp. LEGE 10375 biofilms were the worst-case population conditions, i.e., the conditions that had a greater biofilm amount on the surface material under test. *P. tunicata* alone had an intermediate biofilm-forming ability, while the bacterium-cyanobacterium mixture developed less dense and thinner biofilms when compared to the single-species biofilms of the same marine strains (Figure 6.4.).

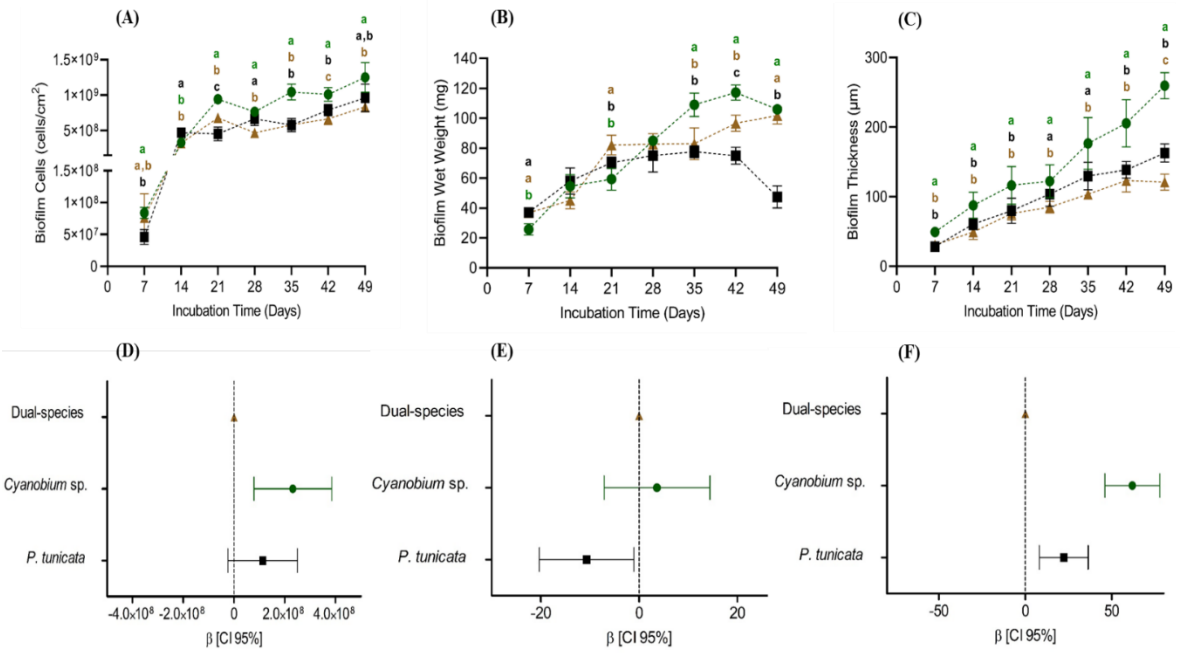

Figure 6.2. (A - C) Single- and dual-species biofilm formation on gel-coated glass surfaces during 49 days: ● - *Cyanobium* sp. LEGE 10375, ■ - *Pseudoalteromonas tunicata*, and ▲ - *Pseudoalteromonas tunicata* - *Cyanobium* sp. LEGE 10375. The biofilm parameters are (**A**) number of cells, (**B**) wet weight, and (**C**) thickness. Letters were assigned in alphabetic order from the highest to the lowest value (from a to c) for each time point. These assignments were made as long as statistically significant differences existed between the biofilms with a confidence level greater than 95% ($p < 0.05$). The color of the letters allows the association with the type of biofilm formed (green - *Cyanobium* sp. LEGE 10375, black - *Pseudoalteromonas tunicata*, and brown - *Pseudoalteromonas tunicata* - *Cyanobium* sp. LEGE 10375). The means ± SDs for three independent experiments are illustrated. (**D** - **F**) Association between the (**D**) number of biofilm cells, (**E**) wet weight, and (**F**) thickness, and single- and dual-species biofilms. Dual-species biofilms were used as the reference condition. Linear regression models were adjusted for incubation days. Results were represented as beta estimates (β) and the corresponding 95% confidence interval (95% CI).

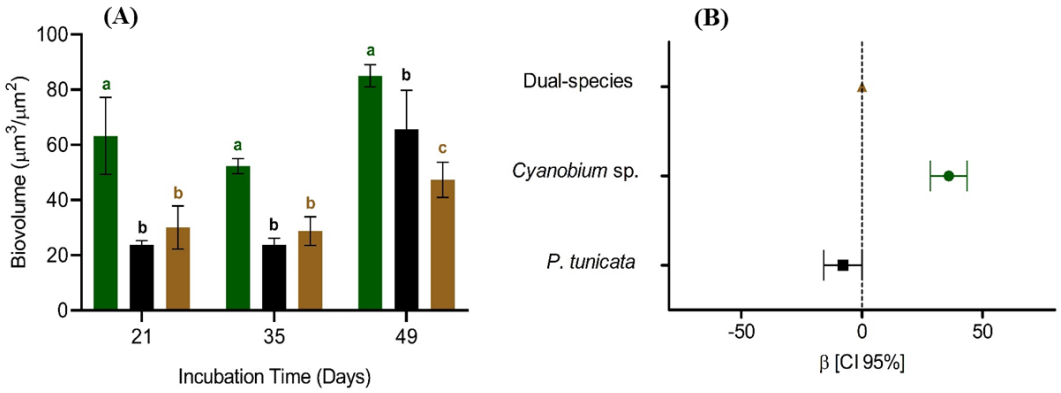

Figure 6.3. (A) Biovolume of single- and dual-species biofilms established on gel-coated glass surfaces at days 21, 35 and 49: ■ - *Cyanobium* sp. LEGE 10375, ■ - *Pseudoalteromonas tunicata*, and ■ - *Pseudoalteromonas tunicata* - *Cyanobium* sp. LEGE 10375. Letters were assigned in alphabetic order from the highest to the lowest value (from a to c) for each time point. These assignments were made as long as statistically significant differences exist between the biofilms with a confidence level greater than 95% ($p < 0.05$). The means ± SDs for three independent experiments are illustrated. **(B)** Association between the biovolume and single- and dual-species biofilms. Dual-species biofilm was used as the reference condition. Linear regression models were adjusted for incubation days. Results were represented as beta estimates (β) and the corresponding 95% confidence interval (95% CI).

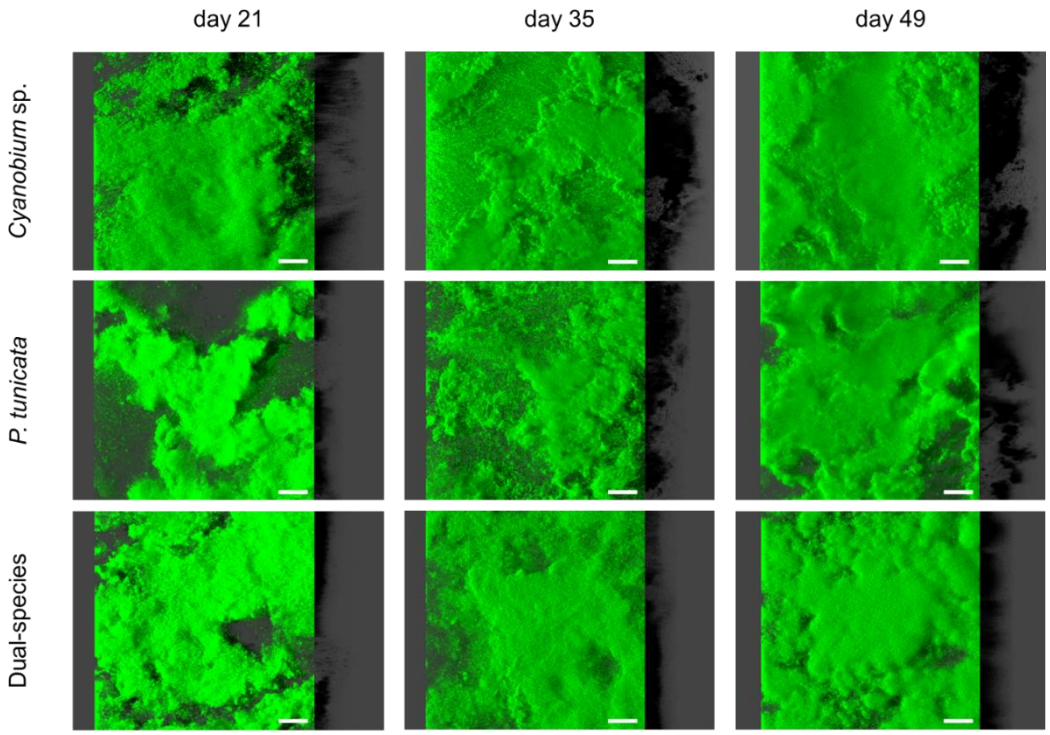

Figure 6.4. 3D-projections of single- (*Cyanobium* sp. and *P. tunicata*) and dual-species biofilms formed on gel-coated glass surfaces after 21, 35 and 49 days. The representative images were obtained from confocal *z*-stacks using IMARIS software and present an aerial view of the biofilms (shadow projection on the right). The white scale bar corresponds to 50 µm.

6.4. Discussion

Present-day awareness of biofilm formation on man-made structures in aquatic environments has prompted the scientific community to develop an increasing number of new materials with AF features. Indeed, the development of AF coatings that can prevent organism adhesion or weaken the biofilm structure has emerged as a promising approach to overcome problems associated with fouling in a marine context, including the reduction of ship speed and the consequent increase of operating costs (Tian et al. 2020). In recent years, modern chemical research has played a prominent role in this area through the synthesis of eco-friendly coatings with improved foul release performance, and also AF properties. Green chemistry has been successful in designing several AF coatings for large and small vessels

made of different materials (steel, aluminum, wood, etc.) that do not contain toxic compounds, limit the extent of environment damage produced by the transportation of non-indigenous species, and improve the hydrodynamic performance of vessels, ensuring significant fuel savings (Ciriminna et al. 2015).

The complexity of marine fouling communities is significant and results from changes in environmental conditions, such as water turbulence, temperature, salinity, light regime, and the number of nutrients (Caruso 2020). Thus, it is within this complex system that marine coatings preventing or reducing biofouling must perform and ultimately be tested. The use of artificial panels to study biofouling communities in natural environments is important for the evaluation of AF systems (Jelic-Mrcelic et al. 2006, Silva et al. 2019). However, it is an arduous task in the development of novel coatings to begin field testing straight away since some of these materials may be very expensive and hard to produce in large quantities. Additionally, there is the issue of a potential release of toxic substances to the marine environment, which must be avoided (Zecher et al. 2018). Furthermore, the sheer number of formulations that are created with the advent of combinatorial approaches requires initial screening in the laboratory. The laboratory assays are relatively quick and easy, so they should be applied in order to eliminate coating formulations that may be expected to have poor AF and physical performances in the *in vivo* ecosystem (Institution 1952).

Although most *in vitro* tests described in the literature grossly simplify the dynamics of fouling in the marine environment, our research group has been particularly concerned in recent years to consider the influence of hydrodynamics on cyanobacterial and *Pseudoalteromonas* sp. biofilm formation (Faria et al. 2020a, Faria et al. 2020b, Romeu et al. 2019). The hypothesis for the current study was that differences in the degree of complexity of marine cultures (single- or dual-species) might impact the preliminary conclusions about the efficacy of new AF coatings. To test this hypothesis, an epoxy resin surface typically used to coat boat hulls was tested with single-species (*Pseudoalteromonas tunicata* or *Cyanobium* sp. LEGE 10375) and dual-species cultures (*P. tunicata* - *Cyanobium* sp. LEGE 10375). Our study demonstrated that the growth kinetics of single-species biofilms of cyanobacteria was different from dual-species biofilms containing this marine microorganism. On the contrary, the growth of *P. tunicata* biofilms during 7 weeks occurred similarly to dual-species biofilms. In general, *Cyanobium* sp. biofilms presented higher cell

density, biomass and thickness than the dual-species biofilms and the single-species biofilms formed by *P. tunicata*. The decrease in the parameters of dual-species biofilms compared to *Cyanobium* sp. biofilm may be related to the presence of *P. tunicata.* Several authors have recognized this microorganisms as a superior competitor able to adapt to high-density communities on surfaces (Rao et al. 2005, Thomas et al. 2008). Additionally, in mixed-species biofilms, *P. tunicata* can inhibit the competing strains. This dominance may be attributed to the ability of this marine bacterium to rapidly form microcolonies and to its capacity for producing extracellular antimicrobial compounds (Rao et al. 2005).

To the best of our knowledge, this is one of the few works that highlights the importance of shorter laboratory-scale trials to study marine biofilms and discloses that monocultures at this scale are as important as, or more important than, mixed cultures when the performance of an antibiofilm material for marine applications is evaluated. There is a preconceived idea among biofilm researchers that microbial diversity in biofilm communities is associated with enhanced survival and growth of the individual biofilm populations (Burmølle et al. 2006, Ren et al. 2015). It has also been shown that this diversity may lead to enhanced tolerance towards antimicrobial compounds (Gomes et al. 2018, Lee et al. 2014). For example, 63% of soil isolates exhibited cooperation when grown as four-member consortia, as determined by quantifying total biofilm biomass by crystal violet staining (Ren et al. 2015). Similarly, on average 54% of the multispecies biofilms formed by isolates from the same habitat exhibited increased biomass relative to when grown as single-species biofilms (Madsen et al. 2016). In a recent study, the influence of intraspecies diversity in biofilm populations composed of up to six different *Escherichia coli* strains isolated from urine was evaluated. Briefly, with the increasing number of strains in a biofilm, an increase in cell culturability and a decrease in matrix production were observed. This suggests that increased genotypic diversity in those biofilms led *E. coli* to direct energy towards the production of its offspring, in detriment of the production of public goods (i.e., matrix components) (Azevedo et al. 2020). Thus, the available data indicates that biofilm development in situations of high microbial diversity may be higher or lower than when each species is individually assessed as a result of the type of interspecies interactions that may occur (cooperation or competition) (Tan et al. 2017).

Another technical challenge of performing *in vitro* assays with multispecies biofilms is the inoculum preparation, as the relative proportions of each type of organism may be difficult to replicate. The fact that these organisms may be at different physiological states further complicates the problem. A common strategy is to use approximately the same cellular concentration of each organism (Azevedo et al. 2017, Gomes et al. 2018), which is, of course, a simplification.

In this chapter, the cyanobacterium alone produced more biofilm than the co-culture of *P. tunicata* and *Cyanobium* sp. It has been suggested for antibiofilm assays, that conditions promoting microbial growth and biofilm formation are desirable so that the positive controls are reproducible (Briand 2009, Martín-Rodríguez et al. 2014) and the differences observed between controls and developed surfaces are effective. Our results indicate that for initial screening, it is probably better to start with a single representative organism (a marine bacterium, a cyanobacterium, or even diatoms) and compare the AF behavior of the coating to a control surface. Parallel studies using a different organism (for instance, marine larvae (Dobretsov and Rittschof 2020) may be performed to strengthen the results. After this initial screening, field tests are necessary and can be performed on a reduced number of surfaces to confirm the real AF activity in the correct environment.

6.5. Conclusions

Even though they are unable to replicate the real marine environment, *in vitro* tests are a useful tool for initial screening and comparing the effectiveness of AF surfaces, having the advantage of easily assessing a broad spectrum of marine conditions.

There is a pressing need for more laboratory work focused on the interactions and dynamics within multispecies biofilms because they are the dominant form in nature, and it is necessary to successfully prevent or control their development. However, when the main goal is to search for new AF surfaces, the present study showed that attention should be given to single-species biofilms, in particular those formed by cyanobacteria, since they can create the worst-case scenarios needed for robust testing of the AF performance. In fact,

monocultures of *P. tunicata* and *Cyanobium* sp. caused denser and thicker biofilms on the polymeric coating than co-cultures with the same marine strains.

The single-strain strategy represents a good compromise between the high complexity of *in vivo* marine ecosystems and the convenience of *in vitro* testing, overcoming the experimental limitations in replicating the cellular concentration of each organism in a dual-species biofilm. Further experiments using a different microfouler (e.g., diatoms), or even a macrofouler (e.g., larvae), should be conducted to support the results.

6.6. References

Amara, I., W. Miled, R. B. Slama and N. Ladhari (2018). "Antifouling processes and toxicity effects of antifouling paints on marine environment. A review." Environmental toxicology and pharmacology **57**: 115-130.

Azevedo, A. S., C. Almeida, L. C. Gomes, C. Ferreira, F. J. Mergulhão, L. F. Melo and N. F. Azevedo (2017). "An in vitro model of catheter-associated urinary tract infections to investigate the role of uncommon bacteria on the Escherichia coli microbial consortium." Biochemical Engineering Journal **118**: 64-69.

Azevedo, A. S., G. P. Gerola, J. Baptista, C. Almeida, J. Peres, F. J. Mergulhão and N. F. Azevedo (2020). "Increased intraspecies diversity in Escherichia coli biofilms promotes cellular growth at the expense of matrix production." Antibiotics **9**(11): 818.

Bakker, D., A. Van der Plaats, G. Verkerke, H. Busscher and H. Van der Mei (2003). "Comparison of velocity profiles for different flow chamber designs used in studies of microbial adhesion to surfaces." Applied and environmental microbiology **69**(10): 6280-6287.

Blain, S., J. Guillou, P. Treguer, P. Woerther, L. Delauney, E. Follenfant, O. Gontier, M. Hamon, B. Leilde and A. Masson (2004). "High frequency monitoring of the coastal marine environment using the MAREL buoy." Journal of Environmental Monitoring **6**(6): 569-575.

Briand, J.-F. (2009). "Marine antifouling laboratory bioassays: an overview of their diversity." Biofouling **25**(4): 297-311.

Brooks, S. and M. Waldock (2009). The use of copper as a biocide in marine antifouling paints. Advances in marine antifouling coatings and technologies. C. Hellio and D. Yebra. Cambridge, UK, Woodhead Publishing**:** 492-521.

Buhmann, M., P. G. Kroth and D. Schleheck (2012). "Photoautotrophic–heterotrophic biofilm communities: a laboratory incubator designed for growing axenic diatoms and bacteria in defined mixed-species biofilms." Environmental Microbiology Reports **4**(1): 133-140.

Burmølle, M., D. Ren, T. Bjarnsholt and S. J. Sørensen (2014). "Interactions in multispecies biofilms: do they actually matter?" Trends in microbiology **22**(2): 84-91.

Burmølle, M., J. S. Webb, D. Rao, L. H. Hansen, S. J. Sørensen and S. Kjelleberg (2006). "Enhanced biofilm formation and increased resistance to antimicrobial agents and bacterial invasion are caused by synergistic interactions in multispecies biofilms." Applied and environmental microbiology **72**(6): 3916-3923.

Caruso, G. (2020). "Microbial colonization in marine environments: overview of current knowledge and emerging research topics." Journal of Marine Science and Engineering **8**(2): 78.

Ciriminna, R., F. V. Bright and M. Pagliaro (2015). "Ecofriendly antifouling marine coatings." ACS Sustainable Chemistry & Engineering - ACS Publications(3): 559-565.

de Carvalho, C. C. (2018). "Marine biofilms: a successful microbial strategy with economic implications." Frontiers in marine science **5**: 126.

Dobretsov, S. and D. Rittschof (2020). "Love at first taste: induction of larval settlement by marine microbes." International journal of molecular sciences **21**(3): 731.

Faria, S. I., R. Teixeira-Santos, L. C. Gomes, E. R. Silva, J. Morais, V. Vasconcelos and F. J. M. Mergulhão (2020a). "Experimental Assessment of the Performance of Two Marine Coatings to Curb Biofilm Formation of Microfoulers." Coatings **10**: 893.

Faria, S. I., R. Teixeira-Santos, M. J. Romeu, J. Morais, V. Vasconcelos and F. J. Mergulhão (2020b). "The Relative Importance of Shear Forces and Surface Hydrophobicity on Biofilm Formation by Coccoid Cyanobacteria." Polymers **12**(3): 653.

Gomes, L., J. Deschamps, R. Briandet and F. J. Mergulhão (2018). "Impact of modified diamond-like carbon coatings on the spatial organization and disinfection of mixed-

biofilms composed of Escherichia coli and Pantoea agglomerans industrial isolates." International journal of food microbiology **277**: 74-82.

Heydorn, A., A. T. Nielsen, M. Hentzer, C. Sternberg, M. Givskov, B. K. Ersbøll and S. Molin (2000). "Quantification of biofilm structures by the novel computer program COMSTAT." Microbiology **146**(10): 2395-2407.

Hoge, J. and C. Leach (2016). "Epoxy resin infused boat hulls." Reinforced Plastics **60**(4): 221-223.

Holmström, C., S. James, B. A. Neilan, D. C. White and S. Kjelleberg (1998). "Pseudoalteromonas tunicata sp. nov., a bacterium that produces antifouling agents." International Journal of Systematic and Evolutionary Microbiology **48**(4): 1205-1212.

Institution, W. H. O. (1952). The Testing of Antifouling Paints. Marine fouling and its prevention. Annapolis, MD, USA, United States Naval Institute**:** 331–348.

Jelic-Mrcelic, G., M. Sliskovic and B. Antolic (2006). "Biofouling communities on test panels coated with TBT and TBT-free copper based antifouling paints." Biofouling **22**(5): 293-302.

Lacoursière-Roussel, A., D. G. Bock, M. E. Cristescu, F. Guichard and C. W. McKindsey (2016). "Effect of shipping traffic on biofouling invasion success at population and community levels." Biological Invasions **18**(12): 3681-3695.

Lee, K. W. K., S. Periasamy, M. Mukherjee, C. Xie, S. Kjelleberg and S. A. Rice (2014). "Biofilm development and enhanced stress resistance of a model, mixed-species community biofilm." The ISME journal **8**(4): 894-907.

Li, Z. and Z. Guo (2019). "Bioinspired surfaces with wettability for antifouling application." Nanoscale **11**(47): 22636-22663.

Madsen, J. S., H. L. Røder, J. Russel, H. Sørensen, M. Burmølle and S. J. Sørensen (2016). "Coexistence facilitates interspecific biofilm formation in complex microbial communities." Environmental microbiology **18**(8): 2565-2574.

Magana, M., C. Sereti, A. Ioannidis, C. A. Mitchell, A. R. Ball, E. Magiorkinis, S. Chatzipanagiotou, M. R. Hamblin, M. Hadjifrangiskou and G. P. Tegos (2018). "Options and limitations in clinical investigation of bacterial biofilms." Clinical microbiology reviews **31**(3).

Martín-Rodríguez, A. J., A. González-Orive, A. Hernandez-Creus, A. Morales, R. Dorta-Guerra, M. Norte, V. S. Martin and J. J. Fernández (2014). "On the influence of the culture conditions in bacterial antifouling bioassays and biofilm properties: Shewanella algae, a case study." BMC microbiology **14**(1): 1-15.

Miller, R. J., A. S. Adeleye, H. M. Page, L. Kui, H. S. Lenihan and A. A. Keller (2020). "Nano and traditional copper and zinc antifouling coatings: Metal release and impact on marine sessile invertebrate communities." Journal of Nanoparticle Research **22**: 1-15.

Ramos, V., J. Morais, R. Castelo-Branco, Â. Pinheiro, J. Martins, A. Regueiras, A. L. Pereira, V. R. Lopes, B. Frazão, D. Gomes, C. Moreira, M. S. Costa, S. Brûle, S. Faustino, R. Martins, M. Saker, J. Osswald, P. N. Leão and V. M. Vasconcelos (2018). "Cyanobacterial diversity held in microbial biological resource centers as a biotechnological asset: the case study of the newly established LEGE culture collection." Journal of Applied Phycology **30**(3): 1437-1451.

Rao, D., J. S. Webb and S. Kjelleberg (2005). "Competitive interactions in mixed-species biofilms containing the marine bacterium Pseudoalteromonas tunicata." Applied and environmental microbiology **71**(4): 1729-1736.

Ren, D., J. S. Madsen, S. J. Sørensen and M. Burmølle (2015). "High prevalence of biofilm synergy among bacterial soil isolates in cocultures indicates bacterial interspecific cooperation." The ISME journal **9**(1): 81-89.

Røder, H. L., S. J. Sørensen and M. Burmølle (2016). "Studying bacterial multispecies biofilms: where to start?" Trends in microbiology **24**(6): 503-513.

Romeu, M. J., P. Alves, J. Morais, J. M. Miranda, E. D. de Jong, J. Sjollema, V. Ramos, V. Vasconcelos and F. J. Mergulhão (2019). "Biofilm formation behaviour of marine filamentous cyanobacterial strains in controlled hydrodynamic conditions." Environmental Microbiology **21**(11): 4411-4424.

Salta, M., J. A. Wharton, P. Stoodley, S. P. Dennington, L. R. Goodes, S. Werwinski, U. Mart, R. J. Wood and K. R. Stokes (2010). "Designing biomimetic antifouling surfaces." Philosophical Transactions of the Royal Society A: Mathematical, Physical and Engineering Sciences **368**(1929): 4729-4754.

Schultz, M., J. Bendick, E. Holm and W. Hertel (2011). "Economic impact of biofouling on a naval surface ship." Biofouling **27**(1): 87-98.

Silva, E., O. Ferreira, P. Ramalho, N. Azevedo, R. Bayón, A. Igartua, J. Bordado and M. Calhorda (2019). "Eco-friendly non-biocide-release coatings for marine biofouling prevention." Science of the Total Environment **650**: 2499-2511.

Tan, C. H., K. W. K. Lee, M. Burmølle, S. Kjelleberg and S. A. Rice (2017). "All together now: experimental multispecies biofilm model systems." Environmental Microbiology **19**(1): 42-53.

Taylor, D. A. (1996). Chapter 16 - Engineering materials. Introduction to marine engineering. D. A. Taylor. Oxford, UK, Butterworth-Heinemann**:** 326–340.

Thomas, T., F. F. Evans, D. Schleheck, A. Mai-Prochnow, C. Burke, A. Penesyan, D. S. Dalisay, S. Stelzer-Braid, N. Saunders and J. Johnson (2008). "Analysis of the Pseudoalteromonas tunicata genome reveals properties of a surface-associated life style in the marine environment." PLoS One **3**(9): e3252.

Tian, L., Y. Yin, H. Jin, W. Bing, E. Jin, J. Zhao and L. Ren (2020). "Novel marine antifouling coatings inspired by corals." Materials Today Chemistry **17**: 100294.

Yu, X., M. F. Polz and E. J. Alm (2019). "Interactions in self-assembled microbial communities saturate with diversity." The ISME journal **13**(6): 1602-1617.

Zecher, K., V. P. Aitha, K. Heuer, H. Ahlers, K. Roland, M. Fiedel and B. Philipp (2018). "A multi-step approach for testing non-toxic amphiphilic antifouling coatings against marine microfouling at different levels of biological complexity." Journal of microbiological methods **146**: 104-114.

7.

The association between the initial adhesion and cyanobacterial biofilm development[e]

Abstract

Although laboratory assays provide valuable information about the AF effectiveness of marine surfaces and the dynamics of biofilm formation, they may be laborious and time-consuming. This study aimed to determine the potential of short-time adhesion assays to estimate how biofilm development may proceed. The initial adhesion and cyanobacterial biofilm formation were evaluated using glass and a polymer epoxy resin surface at two hydrodynamic conditions and compared using linear regression models. For initial adhesion, the polymer epoxy resin surface was significantly associated with a lower number of adhered cells when compared to glass (-1.27 x 10^5 cells/cm^2). Likewise, the number of adhered cells was significantly lower (-1.16 x 10^5 cells/cm^2) at 185 than at 40 rpm. This tendency was maintained during biofilm development and was supported by the biofilm wet weight, thickness, chlorophyll *a* content, and structure. Results indicated a significant correlation between the number of adhered and biofilm cells ($r = 0.800$, $p < 0.001$). Moreover, the number of biofilm cells on day 42 was dependent on the number of adhered cells at the end of the

[e] The content of this chapter was adapted from the following publication(s):

Faria, S. I., R. Teixeira-Santos, J. Morais, V. Vasconcelos and F. J. Mergulhão (2021). "The association between initial adhesion and cyanobacterial biofilm development." FEMS Microbiology Ecology **97**(5): fiab052.

initial adhesion and hydrodynamic conditions (R^2 = 0.795, p <0.001). These findings demonstrated the high potential of initial adhesion assays to estimate marine biofilm development.

7.1. Introduction

The attachment of undesirable molecules and fouling organisms to submerged surfaces is known as marine biofouling (Rajeev et al. 2020, Selim et al. 2017). This process occurs spontaneously in marine ecosystems and may have several economic and environmental implications (Basu et al. 2020). Marine biofouling is detrimental to vessel hulls since the attached fouling organisms exacerbate surface corrosion and increase frictional drag, resulting in higher maintenance and fuel consumption (Rajeev et al. 2020, Tian et al. 2020, Zecher et al. 2018). Similarly, biofouling can damage submerged marine facilities and underwater equipment such as measurement devices or sensors (Tian et al. 2020).

Besides the economic losses for marine industries, marine biofouling is associated with serious environmental issues. This process promotes the bio-invasion of exotic species when the fouling organisms travel in marine vessels (ships, yachts or sailing boats) between different geographic areas, which is aggravated at both community (species richness) and population (genetic diversity) levels by the intense shipping activity in ports (Lacoursière-Roussel et al. 2016, Neves et al. 2020). The negative impact of bio-invasion has motivated the marine conservation entities to seek strategies to reduce the introduction and spread of fouling species in marine ecosystems and, in some countries, strict regulations have already been implemented to maintain the vessel hulls clean (Georgiades and Kluza 2017, McClay et al. 2015).

In general, the consequences of marine biofouling have been stressing the need to develop and evaluate novel marine coatings aiming to control biofilm formation by microfouling organisms (e.g. cyanobacteria and diatoms) since this is the initial colonization stage, building the basis for later settlement by macrofouling organisms (e.g. bryozoans, mollusks, polychaeta, tunicates, coelenterates or fungi) (Arrhenius et al. 2014).

Due to the vast number of fouling organisms and the diversity of biological factors underlying their attachment in the natural environment, the most reliable methods for testing the AF performance of marine surfaces appear to be the immersion of samples in the ocean (Stafslien et al. 2011). However, sea trials require long periods to collect data, are dependent on samples' location and the time of year, and may be ecologically toxic and expensive (Briand 2009, Salta et al. 2010, Zecher et al. 2018). Therefore, the first step for testing new AF coatings usually consists of exposing them to microfouling organisms under laboratory conditions that mimic the marine environments and analyse different biofilm parameters (e.g. number of cells, wet weight and thickness) (Faria et al. 2020, Romeu et al. 2019, Romeu et al. 2020, Zecher et al. 2018). Since numerous extrinsic factors may affect the success of an AF coating, including the microorganisms, temperature and hydrodynamic conditions (Faria et al. 2020), it is important to test its efficacy against a broad spectrum of fouling organisms and marine conditions to obtain a more insightful evaluation (Briand 2009). Although several laboratory assays provide the first indications about AF performance and allow a better understanding of the dynamics of biofilm formation, they may be laborious and time-consuming, requiring on average 6 weeks to provide representative results of a real scenario (Romeu et al. 2019, Zecher et al. 2018). Thus, considering these limitations, the efficacy of AF marine coatings should first be screened before carrying out extensive laboratory tests. Certain adhesion and biofilm formation assays (2 – 48 h) have been developed for screening AF coatings (Leroy et al. 2007, Salta et al. 2010, Stafslien et al. 2011) and some of them showed a correlation with field assays (Briand 2009, Stafslien et al. 2007). Most of these assays are based on the enumeration of the attached cells by direct counting under a microscope after their staining (Briand 2009, Leroy et al. 2007, Salta et al. 2010) or on the spectrophotometric or fluorometric quantification of chlorophyll (Briand 2009). Cell staining usually requires several methodological steps (e.g. cell fixation, staining and washing) to improve analysis specificity and sensitivity, thus increasing the time-to-results and costs (Briand 2009, Leroy et al. 2007, Salta et al. 2010). In turn, the chlorophyll quantification may only be applied to chlorophyll-producing organisms (Briand 2009, Stafslien et al. 2011). Besides, most laboratory assays are conducted under static conditions (Briand 2009, Salta et al. 2010, Stafslien et al. 2007) which can influence AF performance (Nolte et al. 2018, Nolte et al. 2017). Thus, although these assays are very useful as screening tools, it is necessary to

develop rapid, inexpensive, and more accurate and simple to perform alternative short-term assays.

In the present chapter, the association between the initial adhesion and biofilm formation was investigated, aiming to evaluate the potential of short-time adhesion assays to estimate the biofilm development and, consequently, the AF efficacy of a given surface. For this purpose, the initial adhesion and biofilm formation of three coccoid cyanobacteria isolated from different geographic areas were evaluated using different surfaces (glass and a polymer epoxy resin) and hydrodynamic conditions (40 and 185 rpm agitation). Since cyanobacteria are some of the most dominant bacterial phyla colonizing different surfaces at diverse sampling locations (Angelova et al. 2019, de Carvalho 2018), particularly in the early stages of colonization (Azevedo et al. 2020), these microfoulers were chosen for the current study.

7.2. Materials and methods

7.2.1. Surfaces preparation

Cyanobacterial adhesion and biofilm formation were studied using two model surfaces, glass and a polymer epoxy resin. Glass surfaces are commonly found in underwater windows of boats, flotation spheres, moored buoys, underwater cameras, and measuring devices or sensors (King et al. 2006, Taylor 1996), while polymer epoxy resins are used to coat the hulls of small recreation vessels, including powerboats, yachts, and sailing boats (Blain et al. 2004, Taylor 1996).

The surface preparation was performed as described in chapter 3, section 3.2.1.

Before experiments, the initial weight of glass and polymer epoxy resin coupons was registered.

7.2.2. Cyanobacterial strains and growth conditions

Three coccoid cyanobacteria strains from the LEGE-CC, deposited at the CIIMAR, Porto, Portugal, were included in this study. *Synechocystis salina* LEGE 00041 (order Chroococcales) was originally isolated from a seawater sample, collected on June 2000, at Espinho beach (41.00847 N 8.646958 W) located on the north coast of Portugal; *Synechocystis salina* LEGE 06155 (order Chroococcales) was obtained from a rock surface scraping on tide pool, collected on November 2006, at São Bartolomeu do Mar beach (41.57377 N 8.798558 W) located in Esposende, Portugal; and *Cyanobium* sp. LEGE 06097 (order Synechococcales) was isolated from the intertidal zone, on green macroalga, collected in July 2006, at Martinhal beach (37.01869 N 8.926714 W) located in Vila do Bispo, Portugal (Ramos et al. 2018).

Cyanobacterial cells have grown in Z8 broth medium supplemented with 25 mg/mL of synthetic sea salts (Tropic Marin) and vitamin B12 (Sigma Aldrich, Merck, Saint Loius, MO, USA) (Kotai 1972). Cultures were incubated under 14 h light (10 – 30 mol photon m^{-2} s^{-1}, λ = 380 – 700 nm)/ 10 h dark cycles at 25 °C.

7.2.3. Thermodynamic characterization

The thermodynamic characterization was performed as described in chapter 5, section 5.2.2.2.

7.2.4. Initial adhesion assays

Cyanobacterial adhesion assays were performed using 12-well plates (VWR International, Carnaxide, Portugal) under previously optimized conditions (Romeu et al. 2019). Firstly, microplates were UV-sterilized for 30 min. Then, the coupons (glass and polymer epoxy resin) were fixed to the microplate wells using transparent double-sided adhesive tape and inoculated with 3 mL of cyanobacterial suspension at a concentration of 1 x 10^8 cells/mL (as previously described). Microplates were incubated at 25 °C in an orbital shaker with a 25 mm diameter (Agitorb 200ICP, Norconcessus, Ermesinde, Portugal) at 40

and 185 rpm, under a light cycle (10–30 mol photons m^{-2} s^{-1}). Based on computational fluid dynamic studies performed using this type of incubator, a shaking frequency of 40 rpm corresponds to an average shear rate of 4 s^{-1} and a maximum of 11 s^{-1}, while 185 rpm corresponds to an average shear rate of 40 s^{-1} and a maximum of 120 s^{-1} (Romeu et al. 2019). As it is known that lower shear rates promote marine biofouling (Flemming et al. 2009, Minchin and Gollasch 2003), and the estimated shear rate for a ship in a harbour is 50 s^{-1} (Bakker et al. 2003), both shaking frequencies were studied.

Since in marine environments, the bacterial adhesion occurs within the first 24 h (Amara et al. 2018, Brian-Jaisson 2014), the initial adhesion assays were performed during 450 min (seven half hours). Every 90 min, two coupons for each experimental condition (i. glass at 40 rpm; ii. glass at 185 rpm; iii. polymer epoxy resin at 40 rpm; and iv. polymer epoxy resin at 185 rpm) were removed and analysed concerning the number of adhered cells. For this purpose, each coupon was immersed in 2 mL of 8.5 mg/mL NaCl solution and vortexing for 3 min to detach cyanobacteria cells. Then, 10 μL of each cell suspension was placed on each side of a Neubauer chamber and observed in a brightfield microscope (Nikon Eclipse LV100 microscope, Nikon Corporation, Tokyo, Japan). Additionally, the coupons were also observed under the microscope to confirm complete cell detachment.

Experiments were performed in duplicate and in two independent assays.

7.2.5. Biofilm formation assays

Biofilm formation was performed as described in the section above under alternate light cycles of 14 h light (10–30 mol photons m^{-2} s^{-1})/10 h dark, and followed for 6 weeks (42 days) since this period corresponds on average to half of the minimal economically viable interval accepted for the maintenance of underwater systems (Blain et al. 2004) and hulls cleaning (Akinfijevs et al. 2007, Schultz et al. 2011). During this period, the culture medium was replaced twice a week. On days 1, 2, 4, 7, 14, 21, 28, 35 and 42, two coupons of each experimental condition were removed and gently rinsed in a sterile NaCl solution (8.5 mg/mL) to remove loosely attached cyanobacteria. Afterward, coupons were analysed concerning the number of biofilm cells, biofilm wet weight and thickness, and chlorophyll *a* content. Additionally, on day 42, the biofilm structure was analysed by OCT.

Biofilm experiments were performed in duplicate and in two independent assays.

7.2.5.1. Biofilm cell counting

The biofilm cell counting was performed as described in chapter 3, section 3.2.4.1.

7.2.5.2. Biofilm wet weight

To assess the biofilm wet weight, coupons were removed from the wells with a sterile tweezer and weighted. The biofilm wet weight was determined by the difference between the initial weight of the coupon (before inoculation) and the weight measured on the sampling day.

7.2.5.3. Biofilm thickness

Biofilm thickness was determined using a Nikon Eclipse LV100 microscope coupled to a joystick (Prior Scientific Ltd, Cambridge, UK), connected to a camera (Nikon digital sight DS-RI 1, Japan), and analysed using the NIS-Elements AR 4.13.05 software. For each coupon, a minimum of 5 fields was analysed to obtain accurate and reproducible results.

7.2.5.4. Chlorophyll *a* quantification

The chlorophyll *a* quantification was performed as described in chapter 3, section 3.2.4.3.

7.2.5.5. OCT

On day 42, biofilm structures were analysed by OCT using a Thorlabs Ganymede instrument (Thorlabs GmbH, Dachau, Germany) with a central wavelength of 930 nm. After washing, the plate wells were filled with 3 mL of sterile NaCl solution (8.5 mg/mL) and

biofilms formed on coupons were imaged. The captured volume was 3.66 x 1.52 x 2.98 mm^3 (509 x 313 x 1024 pixels). Since biofilms are mainly composed of water (Telegdi et al. 2016), the refractive index was set to 1.40, close to the refractive index of water (1.33).

For each coupon, 2D imaging was performed in a minimum of 5 fields to ensure the accuracy and reproducibility of the results.

7.2.6. Statistical analysis

Descriptive statistics were used to calculate the mean and standard deviations for the contact angles, number of adhered cells, and different biofilm parameters (number of biofilm cells, biofilm wet weight, thickness, and chlorophyll *a* content).

Linear regression models (LRM) between the number of cells and the independent variables (tested surfaces and hydrodynamic conditions) were performed for initial adhesion and biofilm formation. Models were adjusted for strain and incubation periods.

The correlation between the adhered cells at 7.5 hours and biofilm cells on day 42 was determined using the Pearson correlation coefficient (r). In addition, the association between the number of biofilm cells registered on day 42 and the number of adhered cells at 7.5 hours, surface, and hydrodynamic conditions (independent variables) was also estimated using a LRM adjusted for strain.

LRM were also applied between the biofilm wet weight, thickness, and chlorophyll *a* content and the independent variables. Models were adjusted for strain and incubation periods.

For all LRM, glass and 40 rpm were used as the reference conditions. Results were presented as beta estimates (β) and the corresponding 95% confidence intervals (95% CI).

Significant results were considered for p-values < 0.05.

Data analysis was performed using the IBM SPSS Statistics version 24.0 for Windows (IBM SPSS, Inc., Chicago, IL, USA).

7.3. Results

7.3.1. Thermodynamic analysis

The hydrophobicity of the surfaces and cyanobacterial cells was evaluated by contact angle measurement and based on the method of van Oss et al (Oss 1994). Table 7.1. presented the thermodynamic analysis for the tested materials and cyanobacterial cells. Water contact angle (θ_w) values indicated that glass is hydrophilic [θ_w = 39.459 ± 3.505°, (θ_w < 90°)], whereas the polymer epoxy resin surface is slightly hydrophobic [θ_w = 90.194 ± 4.256°, (θ_w > 90°)]. In turn, the free energy of interaction also demonstrated the hydrophilic behaviour of glass [ΔG = 19.383 mJ/m^2, (ΔG > 0 mJ/m^2)] and the hydrophobicity of polymer epoxy resin surfaces [ΔG = - 67.983 mJ.m^{-2}, (ΔG < 0 mJ/m^2)]. Concerning the cyanobacterial cells, water contact angles determined by the sessile drop method in a contact angle meter, and free energy of interaction showed that *Synechocystis salina* LEGE 00041 is relatively more hydrophobic than the other cyanobacteria ($\theta_{w\ 00041}$ = 38.085 ± 4.310° > $\theta_{w\ 06097}$ = 25.698 ± 3.575° > $\theta_{w\ 06155}$ = 19.113 ± 3.498°; ΔG_{00041} = 52.315 mJ/m^2 > ΔG_{06155} = 48.980 mJ/m^2 > ΔG_{061097} = 40.355 mJ/m^2).

The free energy of adhesion (ΔG^{Adh}) calculated for the two surfaces is presented in Table 7.2. ΔG^{Adh} values obtained for the different cyanobacteria strains were very similar and indicated that the cell adhesion on the polymer epoxy resin is thermodynamically favourable (ΔG^{Adh} < 0 mJ/m^2), while on glass it is unfavourable (ΔG^{Adh} > 0 mJ/m^2).

7.1.1. Initial adhesion and cyanobacterial biofilm formation

The number of adhered and biofilms cells were determined for 7.5 h and 42 days, respectively, by direct counting in a Neubauer Camera using a microscope.

Regardless of the surface or hydrodynamic condition, *S. salina* LEGE 00041 exhibited on average a higher number of adhered cells (3.06 x 10^6 ± 5.40 x 10^5 cells/cm^2) than *Cyanobium* sp. LEGE 06097 (6.20 x 10^2 ± 6.87 x 10^2 cells/cm^2) and *S. salina* LEGE 06155 (4.95 x 10^2 ± 6.02 x 10^2 cells/cm^2) (Figure 7.1. 1a). After 42 days of biofilm formation, although the number of biofilm cells had increased, this trend was kept constant with *S. salina*

LEGE 00041, reaching a mean of 3.84 x 10^8 ± 5.83 x 10^8 cells/cm^2, and *Cyanobium* sp. LEGE 06097 and *S. salina* LEGE 06155, reaching a mean of 3.71 x 10^3 ± 6.04 x 10^3 and 5.92 x 10^3 ± 9.89 x 10^3 cells/cm^2, respectively (Figure 7.1. 1b).

Table 7.1. Contact angle measurements, surface tension parameters and free energy of interaction of cyanobacterial strains and tested surfaces.

	Contact angle (º)			**Surface tension parameters (mJ/m^2)**				
	Water	Formamide	α-Bromonaphtalene	γ_s^{LW}	γ_s^{AB}	γ_s^+	γ_s^-	ΔG
Surface								
Glass	39.5 ± 3.5	37.3 ± 4.6	48.1 ± 4.1	30.9	15.7	1.5	41.2	19.4
Polymer epoxy resin	90.2 ± 4.3	69.6 ± 4.3	42.2 ± 3.8	33.7	0.1	0.0	3.2	-67.9
Microorganism								
Synechocystis salina LEGE 00041	38.1 ± 4.3	53.4 ± 3.3	37.3 ± 4.5	35.8	0	0.0	61.0	52.3
Cyanobium sp. LEGE 06097	25.7 ± 3.6	34.2 ± 4.4	31.2 ± 2.3	38.2	7.2	0.2	56.4	40.4
Synechocystis salina LEGE 06155	19.1 ± 3.5	35.4 ± 4.2	39.7 ± 4.4	34.7	9.6	0.4	63.5	48.9

Values represent the average value ± SDs from three independent contact angles measurements.
γ_s^{LW} - apolar component; γ_s^{AB} - polar component; γ_s^+ and γ_s^- - surface tension parameters; ΔG - free surface energy.

Table 7.2. Free energy of the interaction between cyanobacterial strains and tested surfaces.

Microorganism	ΔG^{Adh} **(mJ/m^2)**	
	Glass	**Polymer epoxy resin**
Synechocystis salina LEGE 00041	32.6	-8.0
Cyanobium sp. LEGE 06097	28.6	-8.4
Synechocystis salina LEGE 06155	32.4	-2.3

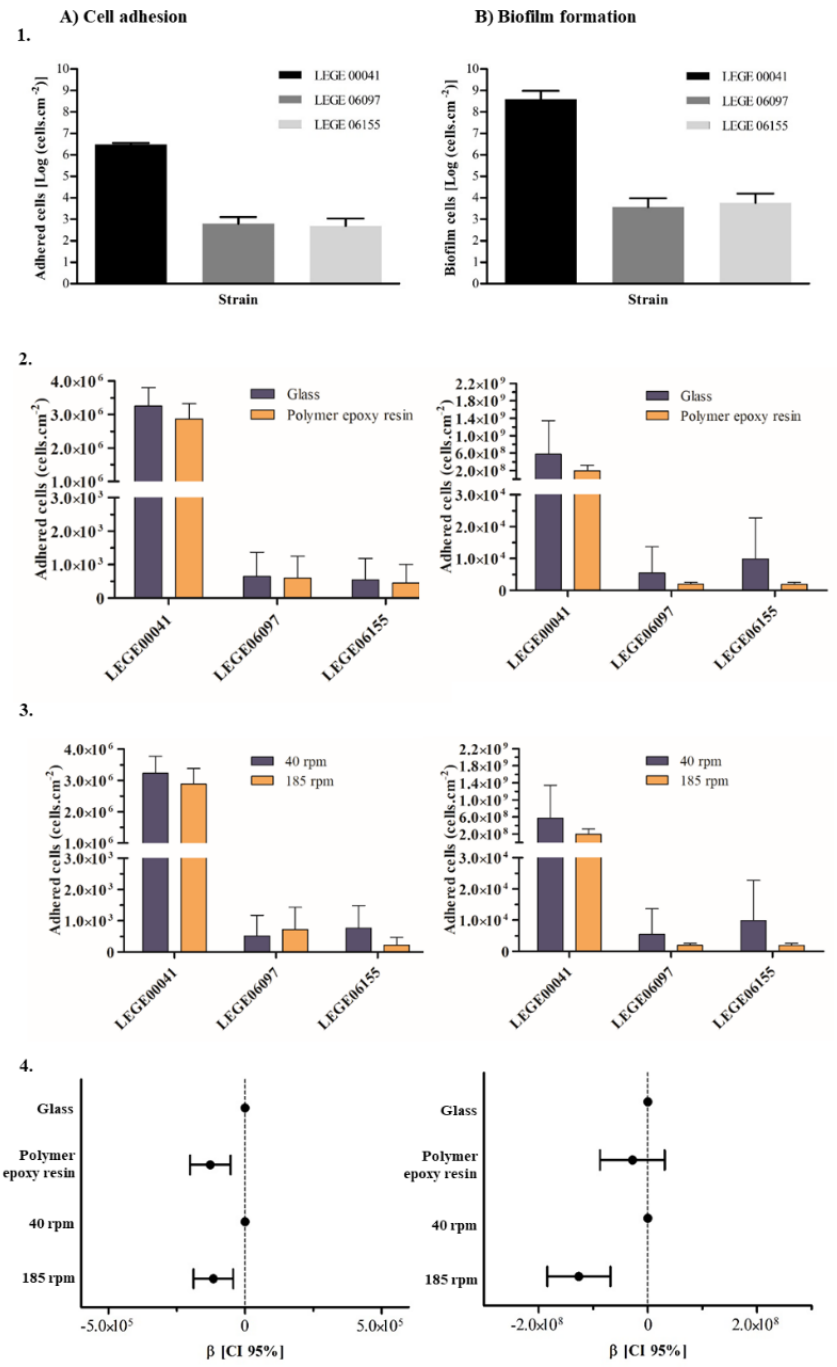

Figure 7.1. Association between initial cell adhesion and biofilm formation of three cyanobacteria strains (*Synechocystis salina* LEGE 00041, *S. salina* LEGE 06155 and *Cyanobium* sp. LEGE 06097) on glass and polymer epoxy resin surfaces under different hydrodynamic conditions. Mean of the cumulative number of cyanobacterial cells attached on glass and polymer epoxy resin surfaces at 40 and 185 rpm for cell adhesion (1**A**) and biofilm formation (1**B**) assays. Bar charts represent the mean of LEGE 00041, LEGE 06155 and LEGE 06097 attached cells on glass and polymer epoxy resin surfaces obtained for cell adhesion (2**A**) and

biofilm formation (2**B**) assays, and the mean of LEGE 00041, LEGE 06155 and LEGE 06097 attached cells under 40 and 185 rpm registered for cell adhesion (3**A**) and biofilm formation (3**B**) assays. Linear regression models (LRMs) between the number of cells and the independent variables performed for initial adhesion (4**A**) and biofilm formation (4**B**). Glass and 40 rpm were used as the reference conditions. LRMs were adjusted for strain and incubation periods. Results are presented as beta estimates (β) and the corresponding 95% confidence interval (CI 95%).

7.1.2. Surface effect on cell adhesion and biofilm formation

For the study of the surface effect on cell adhesion and biofilm formation, cyanobacteria cells were exposed to the glass and polymer epoxy surfaces for 7.5 h and 42 days, respectively, and the number of adhered cells was quantified for each experimental point. The mean adhered cyanobacteria cells on both surfaces is represented in Figure 7.1. 2a. Regarding the surfaces, all cyanobacteria strains had a higher number of adhered cells on glass than on the polymer epoxy resin surface. *Cyanobium* sp. LEGE 06097 and *S. salina* LEGE 06155 strains displayed similar behaviour, reaching a mean value of $6.42 \times 10^2 \pm 7.27 \times 10^2$ and $5.41 \times 10^2 \pm 6.47 \times 10^2$ cell/cm^2 on glass, respectively, and a mean of $5.98 \times 10^2 \pm 6.52 \times 10^2$ and $4.49 \times 10^2 \pm 5.59 \times 10^2$ cell/cm^2 on the polymer epoxy resin, respectively. In the case of *S. salina* LEGE 00041, although the differences are subtle, the number of cells adhered on glass was also higher than on the polymer epoxy resin surfaces ($3.25 \times 10^6 \pm 5.57 \times 10^5$ vs. $2.87 \times 10^6 \pm 4.54 \times 10^5$ cell/cm^2). The same pattern was verified for cyanobacterial biofilms formed on glass and the polymer epoxy resin surfaces for 42 days. *Cyanobium* sp. LEGE 06097 and *S. salina* LEGE 06155 reached a mean value of $5.01 \times 10^3 \pm 7.68 \times 10^3$ and $7.88 \times 10^3 \pm 1.22 \times 10^4$ cells/cm^2 on glass, respectively, and a mean of $2.41 \times 10^3 \pm 3.32 \times 10^3$ and $3.96 \times 10^3 \pm 6.27 \times 10^3$ cells/cm^2 on the polymer epoxy resin surface, respectively (Figure 7.1. 2b). Likewise, the higher biofilm-forming *S. salina* LEGE 00041 presented a higher number of biofilm cells on glass ($4.26 \times 10^8 \pm 6.70 \times 10^8$ cells/cm^2) than on the polymer epoxy resin surface ($3.42 \times 10^8 \pm 4.82 \times 10^8$ cells/cm^2).

7.1.3. Hydrodynamic effect on cell adhesion and biofilm formation

For the study of the hydrodynamic effect on cell adhesion and biofilm formation, cyanobacteria cells were exposed to both glass and polymer epoxy surfaces under 40 and 185 rpm for 7.5 h and 42 days, respectively, and the number of adhered cells was quantified for each experimental point. Regarding the hydrodynamic conditions, the mean adhered cyanobacteria cells registered for two hydrodynamic conditions is represented in Figure 7.1. 3a. For *Cyanobium* sp. LEGE 06097, the mean number of adhered cells at 40 rpm was 5.17 x 10^2 ± 6.61 x 10^2 cells/cm^2, while at 185 rpm it was 7.23 x 10^2 ± 7.05 x 10^2 cells/cm^2. In opposition, *S. salina* LEGE 06155 reached a mean of 7.64 x 10^2 ± 7.25 x 10^2 cells/cm^2 at 40 rpm and 2.26 x 10^2 ± 2.45 x 10^2 cells/cm^2 at 185 rpm. Also, *S. salina* LEGE 00041 registered a higher number of adhered cells at 40 than 185 rpm (3.23 x 10^6 ± 5.36 x 10^5 vs. 2.89 x 10^6 ± 4.92 x 10^5 cells/cm^2). In turn, cyanobacteria biofilms developed for 42 days presented a higher number of cells at low shear forces (Figure 7.1. 3b). *S. salina* LEGE 06155 and *S. salina* LEGE 00041 kept constant the pattern verified for adhesion assays, reaching a mean of 9.93 x 10^3 ± 1.28 x 10^4 and 5.73 x 10^8 ± 7.73 x 10^8 cells/cm^2 at 40 rpm, respectively, and a mean of 1.91 x 10^3 ± 5.84 x 10^2 and 1.95 x 10^8 ± 1.22 x 10^8 cells/cm^2 at 185 rpm, respectively. For *Cyanobium* sp., biofilms developed at 40 rpm also presented a higher number of cells (5.46 x 10^3 ± 8.18 x 10^3 cells/cm^2) than those developed at 185 rpm (1.97x 10^3 ± 5.70 x 10^2 cells/cm^2).

7.1.4. Association between the initial cell adhesion and biofilm development

In order to evaluate the influence of surface properties and hydrodynamic conditions on the number of adhered cells, LRM were performed for initial adhesion and biofilm formation. In general, for initial adhesion, the polymer epoxy resin surface was significantly associated with a lower number of adhered cyanobacteria cells when compared to the glass surface (- 1.27 x 10^5 cells/cm^2 [-2.01 x 10^5: -5.29 x 10^4]) (Figure 7.1 4a). Likewise, for the higher shear force, the number of adhered cells was significantly lower (– 1.16 x 10^5 cells/cm^2 [-1.88 x 10^5: -4.31 x 10^4]) compared to the lower shear force (Figure 7.1. 4a). For biofilm

formation, the polymer epoxy resin was also associated with a lower number of cells (– 2.79 x 10^7 cells/cm^2 [-8.70 x 10^7: 3.13 x 10^7]) compared to glass (Figure 7.1. 4b). Although this association was not significant, the tendency verified for initial adhesion was maintained during biofilm formation. Concerning the hydrodynamic conditions, the high shear force was significantly associated with a lower number of cyanobacteria biofilm cells compared to the low shear force (- 1.26 x 10^8 cells/cm^2 [-1.84 x 10^8: -6.81 x 10^7]) (Figure 7.1. 4b).

Additionally, the correlation between the number of adhered cells after 7.5 h and biofilm cells on day 42 was determined. Regardless of the surface or hydrodynamic conditions, there is a significant correlation between the number of adhered cells and biofilm cells obtained in the last sampling point for each assay (r = 0.800, p < 0.001). Data also indicated that the number of biofilm cells observed on day 42 depends on the number of adhered cells at the end of initial adhesion (7.5 hours) and hydrodynamic conditions (R^2 = 0.795, p < 0.001; Table 7.3.). Additionally, the surface was not significantly associated with the number of biofilm cells on day 42 (p = 0.111), despite playing a significant role in initial adhesion (p = 0.001).

Table 7.3. Association between the number of biofilm cells on day 42 and the number of adhered cells at 7.5 hours, surface, and hydrodynamic conditions. LRM was adjusted for strain. Glass and 40 rpm were used as the reference conditions. Results were represented as beta estimates (β) and the corresponding 95% confidence interval (CI 95%). Significant results were considered for p-values < 0.05.

Independent variables	β	CI (95%)	*p*
Adhered cells	1.28 x 10^3	[7.99 x 10^2:1,77 x 10^3]	**< 0.001**
Surface	1.67 x 10^8	[-3.82 x 10^7:3.72 x 10^8]	0.111
Hydrodynamic condition	-3,75 x 10^8	[-5.70 x 10^8:-1.79 x 10^8]	**< 0.001**

Adjusted R squared = 0.795.

7.1.5. Biofilm parameters analysis

LRM were applied to evaluate the effect of surfaces properties and hydrodynamic conditions on biofilm wet weight and thickness, and chlorophyl *a* content. Considering the biofilm parameters analysis, cyanobacterial biofilms formed on the polymer epoxy resin surface were significantly associated with a lower biofilm wet weight (- 4.62 mg [- 7.32: -1.92], thickness (-14.22 µm [-19.57: -8.86]), and chlorophyll *a* content (- 0.35 µg.mL $^{-1}$ [-

0.55: - 0.14]) compared to those developed on glass (Figure 7.2.). In turn, cyanobacteria biofilms formed at 185 rpm were also associated with a lower biofilm wet weight (- 2.74 mg [- 5.42: - 0.05]), thickness (-16.78 µm [- 21.89: - 11.66]), and chlorophyll *a* content (- 0.78 µg/mL [- 0.97: - 0.59]) compared to those developed at 40 rpm (Figure 7.2.).

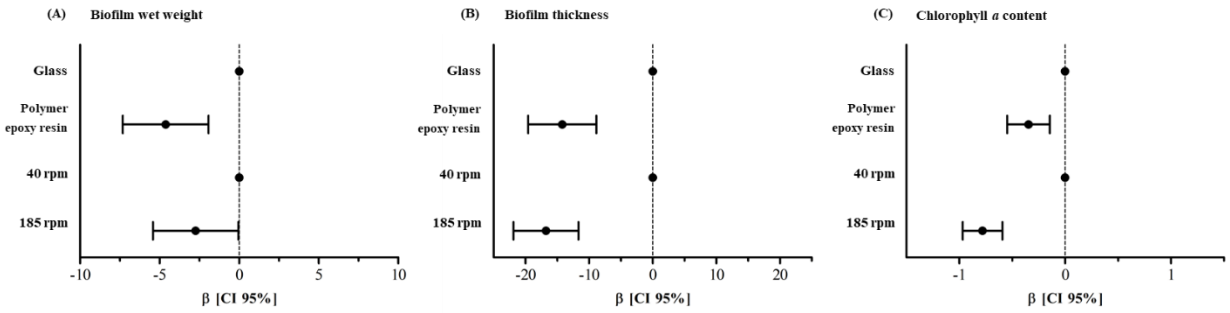

Figure 7.2. Associations between biofilm wet weight **(A)**, thickness **(B)** and chlorophyll *a* content **(C)** and the independent variables. Glass and 40 rpm were used as the reference conditions. LRMs were adjusted for strain and incubation periods. Results are presented as beta estimates (β) and the corresponding 95% confidence interval (CI 95%).

7.1.6. Biofilm structure analysis

Cyanobacterial biofilm structures were evaluated on day 42 using OCT (Figure 7.3.). Regardless of shear forces, biofilms formed on polymer epoxy resin surfaces (Figure 7.3. 1-3.3c and d) exhibited fewer cells and lower thickness than those developed on glass (Figure 7.3. 1-3.3a and b). In addition, for both glass and polymer epoxy resin surfaces, biofilms formed at 185 rpm (Figure 7.3. 1- 3.3b and d) presented a less developed structure than at 40 rpm (Figure 7.3. 1-3.3a and c). These results were verified for the three cyanobacteria strains.

7.2. Discussion

Our study demonstrated that the cyanobacteria behaviour observed for the initial adhesion assays (7.5 h) remained constant during biofilm development (42 days). The association between cell adhesion and biofilm formation was observed for the three

cyanobacteria isolates tested using glass and polymer epoxy resin surfaces at 40 and 185 rpm. Results revealed the potential of short-time adhesion assays (7.5 h) to estimate the biofilm formation at different conditions over 42 days and to provide important insights about the AF performance of marine coatings. Indeed, the tendency verified on initial adhesion assay regarding the cell adhesion on glass and polymer epoxy resin surfaces and at different hydrodynamic conditions was maintained during cyanobacterial biofilm development and was supported by the analysis of the biofilm wet weight, thickness, chlorophyll *a* content, and structure. Furthermore, the number of biofilm cells on day 42 was significantly dependent on the number of adhered cells after 7.5 h.

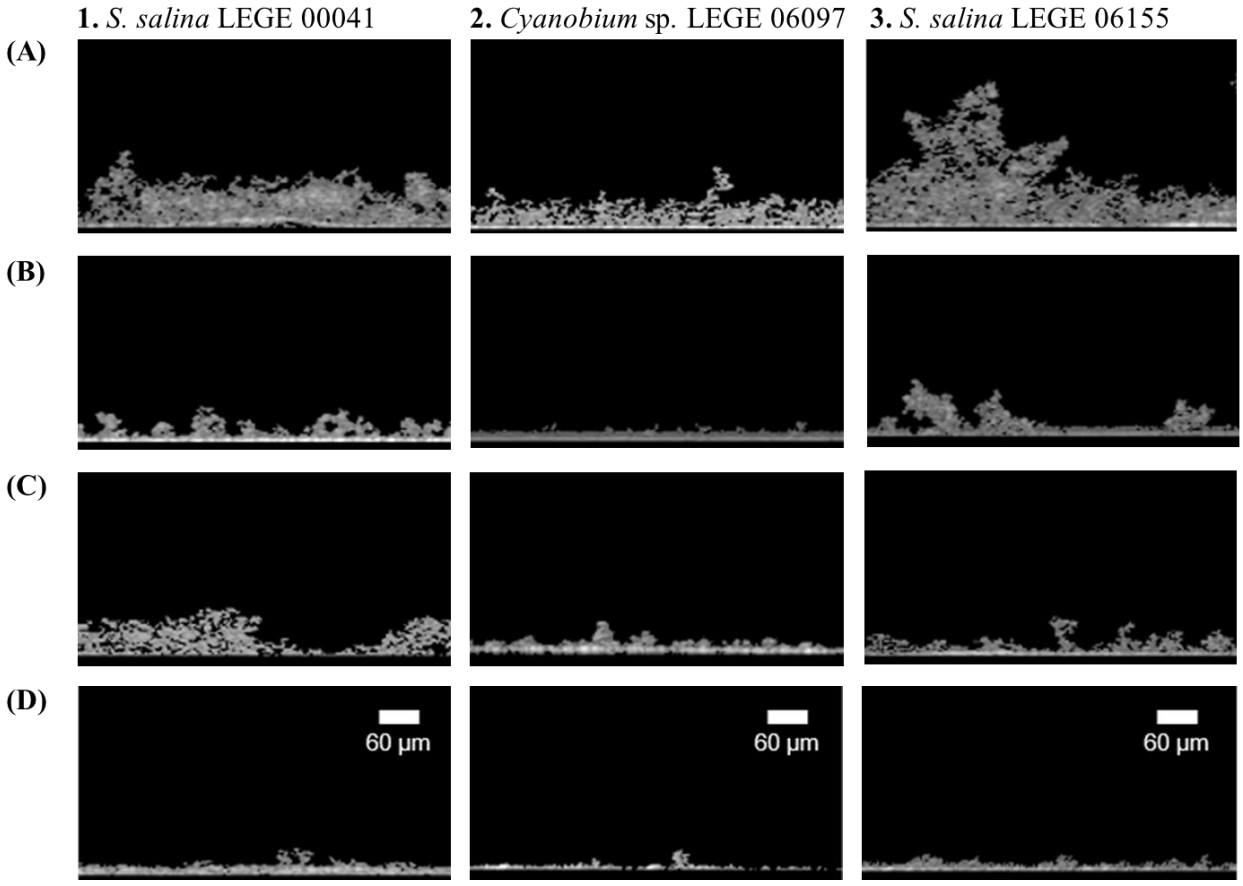

Figure 7.3. Representative images of biofilm structures captured on day 42 using OCT for *S. salina* LEGE 00041 (1), *Cyanobium* sp. 06097 (2) and *S. salina* 06155 (3) biofilms formed on glass at 40 and 185 rpm (**A** and **B**, respectively) and on polymer epoxy resin at 40 and 185 rpm (**C** and **D**, respectively).

The majority of available short-term adhesion methods involve the incubation of a monoculture of microfoulers with a coated surface to allow cell attachment for 2 – 48 h followed by the enumeration of the attached cells by direct counting under a microscope, by staining cells or nucleic acids with dyes, or by spectrophotometric or fluorometric quantification of chlorophyll (Briand 2009, Leroy et al. 2007, Salta et al. 2010, Stafslien et al. 2011, Wendt 2017). The staining of attached cells requires several additional steps in order to increase their specificity and sensitivity (e.g. cell fixation, staining, and washing) (Stafslien et al. 2011), making assays more laborious and expensive and increasing the time-to-results, while the chlorophyll quantification may only be applied to chlorophyll-producing organisms. Although some of these assays correlate with field assays (Briand 2009, Stafslien et al. 2007) and are useful screening tools for AF coatings, the initial adhesion assay proposed in this study is relatively rapid (7.5 h), inexpensive and easy to perform since it does not require specific dyes and additional staining steps and, based on our results, displays high accuracy. However, even though this approach displayed promising results, it is important to highlight that the conditions and materials evaluated in this study are not representative of a real scenario and more tests to assess its correlation with sea trials are needed.

Similarly to the results obtained in this short-term assays, previous studies demonstrated that *Escherichia coli* initial adhesion on different biomedical materials was able to predict biofilm formation for a 24 h period (Alves et al. 2020, Gomes et al. 2015, Lopez-Mila et al. 2018). Altogether, these findings suggest that initial microbial adhesion may provide important cues about the course of biofilm formation regardless of the microorganism type. Indeed, this is possible since microbial adhesion is one of the first steps of biofilm formation, involving physicochemical and molecular interactions (Di Martino 2018).

The adhesion of living microorganisms to a surface is a complex process affected by multiple factors. It is known that surface properties, including the hydrophobicity, influence the cell adhesion and subsequent biofilm formation (Spengler et al. 2019, Zhang et al. 2015). In this study, the results of theoretical adhesion models classified the glass surface as hydrophilic and the polymer epoxy resin surface as hydrophobic. In addition, the calculation of the free energy of adhesion indicated that the cyanobacteria cell adhesion on glass is thermodynamically unfavourable, while being favourable on polymer epoxy resin surfaces.

However, our experimental results showed that for all tested cyanobacteria, the number of both adhered and biofilm cells was higher for glass than for polymer epoxy resin surface. Although a considerable number of studies indicate that hydrophobic surfaces are favourable for bacterial adhesion (Cerca et al. 2005, De-la-Pinta et al. 2019), and in particular, for cyanobacterial adhesion (Ozkan and Berberoglu 2013), other studies found no correlation between surface hydrophobicity and cell attachment (Faria et al. 2020, Irving and Allen 2011, Mazumder et al. 2010, Talluri et al. 2020). These contradictory results may be explained by the existence of conditioning films formed due to the adsorption of (macro)molecules on the substrate that change the adhesion conditions for microorganisms (Hwang et al. 2012, Lorite et al. 2011). The nature of films is related to the material type and the environment that surrounds them (e.g. growth medium and type of microorganism) (Lorite et al. 2011, Talluri et al. 2020). Besides, it was described that conditioning films form few minutes after the surfaces are exposed, with subsequent growth for several hours, playing an important role in cyanobacteria adhesion and in the early stages of biofilm formation (Talluri et al. 2020). Thus, despite the physicochemical properties of the surfaces being fundamental (Zhang et al. 2015), the cyanobacterial adhesion and biofilm formation may be modulated by other factors.

The hydrodynamic conditions have also been pointed out as an important modulating factor of cyanobacterial adhesion and biofilm formation (Faria et al. 2020, Romeu et al. 2019) being able to change protein expression (Romeu et al. 2020). Similar to what happens for initial attachment of other microfoulers (Nolte et al. 2017), our data demonstrated that the number of cyanobacteria cells adhered to surfaces was higher at 40 than 185 rpm. This result was observed for both adhesion and biofilm formation assays, which indicated that shear forces have an influence not only in the early stages of biofilm formation but also during maturation stages. Indeed, higher shear forces may hamper initial cell attachment and facilitate the detachment of adhered microorganisms during biofilm formation (Thomen et al. 2017).

Microbial adhesion is also affected by the physicochemical properties of the microorganisms (Zhang et al. 2015). The thermodynamic characterization of cyanobacterial cells indicated that *S. salina* LEGE 00041 is relatively more hydrophobic than the other cyanobacteria. Indeed, a higher number of adhered and biofilm cells was registered for *S. salina* LEGE 00041 compared to *Cyanobium* sp. LEGE 06097 and *S. salina* LEGE 06155.

Although the association between the initial adhesion and biofilm formation has been verified for the three cyanobacteria, they behaved differently and regardless of their taxonomic order. For this reason, and in order to obtain further knowledge, this association was investigated using linear regression models adjusted for the microorganism and incubation periods. According to LRM, the initial cell adhesion assays were able to estimate that: 1) biofilms formed on glass displayed a higher number of cells than those formed on polymer epoxy resin; 2) biofilms formed at 40 rpm exhibited a higher number of cells than those formed at 185 rpm. Moreover, a significant correlation was found between the number of cells at the end of the initial adhesion period and the number of biofilm cells on day 42. In addition, the latter depends on the initial adhesion and hydrodynamic conditions.

These results were corroborated by the analysis of the different biofilm parameters, with biofilms developed on glass displaying higher values of biofilm wet weight, thickness, and chlorophyll *a* content when compared to biofilms formed on the polymer epoxy resin surface. Likewise, biofilms formed at 40 rpm also exhibited higher wet weight, thickness, and chlorophyll *a* content.

The potential of the initial adhesion assays to estimate the biofilm formation was also confirmed by the OCT analysis. Indeed, cyanobacterial biofilms formed on glass were thicker than those formed on the polymer epoxy resin. Also, biofilms formed at 40 rpm presented a more developed structure than at 185 rpm.

Overall, initial cell adhesion assays revealed a high potential to estimate biofilm development by cyanobacteria. Although thermodynamic studies provide important information about the surface properties and the interaction between surfaces and microorganisms, adhesion assays are crucial since biofilm formation is a complex process that involves a multiplicity of extrinsic factors. Thus, initial adhesion assays performed by cell counting after 7.5 h incubation allow high throughput screening of marine coatings considering different conditions (e.g. hydrodynamic forces and microorganisms type), providing indications about the biofilm behaviour in a short time. Therefore, this approach may be useful as a screening tool for marine coatings development, avoiding, at the first stage, the extensive laboratory assays monitoring biofilm parameters for long periods (6-8 weeks) or field trials often performed without prior evidence of a coating's effectiveness.

Nevertheless, further research is needed to ensure that these short-term adhesion assays may be applied to a broader range of marine engineered surfaces.

7.3. References

Akinfijevs, T., A. Janvaevskis and E. Lavendelis (2007). A Brief Survey of Ship Hull Cleaning Devices. Rīga, Latvia, RTU.

Alves, P., L. C. Gomes, M. Vorobii, C. Rodriguez-Emmenegger and F. J. Mergulhão (2020). "The potential advantages of using a poly(HPMA) brush in urinary catheters: effects on biofilm cells and architecture." Colloids and Surfaces B: Biointerfaces **191**: 110976.

Amara, I., W. Miled, R. B. Slama and N. Ladhari (2018). "Antifouling processes and toxicity effects of antifouling paints on marine environment. A review." Environmental toxicology and pharmacology **57**: 115-130.

Angelova, A. G., G. A. Ellis, H. W. Wijesekera and G. J. Vora (2019). "Microbial Composition and Variability of Natural Marine Planktonic and Biofouling Communities From the Bay of Bengal." Frontiers in Microbiology **10**(2738).

Arrhenius, A., T. Backhaus, A. Hilvarsson, I. Wendt, A. Zgrundo and H. Blanck (2014). "A novel bioassay for evaluating the efficacy of biocides to inhibit settling and early establishment of marine biofilms." Mar Pollut Bull **87**(1-2): 292-299.

Azevedo, J., J. T. Antunes, A. M. Machado, V. Vasconcelos, P. N. Leão and E. Froufe (2020). "Monitoring of biofouling communities in a Portuguese port using a combined morphological and metabarcoding approach." Scientific Reports **10**(1): 13461.

Azevedo, N. F., A. P. Pacheco, C. W. Keevil, M. J. Vieira (2006). " Adhesion of water stressed Helicobacter pylori to abiotic surfaces. " Journal of Applied Microbiology **101**(3): 718-724.

Bakker, D. P., A. van der Plaats, G. J. Verkerke, H. J. Busscher and H. C. van der Mei (2003). "Comparison of Velocity Profiles for Different Flow Chamber Designs Used in Studies of Microbial Adhesion to Surfaces." Applied and Environmental Microbiology **69**(10): 6280.

Basu, S., B. M. Hanh, J. Q. Isaiah Chua, D. Daniel, M. H. Ismail, M. Marchioro, S. Amini, S. A. Rice and A. Miserez (2020). "Green biolubricant infused slippery surfaces to combat marine biofouling." Journal of Colloid and Interface Science **568**: 185-197.

Bayoudhu, S., A. Othmane, F. Bettaieb, A. Bakhrouf, H. Ben Ouada and L. Ponsonnet (2006). " Quantification of the adhesion free energy between bacteria and hydrophobic and hydrophilic substrata." Materials Science and Engineering: C **26**(2-3): 300-305.

Blain, S., J. Guillou, P. Treguer, P. Woerther, L. Delauney, E. Follenfant, O. Gontier, M. Hamon, B. Leilde, A. Masson, C. Tartu and R. Vuillemin (2004). "High frequency monitoring of the coastal marine environment using the MAREL buoy." J Environ Monit **6**(6): 569-575.

Brian-Jaisson, F. (2014). Identification et caractérisation des exopolymères de biofilms de bactéries marines, Universit ´e de Toulon.

Briand, J. F. (2009). "Marine antifouling laboratory bioassays: an overview of their diversity." Biofouling **25**(4): 297-311.

Busscher, H. J., A. H. Weerkamp, H. C. van der Mei, A. W. van Pelt, H. P. de Jong, and J. Arends (1984). " Measurement of the surface free energy of bacterial cell surfaces and its relevance for adhesion." Applied and Environmental Microbiology **48**(5): 980-983.

Cerca, N., G. B. Pier, M. Vilanova, R. Oliveira and J. Azeredo (2005). "Quantitative analysis of adhesion and biofilm formation on hydrophilic and hydrophobic surfaces of clinical isolates of Staphylococcus epidermidis." Research in Microbiology **156**(4): 506-514.

De-la-Pinta, I., M. Cobos, J. Ibarretxe, E. Montoya, E. Eraso, T. Guraya and G. Quindós (2019). "Effect of biomaterials hydrophobicity and roughness on biofilm development." Journal of Materials Science: Materials in Medicine **30**(7): 77.

de Carvalho, C. C. C. R. (2018). "Marine Biofilms: A Successful Microbial Strategy With Economic Implications." Frontiers in Marine Science **5**(126).

Di Martino, P. (2018). "Bacterial adherence: much more than a bond." AIMS microbiology **4**(3): 563-566.

Faria, S. I., R. Teixeira-Santos, M. J. Romeu, J. Morais, V. Vasconcelos and F. J. Mergulhão (2020). "The Relative Importance of Shear Forces and Surface Hydrophobicity on Biofilm Formation by Coccoid Cyanobacteria." Polymers **12**(3): 653.

Flemming, H. C., P. S. Murthy, R. Venkatesan and K. Cooksey (2009). Marine and Industrial Biofouling. Heidelberg, Germany, Springer.

Georgiades, E. and D. Kluza (2017). "Evidence-based decision making to underpin the thresholds in New Zealand's craft risk management standard: biofouling on vessels arriving to New Zealand." Marine Technology Society Journal **51**(2): 76-88.

Gomes, L. C., L. N. Silva, M. Simões, L. F. Melo and F. J. Mergulhão (2015). "Escherichia coli adhesion, biofilm development and antibiotic susceptibility on biomedical materials." Journal of Biomedical Materials Research Part A **103**(4): 1414-1423.

Gomes, L. C., J. Deschamps, R. Briandet and F.J. Mergulhão (2018). " Impact of modified diamond-like carbon coatings on the spatial organization and disinfection of mixed-biofilms composed of Escherichia coli and Pantoea agglomerans industrial isolates." International Journal of Food Microbiology **277**: 74-82.

Hwang, G., S. Kang, M. G. El-Din and Y. Liu (2012). "Impact of conditioning films on the initial adhesion of Burkholderia cepacia." Colloids Surf B Biointerfaces **91**: 181-188.

Irving, T. E. and D. G. Allen (2011). "Species and material considerations in the formation and development of microalgal biofilms." Appl Microbiol Biotechnol **92**(2): 283-294.

Janczuk, B., E. Chibowski, J. M. Bruque, M .L. Kerkeb, F. González Caballero and D. G. Allen (1993). " On the Consistency of Surface Free Energy Components as Calculated from Contact Angles of Different Liquids: An Application to the Cholesterol Surface." Journal of Colloid and Interface Science **159**(2): 421-528.

King, R. K., G. J. Flick, S. A. Smith, M. D. Pierson, G. D. Boardman and C. W. Coale (2006). "Comparison of Bacterial Presence in Biofilms on Different Materials Commonly Found in Recirculating Aquaculture Systems." Journal of Applied Aquaculture **18**(1): 79-88.

Kotai, J. (1972). Instructions for Preparation of Modified Nutrient Solution Z8 for Algae Oslo, Norwegian Institute for Water Research**:** 5.

Lacoursière-Roussel, A., D. G. Bock, M. E. Cristescu, F. Guichard and C. W. McKindsey (2016). "Effect of shipping traffic on biofouling invasion success at population and community levels." Biological Invasions **18**(12): 3681-3695.

Leroy, C., C. Delbarre-Ladrat, F. Ghillebaert, M. J. Rochet, C. Compère and D. Combes (2007). "A marine bacterial adhesion microplate test using the DAPI fluorescent dye: a new method to screen antifouling agents." Letters in Applied Microbiology **44**(4): 372-378.

Lopez-Mila, B., P. Alves, T. Riedel, B. Dittrich, F. Mergulhão and C. Rodriguez-Emmenegger (2018). "Effect of shear stress on the reduction of bacterial adhesion to antifouling polymers." Bioinspir Biomim **13**(6): 065001.

Lorite, G. S., C. M. Rodrigues, A. A. de Souza, C. Kranz, B. Mizaikoff and M. A. Cotta (2011). "The role of conditioning film formation and surface chemical changes on Xylella fastidiosa adhesion and biofilm evolution." Journal of Colloid and Interface Science **359**(1): 289-295.

Ma, Y., X. Cao, X. Feng, Y. Ma and H. Zou (2007). " Fabrication of super-hydrophobic film from PMMA with intrinsic water contact angle below 90°." Polymer **48**(26): 7455-7460.

Mazumder, S., J. O. Falkinham, A. M. Dietrich and I. K. Puri (2010). "Role of hydrophobicity in bacterial adherence to carbon nanostructures and biofilm formation." Biofouling **26**(3): 333-339.

McClay, T., C. Zabin, I. Davidson, R. Young and D. Elam (2015). Vessel biofouling prevention and management options report, U.S. Coast Guard R&D Center.

Meireles, A., R. Fulgêncio, I. Machado, F. Mergulhão, L. Melo and M. Simões (2017). "Characterization of the heterotrophic bacteria from a minimally processed vegetables plant." LWT - Food Science and Technology **85**:293-300

Minchin, D. and S. Gollasch (2003). "Fouling and ships' hulls: how changing circumstances and spawning events may result in the spread of exotic species." Biofouling **19**: 111-122.

Neves, A. R., J. R. Almeida, F. Carvalhal, A. Câmara, S. Pereira, J. Antunes, V. Vasconcelos, M. Pinto, E. R. Silva, E. Sousa and M. Correia-da-Silva (2020). "Overcoming environmental problems of biocides: Synthetic bile acid derivatives as a sustainable alternative." Ecotoxicology and Environmental Safety **187**: 109812.

Nolte, K. A., J. Schwarze, C. D. Beyer, O. Özcan and A. Rosenhahn (2018). "Parallelized microfluidic diatom accumulation assay to test fouling-release coatings." Biointerphases **13**(4): 041007.

Nolte, K. A., J. Schwarze and A. Rosenhahn (2017). "Microfluidic accumulation assay probes attachment of biofilm forming diatom cells." Biofouling **33**(7): 531-543.

Oss, V. C. J. (1994). Interfacial forces in aqueous media. New York, Marcel Dekker Inc.

Ozkan, A. and H. Berberoglu (2013). "Cell to substratum and cell to cell interactions of microalgae." Colloids and Surfaces B: Biointerfaces **112**: 302-309.

Porra, R. J., W. A. Thompson and P. E. Kriedemann (1989). "Determination of accurate extinction coefficients and simultaneous equations for assaying chlorophylls a and b extracted with four different solvents: verification of the concentration of chlorophyll standards by atomic absorption spectroscopy." Biochim Biophysica Acta **975**(3): 384-394.

Rajeev, M., T. J. Sushmitha, K. G. Prasath, S. R. Toleti and S. K. Pandian (2020). "Systematic assessment of chlorine tolerance mechanism in a potent biofilm-forming marine bacterium Halomonas boliviensis." International Biodeterioration & Biodegradation **151**: 104967.

Ramos, V., J. Morais, R. Castelo-Branco, A. Pinheiro, J. Martins, A. Regueiras, A. L. Pereira, V. R. Lopes, B. Frazao, D. Gomes, C. Moreira, M. S. Costa, S. Brule, S. Faustino, R. Martins, M. Saker, J. Osswald, P. N. Leao and V. M. Vasconcelos (2018). "Cyanobacterial diversity held in microbial biological resource centers as a biotechnological asset: the case study of the newly established LEGE culture collection." J Appl Phycol **30**(3): 1437-1451.

Romeu, M. J., P. Alves, J. Morais, J. M. Miranda, E. D. de Jong, J. Sjollema, V. Ramos, V. Vasconcelos and F. J. M. Mergulhao (2019). "Biofilm formation behaviour of

marine filamentous cyanobacterial strains in controlled hydrodynamic conditions." Environ Microbiol **21**(11): 4411-4424.

Romeu, M. J. L., D. Domínguez-Pérez, D. Almeida, J. Morais, A. Campos, V. Vasconcelos and F. J. M. Mergulhão (2020). "Characterization of planktonic and biofilm cells from two filamentous cyanobacteria using a shotgun proteomic approach." Biofouling **36**(6): 631-645.

Salta, M., J. A. Wharton, P. Stoodley, S. P. Dennington, L. R. Goodes, S. Werwinski, U. Mart, R. J. Wood and K. R. Stokes (2010). "Designing biomimetic antifouling surfaces." Philos Trans A Math Phys Eng Sci **368**(1929): 4729-4754.

Schultz, M. P., J. A. Bendick, E. R. Holm and W. M. Hertel (2011). "Economic impact of biofouling on a naval surface ship." Biofouling **27**(1): 87-98.

Selim, M. S., M. A. Shenashen, S. A. El-Safty, S. A. Higazy, M. M. Selim, H. Isago and A. Elmarakbi (2017). "Recent progress in marine foul-release polymeric nanocomposite coatings." Progress in Materials Science **87**: 1-32.

Spengler, C., F. Nolle, J. Mischo, T. Faidt, S. Grandthyll, N. Thewes, M. Koch, F. Müller, M. Bischoff, M. A. Klatt and K. Jacobs (2019). "Strength of bacterial adhesion on nanostructured surfaces quantified by substrate morphometry." Nanoscale **11**(42): 19713-19722.

Stafslien, S., J. Daniels, B. Mayo, D. Christianson, B. Chisholm, A. Ekin, D. Webster and G. Swain (2007). "Combinatorial materials research applied to the development of new surface coatings IV. A high-throughput bacterial biofilm retention and retraction assay for screening fouling-release performance of coatings." Biofouling **23**(1): 45-54.

Stafslien, S. J., J. Bahr, J. Daniels, D. A. Christianson and B. J. Chisholm (2011). "High-Throughput Screening of Fouling-Release Properties: An Overview." Journal of Adhesion Science and Technology **25**(17): 2239-2253.

Talluri, S. N. L., R. M. Winter and D. R. Salem (2020). "Conditioning film formation and its influence on the initial adhesion and biofilm formation by a cyanobacterium on photobioreactor materials." Biofouling **36**(2): 183-199.

Taylor, D. A. (1996). Chapter 16 - Engineering materials. Introduction to Marine Engineering (Second Edition). D. A. Taylor. Oxford, Butterworth-Heinemann**:** 326-340.

Telegdi, J., L. Trif and L. Románszki (2016). 5 - Smart anti-biofouling composite coatings for naval applications. Smart Composite Coatings and Membranes. M. F. Montemor, Woodhead Publishing**:** 123-155.

Thomen, P., J. Robert, A. Monmeyran, A.-F. Bitbol, C. Douarche and N. Henry (2017). "Bacterial biofilm under flow: First a physical struggle to stay, then a matter of breathing." PLOS ONE **12**(4): e0175197.

Tian, L., Y. Yin, H. Jin, W. Bing, E. Jin, J. Zhao and L. Ren (2020). "Novel marine antifouling coatings inspired by corals." Materials Today Chemistry **17**: 100294.

Wendt, D. E. (2017). "Methods of assessing antifouling and foul-release efficacy of non-toxic marine coatings." Green Materials **5**(1): 22-30.

Zecher, K., V. P. Aitha, K. Heuer, H. Ahlers, K. Roland, M. Fiedel and B. Philipp (2018). "A multi-step approach for testing non-toxic amphiphilic antifouling coatings against marine microfouling at different levels of biological complexity." J Microbiol Methods **146**: 104-114.

Zhang, X., Q. Zhang, T. Yan, Z. Jiang, X. Zhang and Y. Y. Zuo (2015). "Quantitatively predicting bacterial adhesion using surface free energy determined with a spectrophotometric method." Environmental science & technology **49**(10): 6164-6171.

8.

Conclusions and suggestions for future work

8.1. Conclusions

The main goal of this thesis was to understand the process of marine biofilm formation, using different strains of coccoid cyanobacteria as model organisms, and develop new strategies to control and evaluate its formation.

This work started with the investigation of the relative importance of shear forces and surface hydrophobicity on cyanobacterial biofilm development by two coccoid cyanobacteria with different biofilm formation capacities (strong and weaker biofilm-forming), since these parameters are recognized as mudolators of biofilm formation. The selected hydrodynamic conditions represent the shear forces found in marine settings which were previously validated using CFD by our research group. In addition, surfaces with different hydrophobicity degrees were used. The overall results demonstrated that hydrodynamics had a stronger impact on biofilm development by coccoid cyanobacterial than surface hydrophobicity. This initial task allowed understanding the process of biofilm development

at an early stage, which provided important information for developing efficient AF solutions to control biofilm formation.

Since marine biofouling begins with surface colonization by microfouling organisms, the inhibition of initial attachment and biofilm formation can be a promising strategy to prevent or delay marine biofouling development. In this context, the second aim of this study was to evaluate the performance of different marine surfaces to prevent biofilm formation, and understand their interactions with microfouling organisms and how these influence biofilm development and structure. Among the tested surfaces, commercial silicone-based paint and an epoxy resin demonstrated a high potential to decrease marine biofilm formation. Additionally, the comprehensive analysis carried out in this study revealed that the surface materials properties, together with the features of the fouling microorganisms and microenvironment conditions, have a considerable role in marine biofouling, affecting not only the amount of biofilm formed but also its architecture. Therefore, understanding how AF surfaces interact with microfouling organisms can clarify and help to improve their efficacy, leading to the development of new AF coatings to control and/or reduce marine biofouling as biofilms with a more opened structure can be more susceptible to cleaning protocols.

The last goal of this study was to optimize the laboratory conditions to be used in the *in vitro* evaluation of marine surfaces, in order to mimic the prevailing conditions in real marine settings, and significantly reduce the time-to-results of available *in vitro* assays.

Firstly, the impact of microorganisms diversity on marine biofilms was assessed in order to understand if biofilms formed by a single microfouler strain are as adequate as mixed species biofilms when testing the AF performance of a given surface. Results demonstrated that the single-strain strategy used is a good compromise between the high complexity of *in vivo* marine ecosystems and the convenience of *in vitro* testing, overcoming the experimental limitations in replicating the cellular concentration of each organism in a multispecies biofilm.

The final accomplished task of this Ph.D. thesis was to determine the potential of short-time adhesion assays to estimate how biofilm development may proceed on a given surface. This evaluation demonstrated that there is a correlation between the number of adhered and biofilm cells, which was supported by other methods as biofilm wet weight,

thickness, chlorophyll *a* content, and structure. These findings demonstrated the high potential of initial adhesion assays to estimate marine biofilm development, and this protocol may be useful as a screening tool for marine coatings development, avoiding, at the first stage, the extensive laboratory assays or field trials often performed without prior evidence of the surface effectiveness.

8.2. Suggestions for future work

Although this thesis contributed to the development of new strategies to control marine biofouling and reduce its negative impact on the marine and environmental sectors, additional studies need to be performed to increase the predictive value of the obtained results.

Marine biofouling formation is a complex and dynamic process, which begins with the adhesion of microorganisms to the surface, and may be affected by several factors such as hydrodynamic conditions, surfaces properties, and microorganisms species (Catão et al. 2019, Chang et al. 2020, Qi et al. 2021, Romeu et al. 2019, Telegdi et al. 2016). These factors influence intracellular communication, including QS mechanisms, and the access of marine organisms to the nutrients, modulating the architecture and structure of microbial communities and their phenotype diversity and synergism (Aufrecht et al. 2019, Salta et al. 2013). The heterogeneous structures featured in marine biofilms may influence their resistance to mechanical and chemical challenges, such as fluid shear, detergents, and AF compounds, modulating their activity (Grzegorczyk et al. 2018, Hou et al. 2019, Srinandan et al. 2012). Therefore, biofilm architecture studies deserve special attention since they can provide critical information for the development of AF approaches for the control of bio-encrustation.

In this Ph.D. project, the impact of different marine surfaces on biofilm architecture was evaluated at the endpoint of the assays. In order to obtain a more insightful knowledge about the dynamics of biofilm formation and how surface properties modulate the structure of biofilm during both the initial and later stages of its development, the analysis of biofilm architecture and the presence of empty spaces should be monitored over time. Our group also

reported that hydrodynamics and surface properties can affect protein expression in filamentous cyanobacterial biofilms (Romeu et al. 2020, Romeu et al. 2021). Quantitive proteomic studies for coccoid cyanobacteria are still missing to understand the physiological effects of AF surfaces better, leading to the identification of new targets for biofilm control.

On the last study of this thesis, the short-time assays demonstrate potential to provide indications about the biofilm behaviour. Thus, this approach may be useful as a screening tool for marine marine engineered surfaces, at the first stage. Nevertheless, further research is needed to ensure that these short-term adhesion assays may be applied to a broader range of marine engineered surfaces and microorganisms.

In this study, the selected model microorganism was marine cyanobacteria, since it is considered one of the primordial colonizers of submerged surfaces, bulding the basis for the later settlement of macrofouling organisms (e.g. bryozoans, mollusks, polychaeta, tunicates, coelenterates or fungi) (Angelova et al. 2019, Arrhenius et al. 2014, Azevedo et al. 2020, de Carvalho 2018). However, other microorganisms, such as diatoms and marine bacteria, are also being described as earlier colonizers (Antunes et al. 2019, Arrhenius et al. 2014). As such, it would be important to extend the tests performed in the framework of this thesis to other microfouling organisms.

According to the literature review, there are several studies about the AF potential of different polymers either alone or functionalized with a wide variety of compounds (e.g., metals and carbon materials) (Aldred et al. 2008, Chen et al. 2008, Yang et al. 2021). In addition, marine organisms have also been identified as a rich resource of natural compounds with antimicrobial and antifouling properties, which are non-toxic for non-target marine organisms (Palanichamy and Subramanian 2017, Satheesh et al. 2016). Marine cyanobacteria are able to produce compounds that delay biofilm development and/or have antimicrobial properties that inactivate the biofilm growth through the inhibition of bacterial signals and production of enzymes that destroy biofilm matrix (Dobretsov et al. 2013). Within the scope of the CVMAR+i project, several extracts obtained from cyanobacterial strains were screened regarding their potential to inhibit biofilm formation by marine bacteria, which

show promising results. In this context, it would be interesting to immobilize these compounds on polymeric matrices and evaluate the AF potential of synthesized surfaces.

8.3. References

Aldred, N., I. Y. Phang, S. L. Conlan, A. S. Clare and G. J. Vancso (2008). "The effects of a serine protease, Alcalase®, on the adhesives of barnacle cyprids (Balanus amphitrite)." Biofouling 24(2): 97-107.

Angelova, A. G., G. A. Ellis, H. W. Wijesekera and G. J. Vora (2019). "Microbial composition and variability of natural marine planktonic and biofouling communities from the Bay of Bengal." Frontiers in microbiology 10: 2738.

Antunes, J., P. Leão and V. Vasconcelos (2019). "Marine biofilms: diversity of communities and of chemical cues." Environmental microbiology reports 11(3): 287-305.

Arrhenius, Å., T. Backhaus, A. Hilvarsson, I. Wendt, A. Zgrundo and H. Blanck (2014). "A novel bioassay for evaluating the efficacy of biocides to inhibit settling and early establishment of marine biofilms." Marine pollution bulletin 87(1-2): 292-299.

Aufrecht, J. A., J. D. Fowlkes, A. N. Bible, J. Morrell-Falvey, M. J. Doktycz and S. T. Retterer (2019). "Pore-scale hydrodynamics influence the spatial evolution of bacterial biofilms in a microfluidic porous network." PloS one 14(6): e0218316.

Azevedo, J., J. T. Antunes, A. M. Machado, V. Vasconcelos, P. N. Leão and E. Froufe (2020). "Monitoring of biofouling communities in a Portuguese port using a combined morphological and metabarcoding approach." Scientific reports 10(1): 1-15.

Catão, E. C., T. Pollet, B. Misson, C. Garnier, J.-F. Ghiglione, R. Barry-Martinet, M. Maintenay, C. Bressy and J.-F. Briand (2019). "Shear stress as a major driver of marine biofilm communities in the NW Mediterranean Sea." Frontiers in microbiology 10: 1768.

Chang, J., X. He, X. Bai and C. Yuan (2020). "The impact of hydrodynamic shear force on adhesion morphology and biofilm conformation of Bacillus sp." Ocean Engineering 197: 106860.

Chen, M., Y. Qu, L. Yang and H. Gao (2008). "Structures and antifouling properties of low surface energy non-toxic antifouling coatings modified by nano-SiO 2 powder." Science in China Series B: Chemistry 51(9): 848-852.

de Carvalho, C. C. (2018). "Marine biofilms: a successful microbial strategy with economic implications." Frontiers in marine science 5: 126.

Dobretsov, S., R. M. Abed and M. Teplitski (2013). "Mini-review: Inhibition of biofouling by marine microorganisms." Biofouling 29(4): 423-441.

Grzegorczyk, M., S. J. Pogorzelski, A. Pospiech and K. Boniewicz-Szmyt (2018). "Monitoring of marine biofilm formation dynamics at submerged solid surfaces with multitechnique sensors." Frontiers in Marine Science 5: 363.

Hou, J., C. Wang, R. T. Rozenbaum, N. Gusnaniar, E. D. de Jong, W. Woudstra, G. I. Geertsema-Doornbusch, J. Atema-Smit, J. Sjollema and Y. Ren (2019). "Bacterial density and biofilm structure determined by optical coherence tomography." Scientific reports 9(1): 1-12.

Palanichamy, S. and G. Subramanian (2017). "Antifouling properties of marine bacteriocin incorporated epoxy based paint." Progress in Organic Coatings 103: 33-39.

Qi, L., T. Jiang, R. Liang and W. Qin (2021). "Polymeric membrane ion-selective electrodes with anti-biofouling properties by surface modification of silver nanoparticles." Sensors and Actuators B: Chemical 328: 129014.

Romeu, M. J., P. Alves, J. Morais, J. M. Miranda, E. D. de Jong, J. Sjollema, V. Ramos, V. Vasconcelos and F. J. Mergulhão (2019). "Biofilm formation behaviour of marine filamentous cyanobacterial strains in controlled hydrodynamic conditions." Environmental microbiology 21(11): 4411-4424.

Romeu, M. J., D. Domınguez-Pérez, D. Almeida, J. Morais, A. Campos, V. Vasconcelos and F. J. Mergulhão (2020). "Characterization of planktonic and biofilm cells from two filamentous cyanobacteria using a shotgun proteomic approach." Biofouling 36: 631–645.

Romeu, M. J., D. Domınguez-Pérez, D. Almeida, J. Morais, M. Araújo, H. Osório, A. Campos, V. Vasconcelos and F. J. Mergulhão (2021). " Quantitative proteomic analysis of marine biofilms formed by filamentous cyanobacterium." Environmental Reseach (in press).

Salta, M., J. A. Wharton, Y. Blache, K. R. Stokes and J. F. Briand (2013). "Marine biofilms on artificial surfaces: structure and dynamics." Environmental microbiology 15(11): 2879-2893.

Satheesh, S., M. A. Ba-akdah and A. A. Al-Sofyani (2016). "Natural antifouling compound production by microbes associated with marine macroorganisms: a review." Electronic Journal of Biotechnology 19(3): 26-35.

Srinandan, C., G. D'souza, N. Srivastava, B. B. Nayak and A. S. Nerurkar (2012). "Carbon sources influence the nitrate removal activity, community structure and biofilm architecture." Bioresource Technology 117: 292-299.

Telegdi, J., L. Trif and L. Románszki (2016). Smart anti-biofouling composite coatings for naval applications. Smart Composite Coatings and Membranes, Elsevier: 123-155.

Yang, H., S. Wang, C. Li and H. Li (2021). "Three-Dimensional Numerical Simulations and Antifouling Mechanism of Microorganisms on Microstructured Surfaces." Processes 9(2): 319.